Translation of a Chemical Reaction from Batch to Continuous Flow via Process Analytical Technology and Chemometrics

Michael F. Roberto

A dissertation submitted in partial fulfillment of the requirements for the degree of

Doctor of Philosophy

University of Washington

2014

Reading Committee:

Brian J. Marquardt
Philip Reid, Chair
Frank Turecek

Program Authorized to Offer Degree:

Department of Chemistry

University of Washington

Abstract

Translation of a Chemical Reaction from Batch to Continuous Flow
via Process Analytical Technology and Chemometrics

Michael F. Roberto

Chair of the Supervisory Committee:

Professor Philip J. Reid

Chemistry

Research Advisor

Dr. Brian J. Marquardt

Applied Physics Laboratory

Current continuous flow reactor (CFR) development and optimization primarily involves the investigation of process parameters such as flow and temperature to optimize a reaction. The advantages of CFRs for stable production – including improved heat transfer, reproducible results, safety and cost considerations, and others – generally result in comparable or improved yield compared to batch chemistry. However, the translation of a reaction from batch to continuous flow may be significantly improved following the thorough investigation of a batch reaction with analytical instrumentation.

In this work, the Swern oxidation of S-1-phenylethanol is optimized for continuous flow production via the combination of information discovered in batch and continuous flow validation methods. A model chemistry is investigated with Raman spectroscopy and chemometric modeling in continuous flow, demonstrating the capability of real-time monitoring conversion in a CFR. The Swern oxidation is investigated in batch using Raman spectroscopy, high performance liquid chromatography (HPLC), and gas chromatography tandem mass spectrometry (GC-MS), yielding new information about intermediate kinetics, product formation, and side-product decomposition pathways. A technique for rapidly determining steady state in a CFR is described, using the Swern oxidation as a model chemistry. Finally, the Swern oxidation of S-1-phenylethanol is optimized in a CFR using real-time quantitative Raman monitoring and the mechanistic information uncovered in the batch investigation. This improved CFR development and optimization pathway – a thorough investigation of batch, coupled with optimization of a reaction through understanding of a chemistry – offers significant advantages over the current paradigm, and is applicable to most CFRs.

Dedicated to David S. Roberto

1989-2011

Acknowledgements

I would like to thank my advisor, Brian Marquardt, for guiding me, encouraging me, and putting up with me for the last five years. It's been a long ride, and I've enjoyed... some of it. If I had to guess, I'd say probably more than half. Drs. Tom Dearing and Chuck Branham have been great mentors, keeping me on track and helping me with the day-to-day stuff. Jessica, who's kept me sane throughout this extensive writing period. My wonderful family, encouraging me from afar and, when feasible, in person. Brian and Linda at Medicinal Chemistry for their generous help in instrumentation in the final two years of my research. CPAC and the FDA for funding support, and encouragement of my professional development. Olav Bleie, the best magpie I've ever collaborated with. My extended Enforcer family, a limitless fountain of positivity, friendship, and Expo Mode that kept my head above water. And all of my other friends, near and far, that provide diversions, distractions, and terrible ideas for thesis titles. Though actually, "My First Thesis" was pretty good.

Chapter 1

Introduction

Today, pharmaceutical and specialty chemical manufacturing are produced in large scale batch reactions. This is a time- and energy-intensive procedure and requires multiple engineering cycles of scaling the reaction from discovery, development pilot and production-scale. Monitoring a production process, and validation of final products, is a complicated and time-consuming method, requiring hours of processing and energy consumption for various analytical validation techniques [1]. In addition, batch reactions have numerous potential failure points for large-scale production:

- Handling of unsafe chemicals in large scales requires appropriate safety facilities,
- Stepped operations require frequent interaction and process monitoring,
- Heating inefficiencies in large-scale reactors limit the capability of employing temperature-sensitive reactions
- Reproducibility is limited outside research laboratories.

Continuous flow reactors (CFRs) are an emerging technology in the chemical production world, having found use in both research and industry settings [2]. CFRs are small volume flow cells optimized for continuous, consistent production of a target compound, addressing many of the inefficiencies associated with large-scale batch production.

Advantages of CFR Technology

When conducting reactions on a laboratory-scale that may eventually be scaled to production, the exothermicity of a reaction is a critical consideration for process safety. A reaction that requires a cryogenic ice bath at a 50 mL scale quickly becomes unfeasible in a large-scale production facility. Reactions that require reflux in batch are frequently infeasible at large scales. From the perspective of both safety and cost, the pharmaceutical

and specialty chemical manufacturing industries prefer production schemes that do not require heat management. CFRs can overcome these challenges by significantly reducing the heat management costs associated with production. CFR reaction plates are typically manufactured with millimeter-wide channels and a high surface-to-volume interface, resulting in a multi-fold reduction in the average distance to temperature control channels (Figure 1.1). The design results in a reduction of temperature gradients and improved homogeneity in CFRs [12-14]. This significantly reduces the possibility of runaway exothermic reactions. In addition, only a small volume of material is committed to the reaction at any given time should control of the reaction be lost.

Figure 1.1. Schematic side-view of continuous flow reactor mixing chip showing heat exchange and mixing areas. Each layer has a width of 1.5 mm, and is separated by 1 mm of glass.

In addition to ensuring process safety, CFRs reduce the volume of chemical waste generated. Efficient heating, homogenous mixtures, and improved safety against runaway exothermic reactions allows for a large reduction of solvent required compared to batch synthesis. With pharmaceutical processes generating typically 25 kg of waste for every kilogram of product prepared [2], CFRs offer a reprieve from such large volumes of waste. This enables an expansion of green chemistry in industrial manufacturing, assisting with cost saving while reducing the environmental footprint.

CFRs have been fabricated from an array of substrates, including glass [3], quartz [4], diamond [5], stainless steel [6], and others [7-9]. Each substrate includes its own

considerations for solvent use, temperature and pressure ranges, cost, and ability to interface with flow channels. Due to its broad compatibility with organic compounds, glass microreactors are heavily favored for most CFR use. Aside from hydrofluoric acid chemistry, which can etch glass, there are few chemistries that are incompatible with the glass substrate.

The volumes and channels of CFRs can range from milliliter to microliter scale [10]. The simplest CFR is a T-microreactor (Figure 1.2), which works by bringing two reactant streams together at a T-junction. In these reactors, reactions only occur by diffusion. As the scale of CFRs increases to the milliliter-scale, the cross-sectional area of reagents would require lengthy reaction times to obtain homogeneity via diffusion [11]. A reaction with slow kinetics would further require a prohibitively long amount of time in a diffusion channel to reach its conclusion. Micromixers have been developed that ensure turbulence

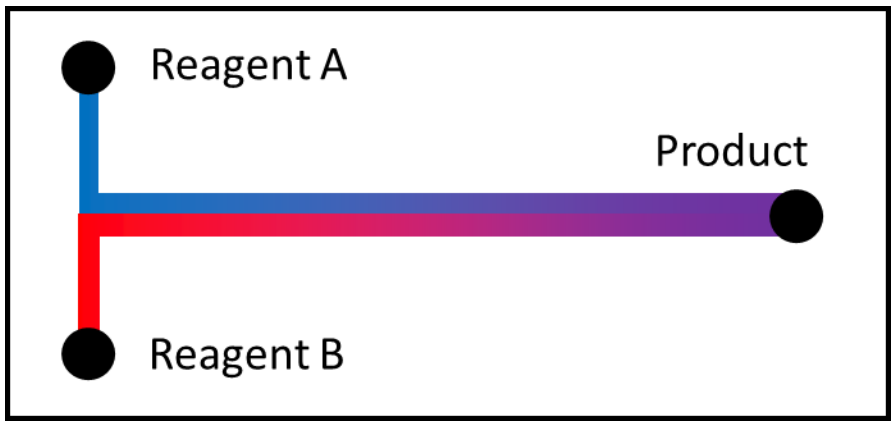

Figure 1.2. T-junction micromixer schematic. Two reagents (red and blue) mix slowly via diffusion on the path towards the reactor exit.

throughout the length of the reactor [4]. Turbulent mixing ensures that reagents are continually well-mixed, such that the limiting step is the kinetics of the reaction itself rather than the diffusion time. These CFRs typically employ reaction plates designed for turbulent mixing (Figure 3). In addition to more efficient mixing, turbulent mixing schemes allow for larger volume CFRs, increasing product throughput.

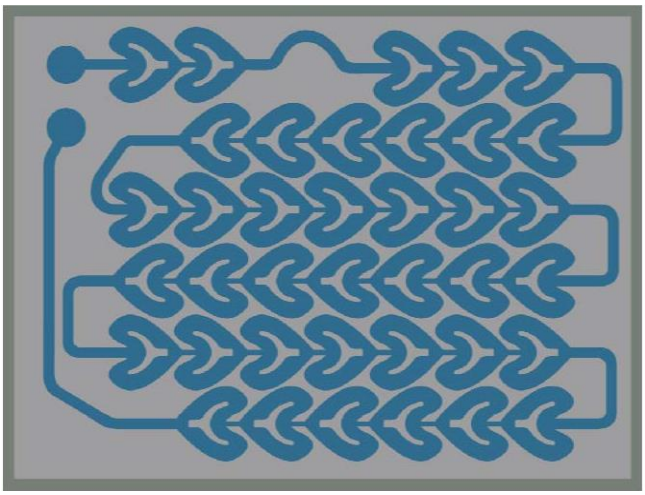

Figure 1.3. Top view of continuous flow reactor mixing chip. Heart-shaped mixers are employed to ensure turbulent mixing throughout

Implementation of CFRs

Continuous flow reactors have been optimized for production in numerous ways. Reactions investigated in continuous flow are frequently a direct translation of the batch chemistry, optimized via flow and temperature studies. In a typical example, Wiles *et. al.* investigated the esterification of benzoic acid at multiple temperatures and residence times using HPLC [12]. The process was time-intensive, requiring equilibrium to be reached in the microreactor and 20+ minutes of time for HPLC analyses. Baek *et. al.* experienced similar

results in their investigation of indium phosphate [13]. In these and nearly every other example, HPLC run times represent the vast majority of time associated with reaction optimizations. Jensen *et. al.* have had the most success trying to reduce the time required to optimize a reaction without sacrificing a proper design of experiments. Most notably towards this goal, the group constructed a self-optimizing reactor using in-line HPLC and the Nelder-Mead simplex method [14]. The controller program interpreted the yield results from the HPLC every 20 minutes, determining via algorithm another design point to investigate until a maximum was obtained. While this reduced the number of design points required to determine a reactor was optimized, it still relied upon a time-intensive chromatographic method to validate reaction yield. Additionally, real-time optimization strategies generally rely upon peak-height ratios monitoring specific species, unable to detect process upsets in a CFR due to a lack of full-spectrum multivariate analysis.

Additional inefficiencies in CFRs exist in how reactions are designed for continuous flow. In the previous examples, which constitute only a small sample of similar studies, the continuous flow production scheme is directly translated from the batch production scheme, taking advantage of the efficient temperature gradients and thermal capabilities of continuous flow. However, continuous flow allows not only for a translation of batch production paradigms, but for an informed production scheme by designing for continuous flow from scratch. This is possible following a thorough investigation of a reaction in batch. Through the understanding of intermediate formation rates, production pathways, target chemical formation mechanisms, and understanding of batch design limitations, a chemistry pathway can be fundamentally improved.

Chromatographic Validation

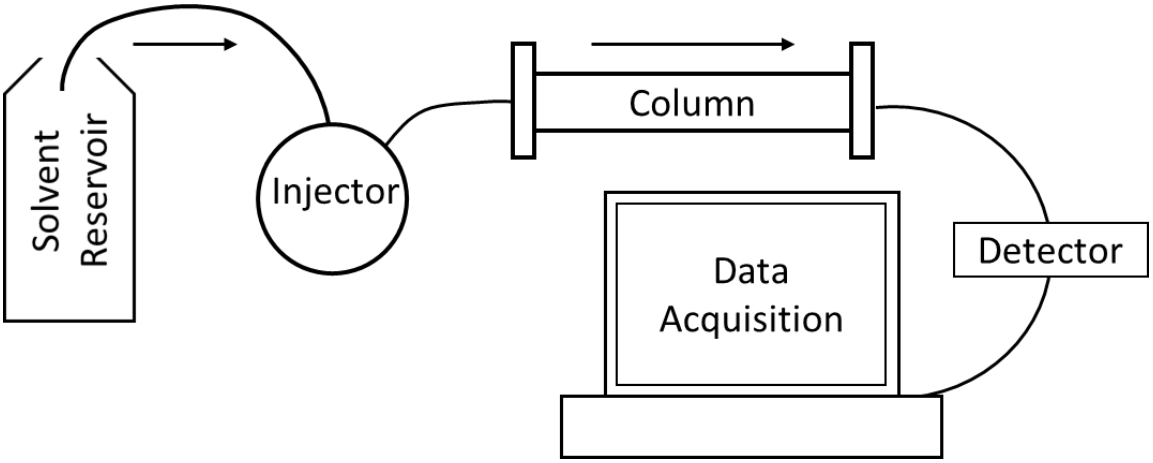

Figure 1.4. A basic schematic of an HPLC. HPLC is a highly quantitative technique able to separate a mixture of compounds. The core components are: Solvent reservoir or reservoirs, a mixture injector, a packed column, a detector (FID or UV), and data acquisition software.

Chromatographic methods are frequently used validation methods to determine chemical steady state and conversion in CFRs [12,15-18]. High performance liquid chromatography (HPLC) is a technique used to separate the components in a mixture, to identify components, and to quantify components. HPLC is capable of separating analytes in a mixture based on their polarity, which is dictated by the analyte's adsorptivity to the stationary phase. Figure 1.4 shows a basic schematic of an HPLC and each of its key components. A solvent or a mixture of solvents (shown in Figure 1.4) is pumped at high pressure, forming the mobile phase in this chromatography. An injector introduces a small amount of the mixture, and the eluent is sent into the stationary phase column typically packed with long-chain hydrocarbons. After separation, a detector (Figure 1.4) such as a flame ionization detector (FID) or UV detector generates a signal proportional to the amount of sample component emerging from the column, hence allowing for quantitative

analysis of the sample components. HPLC has proven popular for CFRs and microreactors as material produced is frequently well-suited for separation via polarity.

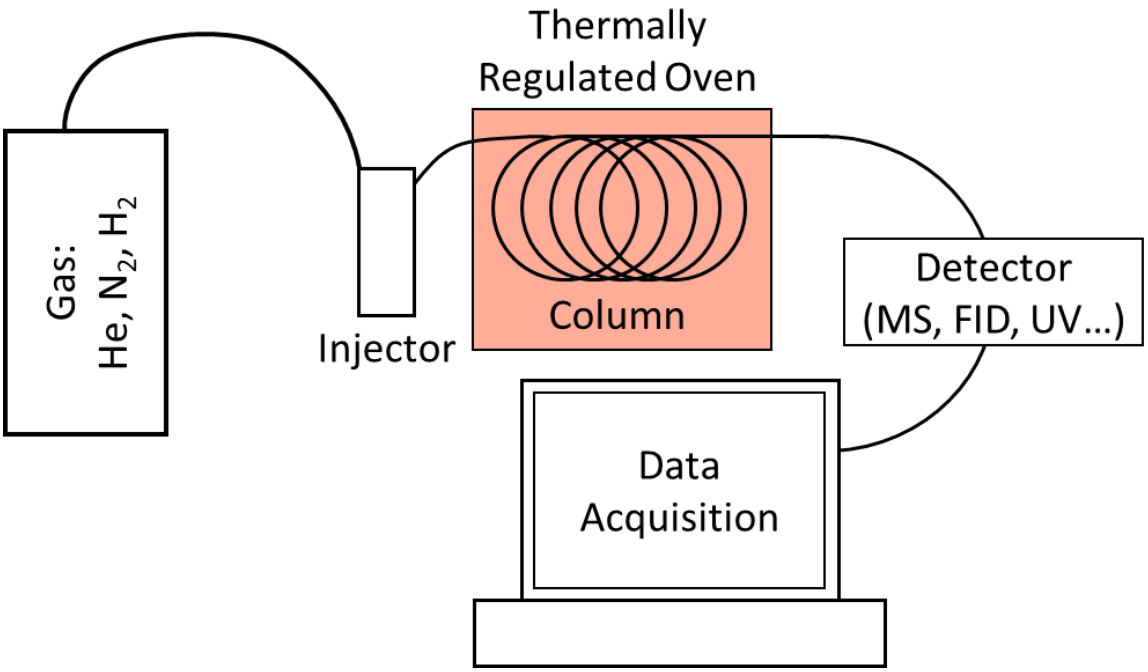

Figure 1.5. A basic schematic of a GC. GC is regarded as the "gold standard" for separation of a mixture. The core components are: gas supply, sample injector, a packed column, a detector (MS, FID, UV…) and data acquisition software.

Gas chromatography (GC) is less frequently used in continuous flow applications than HPLC [2]. GC separates analytes in a mixture based on their boiling point through a temperature ramp in the oven containing the stationary phase (Figure 1.5). Instead of a solvent as the mobile phase, inert gas is used to carry a mixture through the instrument. An injector introduces a small amount of a mixture, carried into a packed column that is frequently meters long. As the components of the mixture are separated and exit the column, they are detected via UV, FID, mass spectrometry (MS), or another detector,

generating signal proportional to concentration that is collected by data acquisition software.

These chromatographic methods yield reproducible results but can have analysis times in excess of fifteen minutes, and cycle times that approach 30 minutes. Confirmation of chemical steady state in a CFR over multiple aliquots requires an hour or more using chromatographic methods. A design of experiments (DoE) with 25 points would require more than a day to determine optimal conditions. Other validation techniques, such as spectroscopic methods, offer significant time improvements compared to chromatographic methods.

Spectroscopic Validation

Raman spectroscopy is a spectroscopic technique used to study vibrational and rotational energy states of a chemical system through inelastic Stokes scattering [19]. To create Stokes scattering, a molecule is excited via photons emitted by a laser to a virtual energy state (Figure 1.6). The majority of molecules in such a system will relax to the original ground state, emitting light at the same energy called Rayleigh scattering. A fraction of the excited molecules will relax to a higher vibrational state in the ground electronic state, producing Stokes Raman scattering at a lower frequency than the incident light. A smaller fraction of molecules will have been excited from this excited vibrational state by the laser to a virtual energy state, relaxing to ground state and emitting light at a higher frequency than the incident light, causing anti-Stokes Raman scattering. Most Raman spectroscopy is performed in the Stokes scattering regime, yielding information about the vibrational

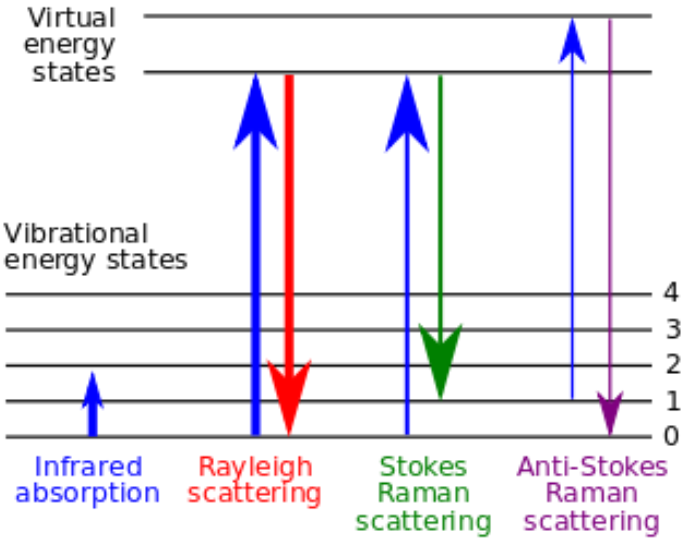

Figure 1.6. Raman spectroscopy mechanism, showing Rayleigh scattering and other vibrational mechanisms.

modes of the molecule. Typically, after a sample has been illuminated with laser light, the desired Stokes Raman scattering is collected into a fiber optic cable and passed through a spectrometer, rejecting anti-Stokes and Rayleigh scattering while the rest of the collected light is dispersed onto a detector.

Chemometrics

Deconvolution of Raman spectral data can be challenging in complex chemical systems. Chemometric tools such as principal component analysis (PCA) and partial least squares (PLS) are often used to process and analyze this spectral data quickly and effectively [20-23]. PCA is a multivariate statistical analysis method that is able to separate a series of spectra into a set of linearly uncorrelated variables called principal components. This transition is such that the greatest variance by some projection of the data lies on the first

coordinate (called the first principal component (PC)), the second greatest variance on the second coordinate, and so on. Each PC accounts for the largest amount of variability while maintaining orthoganality to all previous PCs [24]. The signal (in the case of Raman spectroscopy, the Raman response) that accounts for the most variance across the dataset (in Raman, the series of spectra) is titled the loading of the principal component. Each row of data is given a score on that loading, indicating how well the data varies along the vector of the loading. The first PC generated cannot account for all of the variation in a dataset, and subsequent PCs account for further covarying signals in the dataset. Used in tandem, Raman spectroscopy and PCA have allowed for robust process monitoring and effective process control [23,25-27].

Spectroscopy and chemometrics have also been used in tandem to quantitatively monitor batch reaction progress in real-time using PLS. This regression model technique bears some relation to PCA. Instead of constructing loadings based on maximizing orthogonal variance, it creates a linear regression model by projecting the predicted variables and the observable variables to a new matrix space. Each latent variable (compared to principal component in PCA) describes a response signal that best correlates to a measured variable. In using PLS to correlate Raman analysis with a known quantity such as % yield, this will generate a loading that best describes the set of Raman variables that correlate with % yield across the entire dataset. Model construction errors are typically calculated with root mean square error of calibration (RMSEC) and root mean square error of prediction (RMSEP). The equation for these calculations is:

$$x_{\mathrm{rms}} = \sqrt{\frac{1}{n}\left(x_1^2 + x_2^2 + \cdots + x_n^2\right)}. \qquad \text{Eq. 1}$$

where x_n represents the error between predicted and measured values in the calibration dataset (RMSEC) or the validation dataset (RMSEP).

PLS and vibrational spectroscopies have been used in conjunction to predict yield or monitor systems in numerous cases. Sivakesava *et. al.* demonstrated real-time monitoring of ethanol production using PLS and Raman spectroscopy. In this batch system, Raman spectra were used to detect reaction completion without the need for manual sampling or long HPLC analyses. Sulub *et. al.* demonstrated accurate prediction of active pharmaceutical ingredient (API) dosage in real-time using near infrared, after constructing a calibration model off-line [28]. Physical processes, such as drying of chemicals, have also been predicted in real-time as demonstrated by Peinado *et. al* [29]. Regardless of specific application, real-time PLS modeling of spectra has allowed for fast and accurate quantitative information to be acquired from batch systems. However, to apply Raman spectroscopic monitoring to a continuous flow system requires a reactor that is able to interface sensors and probes with a continuous flow path.

Reactor Construction and NeSSI

Throughout this work, univariate sensors such as thermocouples, pressure transducers and flow meters, and multivariate spectroscopies such as Raman must interface with the flow streams of CFRs. Proper sampling ensures that measurements are accurate, reproducible, and representative of the system. New Sampling/Sensor Initiative (NeSSI) sampling systems are commercially available flow components that enable users to construct custom

flow systems using interchangeable pieces. Figure 1.7 shows the components of a model NeSSI system and emphasizes the modular nature of the platform.

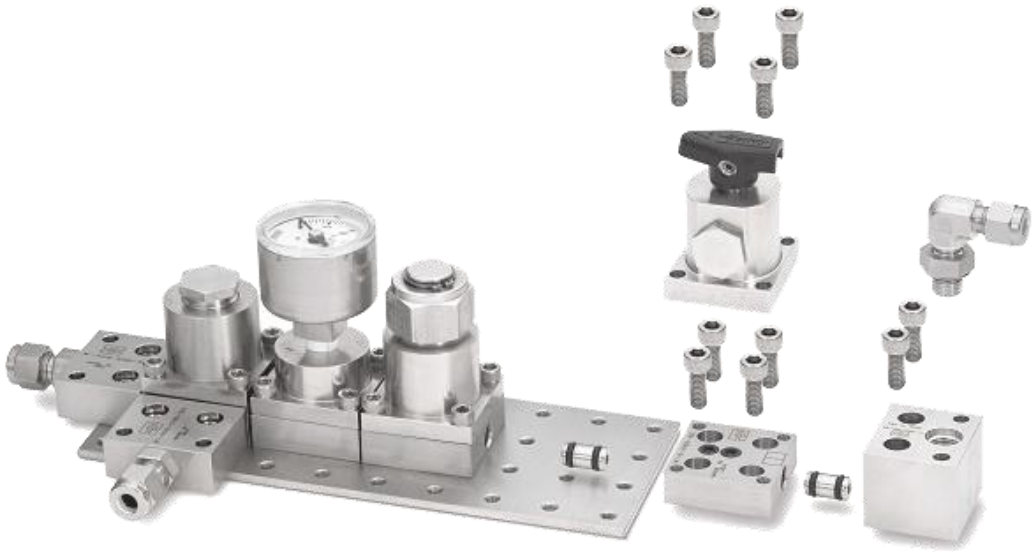

Figure 1.7. Example NeSSI sampling system and parts schematic, courtesy of Parker Hannifin, Inc. (Cleveland, OH). This schematic shows

This modularity enables rapid prototyping and development of sampling platforms for flow systems. NeSSI has been used to interface sensors with flow control systems in both fluid and gas systems [30,31], and as interfaces for continuous flow reactor analytics [31]. NeSSI as a platform has been developed to include interfaces for advanced analytics, such as immersion Raman probes. The design shown in Figure 1.8 ensures flow across the sampling tip of the probe, ensuring a well-sampled flow system. The coupling of NeSSI with appropriate process analytical technology (PAT) creates a dependable interface for the sampling of a flow channel [30,32].

Figure 1.8. A schematic of a Raman BallProbe™ interfaced with the flow channel of a NeSSI sampling piece.

In this work, the described technologies and others are combined to form a compelling case for a more thorough investigation of a chemical reaction in batch before transitioning to production-scale CFRs. In addition, this work describes how real-time modeling of product conversion via Raman spectroscopy and PLS allows for a significantly improved CFR optimization process. In Chapter 2, a proof of concept reaction is investigated in a CFR to test technologies and demonstrate the capabilities of Raman spectroscopy in continuous flow modeling. In Chapter 3, the Swern oxidation of S-1-phenylethanol is monitored in batch via Raman spectroscopy, HPLC, and GC-MS offering unprecedented mechanistic information for this reaction. In Chapter 4, a CFR is described allowing for real-time monitoring of both physical and reaction stability allowing for rapid determination of steady-state. Chapter 5 describes a redesign of the reactor from Chapter 4, taking into consideration the findings from Chapter 3 and implementing the real-time modeling developed in Chapter 2. Together, this thesis describes the application of analytical measurements and chemometrics towards the design of a chemical reaction in a CFR from information gained while monitoring the reaction in batch, and the implementation of real-time optimization in a CFR.

Chapter 2

The Esterification of Benzoic Acid

Introduction

Continuous flow reactors (CFRs) are an emerging technology that offer several advantages over traditional batch synthesis methods, including more efficient mixing schemes, rapid heat transfer, and increased user safety. [33-35] CFRs are capable of producing thousands of pounds of target chemicals through scale-out of production by using multiple parallel flow reactors. Modular scale-out eliminates extensive engineering costs associated with large volume production scale-up from a batch reactor system used for chemical development or optimization. For example, if a CFR yields 1 ton of target product per year, 100 identical, parallel systems would yield 100 tons of target product per year with no reaction adaptation required [36]. To achieve a similar increase in production using a batch reactor would require extensive engineering and adaptation to account for the changes in heat and mixing profiles at different scales.

Currently, quantitative validation of chemical synthesis on flow reactors largely requires off-line validation [10,15,16,37]. This involves acquiring an aliquot from the reactor and performing the analysis using the appropriate off-line instrumentation. The time from sample acquisition to analytical results frequently requires 10-30 minutes depending on the application and the analytical technique. Using HPLC analysis frequently requires more than 20 minutes of cycle time for each sample. This introduces a large delay between sampling from the product stream and the generation of actionable information which can lead to a variety of problems including off-specification material or unsafe reactor conditions persisting for an extended period of time. In addition, continuous sampling is often time-consuming and resource-intensive, both in solvent consumption and personnel

requirements [38,39]. Spectroscopic methods, such as NIR, IR, and Raman, allow for rapid analysis of a reaction system, provide high resolution chemical information, and have seen use in the petrochemical and pharmaceutical fields as alternative validation techniques [40-47].

Raman spectroscopy is an information rich vibrational spectroscopic method. It has previously been used for in-line process monitoring in batch and flowing systems in a variety of industries [48]. Raman spectroscopy has also been used for quantitative modeling of simple chemistry in microreactor systems using peak-height ratios [37]. Though Raman spectra contain chemical and physical information, deconvolution of spectral data is not easy in complex chemical systems that contain many Raman active species. Chemometric tools, such as principal component analysis (PCA) and partial least squares (PLS) are often used to process and analyze the spectral data quickly and effectively [20,21]. Used in tandem, these techniques allow for robust process monitoring and effective control [25-27].

Once analytical techniques have been defined, a system's performance can be tested. Design of Experiments (DoE) provides a statistically sound method of evaluating the performance of a CFR, and determining what variables can affect the chemical yield of the system. Reactions such as the Fischer esterification [12], which is highly dependent on residence time and temperature, make ideal candidates for applying DoE principles. The flow, temperature, and stoichiometry in the CFR are all readily controlled using custom control hardware and software. The Yates method [49] is a factorial design that allows for the deconvolution of contributions each of these critical process parameters (CPPs) has

towards the system's critical response factor (yield). Table 2.1 shows the process for calculating the Yates factor in a 2-factor design. In this example, YA indicates the contribution of variable A towards the response, YB indicates the contribution of variable B towards the response, and YAB indicates the combined effect of variables A and B towards the response. A full understanding of the effect each CPP has on the yield of the system allows for optimization and control [50,51].

	Factor (0 = Low, 1 = High)				
Experiment	A	B	Response	Col. 1	Yates Factor
0	0	0	R0	R4 = R1+R0	Y0 = N/A
A	1	0	R1	R5 = R3+R2	YA = R7+R6
B	0	1	R2	R6 = R1-R0	YB = R5-R4
AB	1	1	R3	R7 = R3-R2	YAB = R7-R6

Table 2.1. The Yates analysis methodology. Final calculated Yates factor indicates contribution towards response.

The main goal of this chapter is to demonstrate that Raman spectroscopy can provide real-time validated quantitative monitoring of CFRs when used in tandem with multivariate modeling. This proof of concept will be utilized in future chapters for investigation of a complex reaction. In this study, the esterification of benzoic acid was performed in a continuous flow reactor. Raman spectroscopy and DoE were used to determine the effects of the CPPs (flow, temperature, and stoichiometry) on the chemical yield of the system. PLS models were used to assess the capability of Raman spectroscopy to quantitatively determine chemical yield. The overall results demonstrate the capability of Raman

spectroscopy coupled with multivariate PLS models to quantitatively predict chemical yield in a flowing system in real-time.

Experimental

The esterification (Figure 2.1) of benzoic acid (**1**) in methanol (**2**) to methyl benzoate (**3**) was investigated in a continuous flow reactor system. Stock solutions of 1.1 M benzoic acid (Sigma-Aldrich) and 1.1 M methyl benzoate (Sigma-Aldrich) were prepared in methanol (Sigma-Aldrich). Sulfuric acid (Sigma-Aldrich) stock solutions of 0.275 M and 1.1 M were prepared in methanol. Calibration standards were prepared from the stock solutions with 20 mL of sulfuric acid and 20 mL of benzoic acid / methyl benzoate mixtures, ranging from 0% to 100% methyl benzoate, for a total of 11 calibration standards.

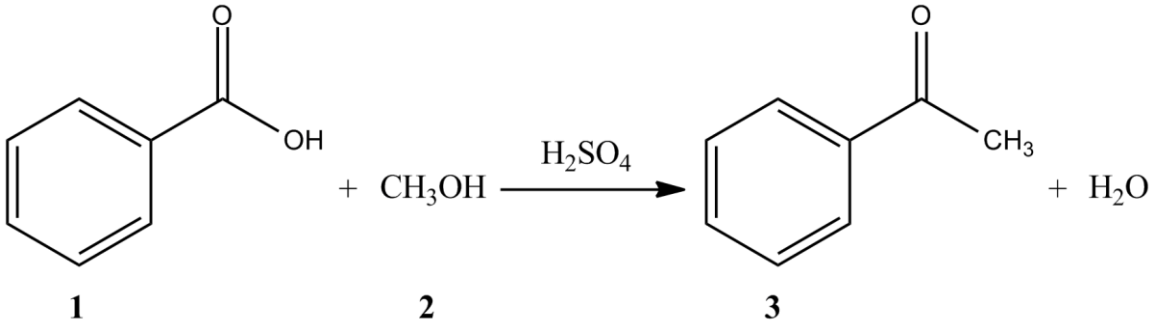

Figure 2.1. Reaction Schematic. Benzoic acid (**1**) and methanol (**2**) react in sulfuric acid to form methyl benzoate (**3**).

The continuous flow reactor system (Figure 2.2) consisted of three main components: an Intraflow NeSSI sampling system, continuous flow mixers, and on-line sensors. The Intraflow sampling system (Parker Hannifin, Cleveland, OH) contained two reagent lines

which combined to a single stream at the reactor mixing plates where the esterification occurred. The Advanced-flow™ LF continuous flow reactors (Corning Inc., Corning, NY) employed heart-shaped mixers to ensure turbulent flow throughout the reactor. Five sequential mixing plates were used with parallel flow heating. The reactor terminated in a pressure controlled Intraflow product line equipped with pressure, temperature, and flow analytical instruments.

A multichannel Raman system (Kaiser Optical Systems, Ann Arbor, MI) equipped with BallProbe™ immersion optics (MarqMetrix, Seattle, WA) was used to monitor each of the reagent lines and the product line. On-line sensors consisting of flow meters pressure transducers, and thermocouples were also employed in each of the three lines. Data from these analyzers were collected using in-house software developed in LabVIEW.

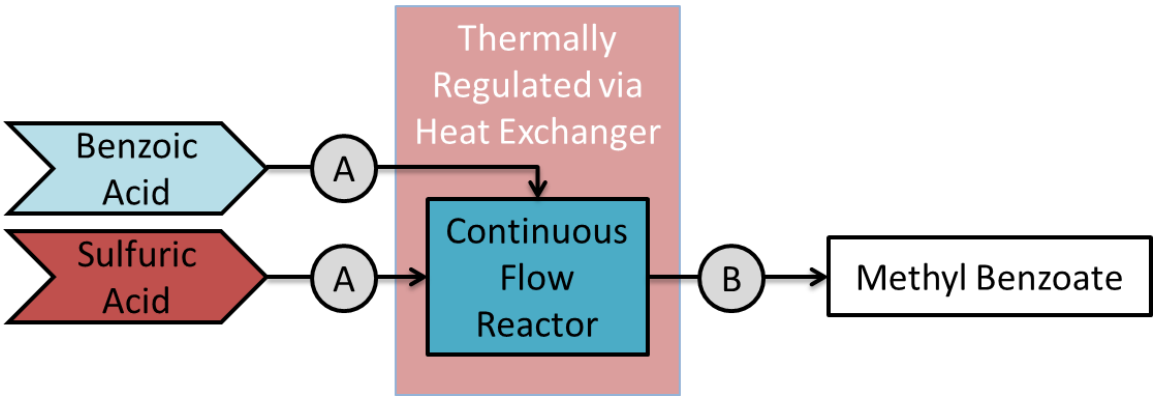

Figure 2.2. Schematic of continuous flow reactor. Each reagent line is equipped with identical suite of analytics (labeled as A) – flow meter, pressure sensor, and Raman probe – and safety valves for operator safety. The product line (B) contains a Raman probe, a pressure regulator, and a pneumatic valve to route the completed reaction material to product or to waste, depending on product quality.

In-house software developed in LabVIEW (National Instruments Corporation, Austin, TX) was also used to control the physical reaction parameters. Residence time was controlled by the flow rate of the two HPLC pumps, (Flom Co., Ltd., Tokyo, Japan) connected to each of the reagent lines. To ensure effective flow control and minimize pulsation in the reactor, the reactor was equipped with 2.0 MPa backpressure regulators (Parker Hannifin). The on-line sensors consisted of flow meters (FCI Incorporated, San Marcos, CA), pressure transducers (Heise, Stratford, CT), and thermocouples (Omega Engineering, Stamford, CT). Pressure in the reactor was maintained via a variable backpressure regulator to ensure proper mixing in the liquid phase. Reaction temperature was controlled via a Huber Tango heat exchange pump (Huber USA, Northport, NY) which supplied heat exchange fluid to channels surrounding each reactor plate.

Raman calibration was performed prior to initiating the esterification. Calibration was performed by injection of an aliquot of each calibration standard into the product line and recording the resulting Raman spectrum. Three Raman spectra of the calibration standards were collected in this fashion, each consisting of five three-second exposures, for a total of 33 calibration spectra. A separate reference sample was collected and diluted into methanol for off-line HPLC validation. All off-line samples were run using an Agilent 1100 Series HPLC (Agilent Technologies, Santa Clara, CA) using a reverse-phase column (Agilent C18 Column). The liquid chromatography was performed using two mobile phases: 0.1% acetic acid in water, and acetonitrile. A gradient of 20% acetonitrile to 95% acetonitrile over 5.5 minutes resulted in clearly defined peaks for benzoic acid and methyl benzoate. The methyl benzoate peak percentage was used to determine reaction progress.

Residence time (controlled via flow rate), temperature, and catalyst concentration were investigated to determine how each affects the product yield. A full factorial design using three factors with two levels per factor was used in conjunction with the Yates algorithm to determine which factors had the largest main total effect upon product yield. Consequently, synthesis was performed in the reactor at 60°C and 150°C, at flow rates of 1 mL/min and 8 mL/min, with 0.275 M and 1.1 M sulfuric acid. After the reactor reached a steady-state at each of the design conditions, five aliquots were collected from the product stream for off-line HPLC validation. These were paired with corresponding Raman spectra acquired in-line during the synthesis, each consisting of five three-second acquisitions, for a total of 40 validation samples.

All Raman spectra were imported into MATLAB (Mathworks, Natick, MA) for analysis and modeling. All spectra were preprocessed using a 1^{st} order baseline removal [52,53] to remove unwanted baseline variations between spectra. PCA was performed using mean-centered background corrected spectra to monitor the reaction progress (Eigenvector Research, Inc., Wenatchee, WA). A PLS model was constructed from the calibration samples to enable predictions of chemical yield through correlations between Raman signal and off-line HPLC validation data. The number of latent variables (LVs) used was determined from the total variance captured and *a priori* knowledge. Model performance was determined with the root mean square error in calibration and prediction.

Results and Discussion

The esterification of benzoic acid is an equilibrium reaction performed in reflux in batch, requiring more than an hour for full conversion to methyl benzoate. This reaction is temperature driven, and the low boiling point of methanol (65°C) results in a lengthy reaction time. Performing reflux reactions at higher temperatures through increased reaction vessel pressure in batch is infeasible due to safety considerations. In continuous flow, however, reactions can be performed at significantly higher pressures, increasing potential reaction temperatures to higher than a solvent's boiling point in atmospheric pressure. To ensure safe operating procedures, reactor conditions were investigated while performing the esterification of benzoic acid in methanol. Initial reactor testing established upper and lower levels for three design factors: residence time – as determined by flow rate, temperature, and catalyst concentration.

Reactor Optimization

Residence time ranges were dictated by reactor flow rate limitations. The reactor used for this work required total flow above 1 mL/min to maintain turbulent flow. Lower flow rates led to laminar flow, which resulted in inconsistent mixing and poor reaction progress. An upper flow limit of 8 mL/min maintained stable pressures in the reactor. Flow rates higher than 8 mL/min led to a destabilized reactor system and runaway pressures. Temperatures as high as 150°C were safely attainable while maintaining liquid phase. This temperature reduced the time required for complete product formation from 1 hour in batch reflux to

less than 5 minutes in continuous flow. This allowed for a design of temperatures, pressures, and reaction times to extend further than is possible in a batch system.

The esterification reaction was performed at each combination of low and high factor levels for a total of 8 experimental conditions (Table 2.2). Yield was determined through off-line HPLC. The factorial design experiment results indicated a direct correlation to percent yield (as measured via HPLC) across the three studied factors of residence time, temperature, and catalyst concentration. The Yates algorithm was applied to the data to find total factorial effects across these independent variables. Temperature and residence time were shown to have the strongest main total effect on the yield, while catalyst concentration was shown to have the least main total effect. As a result, subsequent experiments were performed only at the high catalyst concentration, 1.1M H_2SO_4, which resulted in yields between 0.3% and 93.8%.

Experiment	Yield (%)	Yates Factor
0	0.72	N/A
A	4.5	104
B	23.4	223
AB	70.6	75
C	0.3	57
AC	11	2
BC	51.5	45
ABC	93.8	-12

Table 2.2. Results of the Factorial Design Experiment (Yates Factor determination). Yield determined via off-line HPLC. High Yates Factor indicates that combination of variables strongly correlates to change in Yield.

Raman Investigation

Both reagent and product were Raman active, with clear and separate peaks throughout the spectrum. Methyl benzoate had strong Raman emissions at 350 cm^{-1} and 816 cm^{-1} (representing the carbonyl stretch), and benzoic acid had strong emissions at 390 cm^{-1} and 780 cm^{-1} (representing the carboxylic acid C=O stretch). Figure 2.3 demonstrates the variation throughout the spectrum as the ratio of benzoic acid (reagent) to methyl benzoate (product) is varied from 0% to 100% at 10% increments. Figure 2.3's insert shows a highly active region of interest in the Raman spectrum, clearly showing the changing peak heights

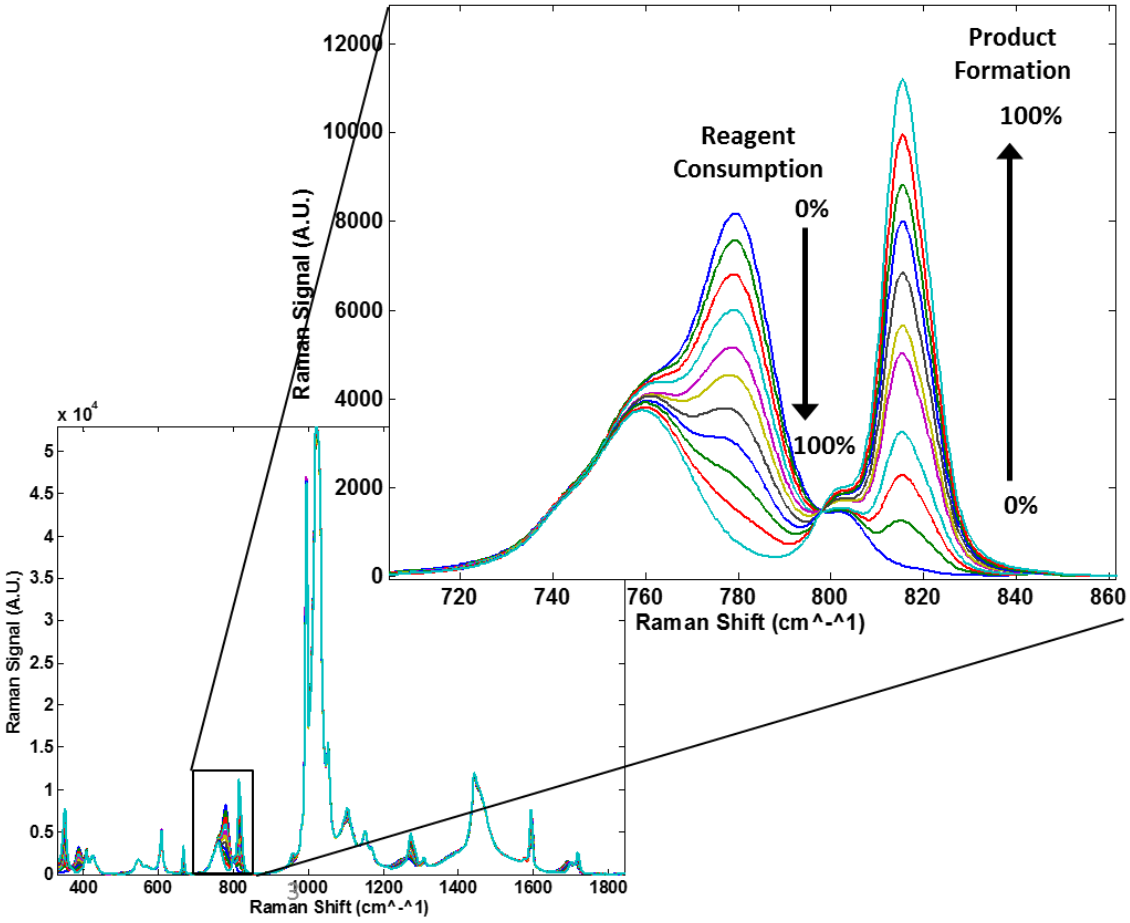

Figure 2.3. Raman spectra of 0-100% conversion standards (10% increment). Subset shown to highlight active spectral regions. Spectra have 1st order polynomial fit to maintain common baseline. Subset of spectra show the product peak for methyl benzoate is at 816 cm^{-1} and the reactant benzoic acid peak is at 780 cm^{-1}.

Multivariate Model Construction and Validation

11 calibration standards from 0% methyl benzoate to 100% methyl benzoate were prepared offline for the generation of a calibration model. Three aliquots from each calibration standard were analyzed using HPLC as a reference. Separate aliquots from each standard were injected into the product line of the reactor after the mixing plates and before the on-line sensors (Figure 2.2) to replicate measurement conditions in synthesis. Three spectra were collected of each standard, and matched to HPLC samples, for a total of 33 calibration spectra. Additionally, 20 validation samples were collected during continuous synthesis in the reactor. Once steady-state had been established in the CFR, 5 samples were collected for HPLC analysis and validation, each used to validate a Raman spectrum collected during continuous synthesis.

The 33 calibration spectra were preprocessed with a baseline variation removal technique and mean centering. The spectrum was truncated from 300 cm^{-1} to 850 cm^{-1} to include only relevant spectral information. PCA in conjunction with online Raman spectra was used to model reaction progress. Two principal components were used within the model, which accounted for 99.5% of the variation. Figure 2.4 shows the same truncated region and subset of spectra (solid lines), with the loadings of principal component one overlaid (dashed line). The positive regions of the loadings spectrum correlate to the product formation, and the negative regions correlate with the reagent consumption. This inverse correlation between the product and reactant peaks is demonstrated in the anti-correlated intensities of the PCA loadings plot shown in Figure 2.5. From these results it was concluded that the real-time Raman spectral data collected in the CFR was capable of monitoring reaction progress and could be used for product yield determination.

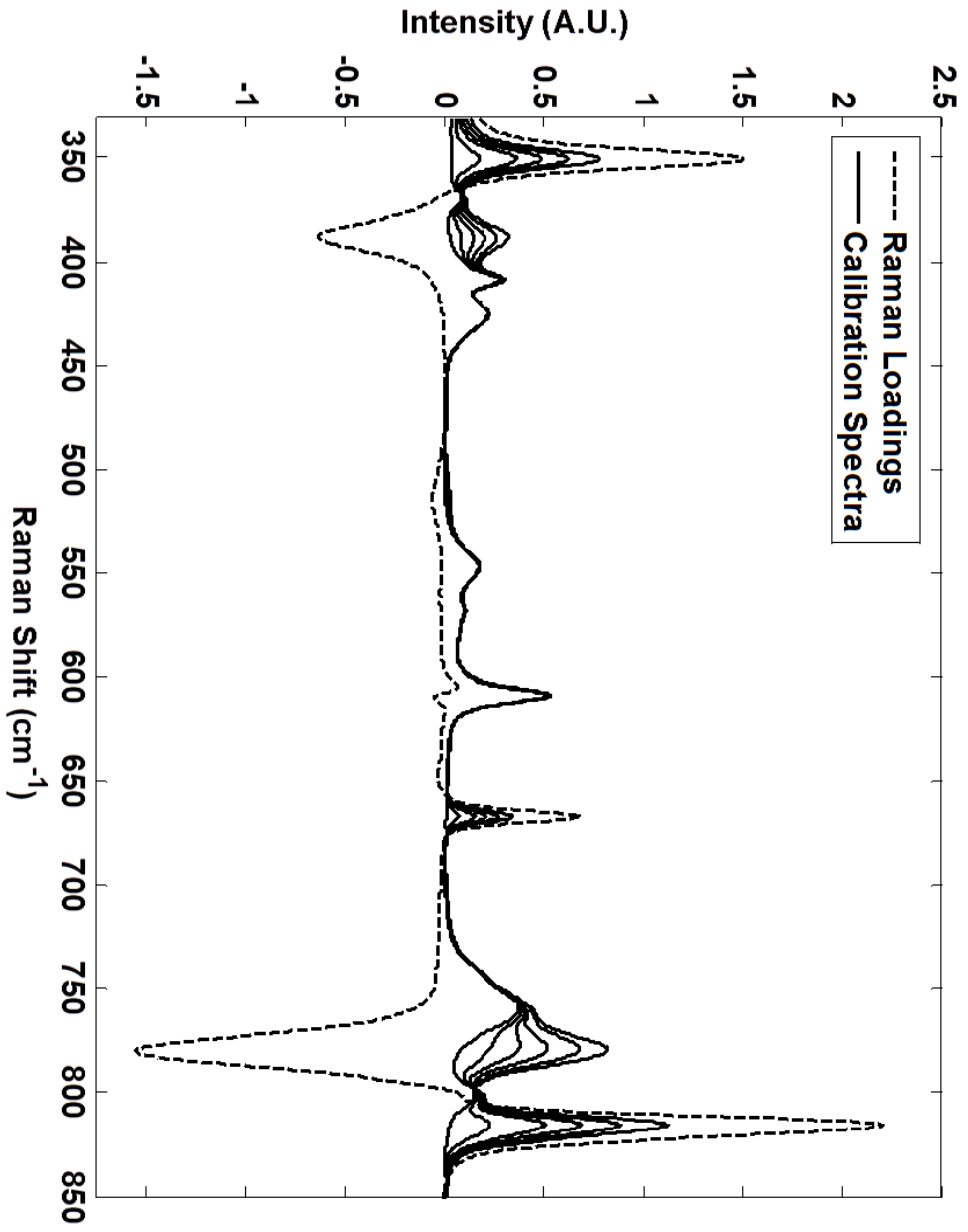

Figure 2.4. Raman calibration standards (solid line) with the loadings plot from principal component 1 (dashed line) overlaid. Negative loadings indicate the regression of a peak, positive loadings indicate peak formation in this figure.

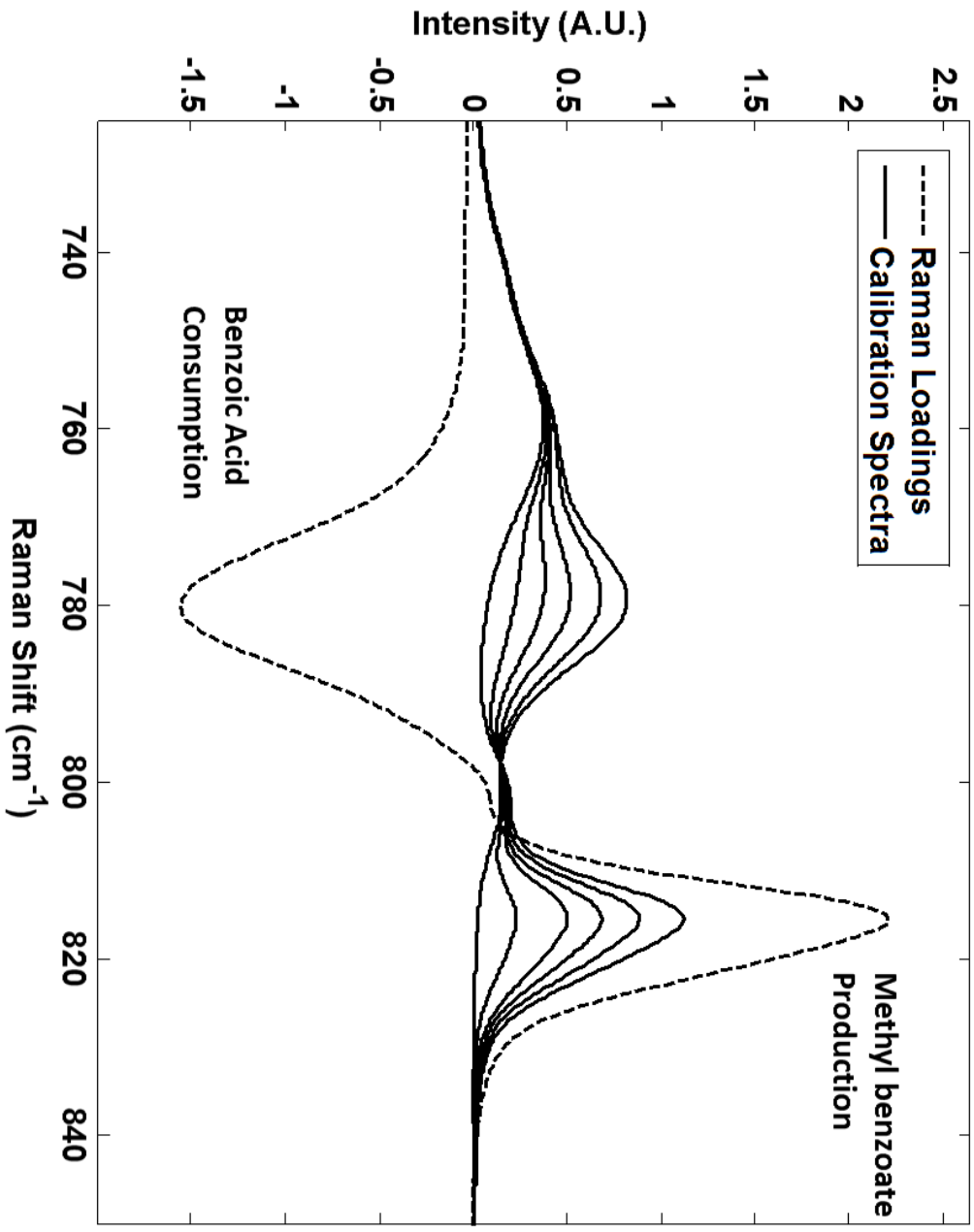

Figure 2.5. Subset of Fig. 4, illustrating the active Raman spectral region containing the benzoic acid and methyl benzoate C=O peaks. Inverse correlation of the loadings plot (dashed line) indicates the production of methyl benzoate (peak at 818cm^{-1}) and consumption of benzoic acid (peak at 780 cm^{-1}).

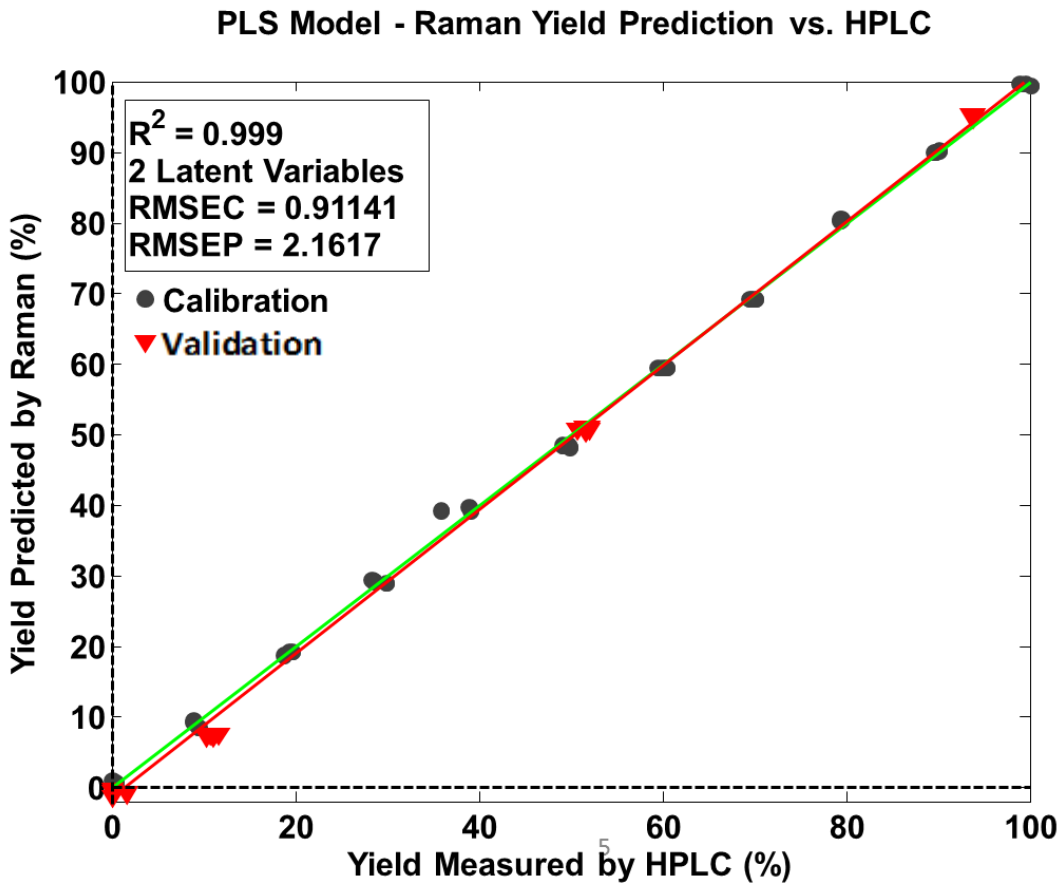

Figure 2.6. Partial Least Squares (PLS) regression model of percent conversion to methyl benzoate measured (via HPLC) versus predicted (via Raman). Calibration samples were prepared offline, validation samples were collected online during the esterification reaction.

The success of the initial modeling lead to the development of a PLS calibration model that would allow direct prediction of product yield. The calibration model was constructed using the 33 spectra collected offline (Figure 2.6, black circles) and corresponding HPLC reference measurements. Two latent variables were included within the calibration model that captured 99.7% of the variance. The RMSEC of the model was 0.9% yield. The calibration model was applied to a series of test spectra collected during a reaction to determine product yield, (Figure 2.6, red triangles). The RMSEP prediction error of the model was determined to be 2.1% yield. The strong agreement between the calibration and

prediction datasets resulted in a low prediction error. This demonstrated that calibration standards can be prepared offline and used to predict yield online in a CFR.

Real-Time Monitoring of Product Formation

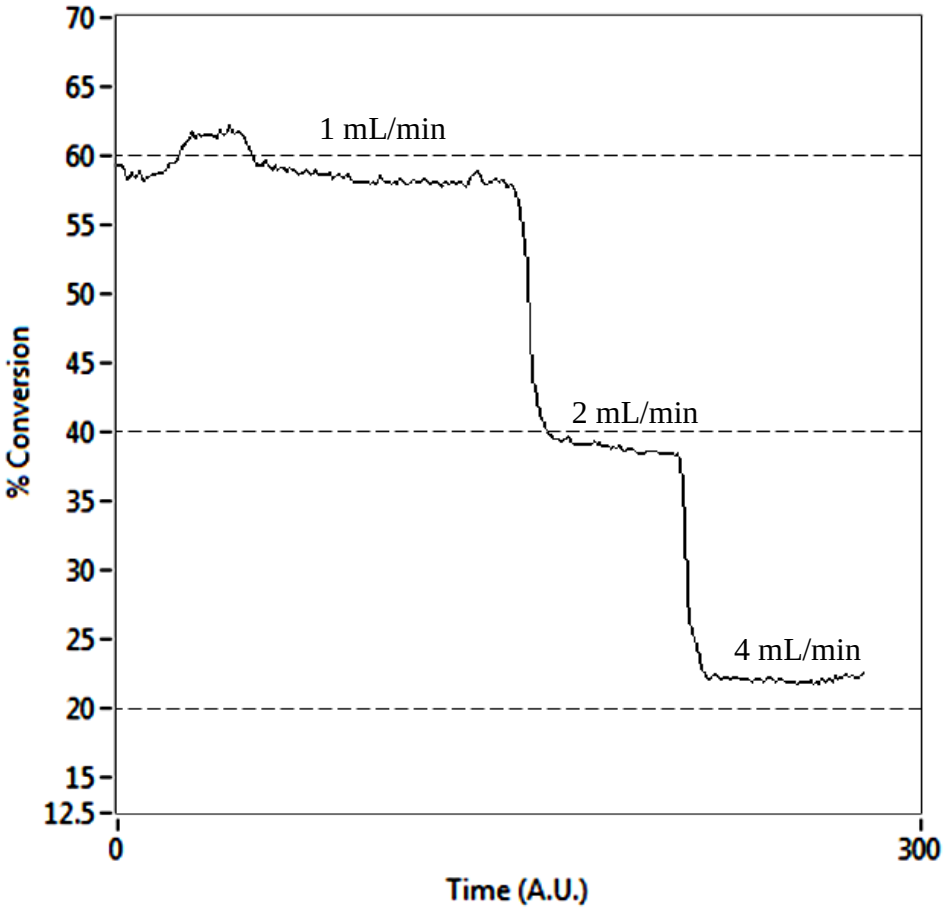

Figure 2.7. Real-time trace of % conversion of methyl benzoate at three different flow rates.

After the PLS model construction, an experiment was performed in the reactor to demonstrate real-time monitoring of product yield. While maintaining a constant

temperature of 150°C, the total flow rate was stepped from 1 to 2 to 4 mL/min. Aliquots were taken as soon as the reactor was confirmed to be at equilibrium. Figure 2.7 is a screen shot that shows the real-time predicted yield at each flow rate, as displayed in the control software. This real-time information was updated every 15 seconds, and allowed for rapid, accurate determination of % yield in the CFR. The PLS validation model was found to have a prediction error of 1.2% yield (Figure 2.8, red triangles) after HPLC analysis of the design point samples. This conclusively demonstrated the ability to accurately model a simple, one-step chemistry in real-time using Raman spectroscopy.

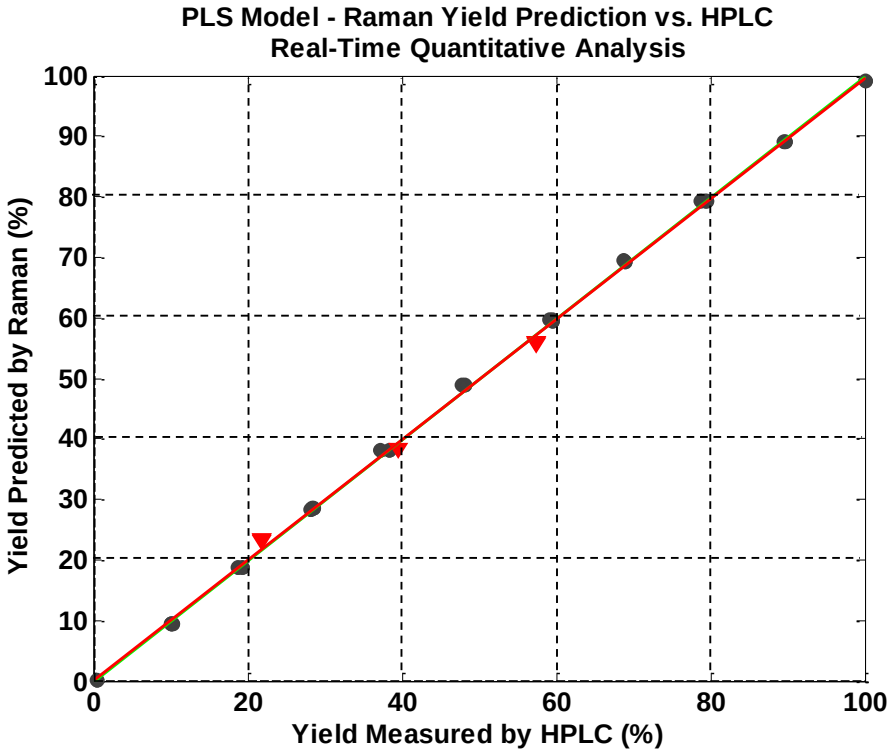

Figure 2.8. PLS validation of real-time monitoring of the esterification of benzoic acid. Red triangles represent aliquot samples taken from CFR. Calibration model is the same as Figure 2.6.

Calibration samples prepared off-line allowed for easy model construction and calibration. The in-line Raman predictions occurred every 30 seconds, offering a significant speed improvement compared to HPLC aliquot preparation. Real-time optimization provided a significant advantage over batch chemistry by minimizing optimization time, mitigating waste, and reducing thermal loss. The optimization and control of product yield through the use of online PAT and multivariate modeling also provides the potential for real-time release testing in highly regulated industries where product quality is essential.

Conclusions

In this chapter, the esterification of benzoic acid was investigated in continuous flow. This model chemistry confirmed the capability of Raman spectroscopy to monitor chemical reactions. Raman spectroscopy was then used to create a PLS model predicting conversion to product. Of particular interest the model was capable of being constructed using prepared standards. The model accurately predicted yield of methyl benzoate, and was deployed in the control software for real-time quantitative conversion in the continuous flow reactor. This investigation of a simple system served as a proof of concept for integrating Raman into a continuous flow reactor and predicting yield in real-time. Later chapters will expand on these techniques for a more complicated reaction: the Swern oxidation of S-1-phenylethanol.

Work from this chapter was published in the Journal of Pharmaceutical Innovation in 2012 [31].

Chapter 3

The Moffat-Swern Oxidation of S-1-Phenylethanol in Batch

Introduction

The Moffat-Swern Oxidation

The Moffatt-Swern oxidation [54] is a multistep, versatile, metal-free reaction by which alcohols are transformed into aldehydes and ketones (Figure 3.1). The oxidation requires low temperatures (-70°C) due to the highly exothermic production of intermediates. In addition, the intermediates – a trifluoroacetoxydimethylsulfonium salt (**3**) ("intermediate 1") and an alkoxydimethylsulfonium salt (**5**) ("intermediate 2") – are very reactive, posing a risk of thermal runaway should the temperature raise too high. van der Linden et. al. [18] describe the process:

> "The exotherm causing the runaway can be attributed to the Pummerer rearrangement of intermediates **3** and **5** which takes place above-30°C and leads to the formation of trifluoroacetoxymethyl methyl sulfide (**7**) and methylthiomethyl ether (**8**), respectively. The trifluo-roacetoxymethyl methyl sulfide (**7**) can subsequently react with benzyl alcohol to benzyltrifluoroacetate (**9**) ["side-product 9"] under the basic conditions after the quench. Obviously the uncontrolled decomposition of intermediates **3** and **5** is also detrimental to the yield of the process."

Trifluoroacetic anhydride (TFAA) as an electrophile for activation of DMSO was first tried unsuccessfully in room temperature by Albright and Goldman in 1965 [55]. Swern et al. proved later that the TFAA activated DMSO is stable at low temperatures and can be used successfully in oxidation of alcohols [56]. DMSO (1) and TFAA (2) in DCM react at low temperatures to form intermediate 1 (**3**). This compound can form a white precipitate [54], and is only stable below -30 C [57]. Above this temperature, intermediate 1 (**3**) can

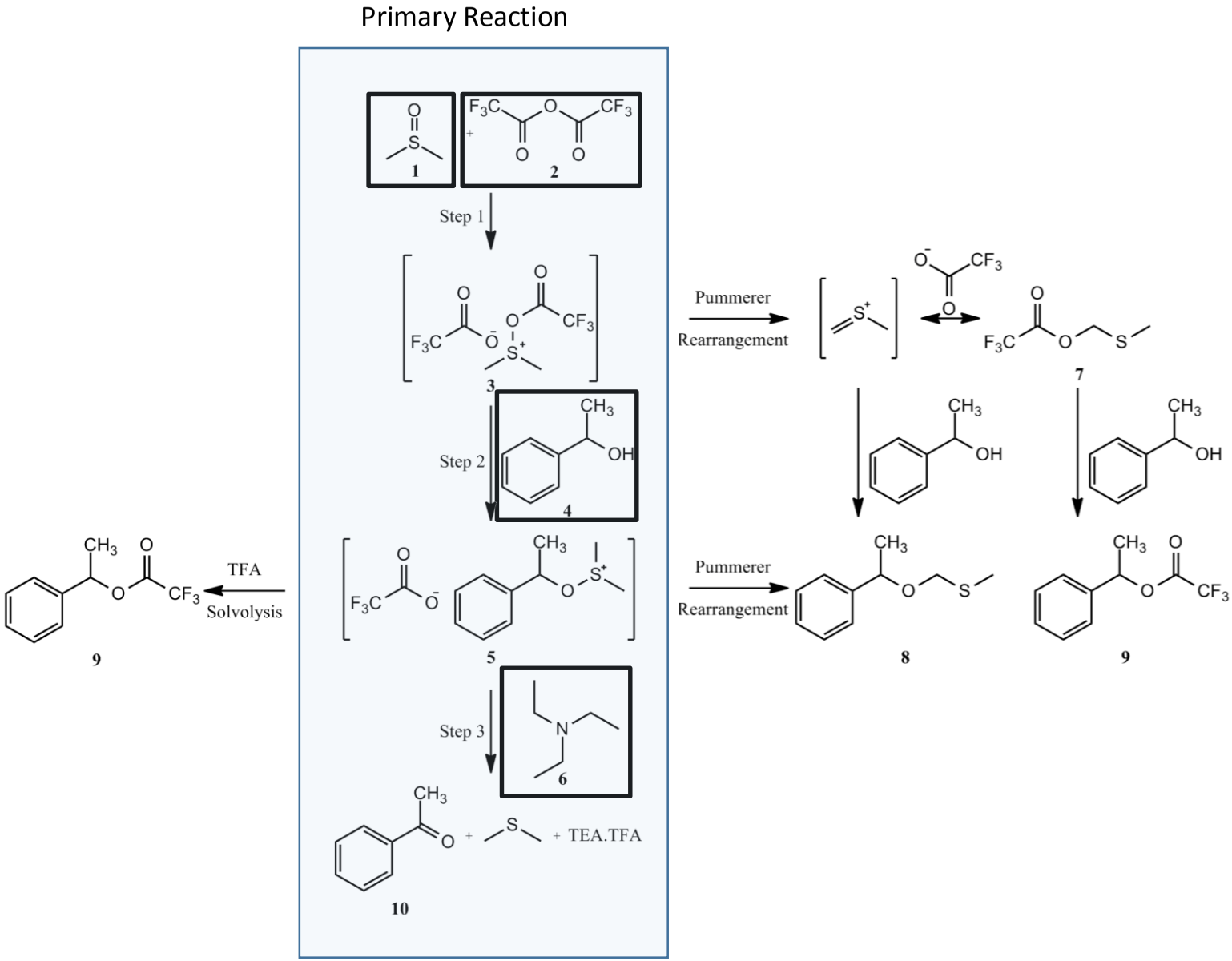

Figure 3.1. The Swern Oxidation. In the primary reaction pathway, DMSO (**1**) reacts with TFAA (**2**) to form intermediate 1 (**3**) quickly. S-1-phenylethanol (**4**) then reacts with intermediate 1 to form intermediate 2 (**5**). TEA (**6**) quenches the reaction, resulting in product acetophenone (**10**). Possible side-products include **8** and **9** through Pummerer rearrangements or solvolysis.

undergo a Pummerer rearrangement reaction and form methylthiometyl trifluoroacetate (**7**). In the presence of base, (**7**) can experience a base catalyzed alcoholysis with (**4**) to form the trifluoroacetate (**9**), referred to as side-product **9** hereafter.

In the absence of the Pummerer rearrangement occurring, intermediate 1 (**3**) reacts as desired with 1-phenylethanol (**4**) to form intermediate 2 (**5**), with the free electron pair on the hydroxyl group of (**4**) attacking the positive charge on the sulfur on (**3**). Trifluoroacetate is cleaved off together with the excess hydrogen on the hydroxyl. If intermediate 2 (**5**) is subjected to room temperature in an acidic environment it will solvolyse to sec-phenethyl trifluoroacetate (**9**) [56]. Swern's 1978 paper [54] established the formation of intermediate 2 (**5**) via intermediate 1 (**3**) as "extremely fast irrespective of reaction temperature, at least down to -70°C."

Adding the base triethylamine (**6**) (TEA) to (**5**) will deprotonate one of the methyl groups attached to sulfur on (**5**) to form an ylide (metylcarbanion). The ylide can now collapse by intermolecular hydrogen transfer to form the carbonyl product (**10**) and dimethylsufide. The ylide may also collapse in a Pummerer style side reaction into a methylmethylensulfonium ion and an alkoxide. The alkoxide ion can either receive a proton reform the alcohol, or recombine with the methylmethylensulfonium to form the side-product sec-phenethyl methylthiomethyl ether (**8**) ("side-product 8").

Analytical Investigation

Raman spectroscopy has previously been shown to be an effective tool for monitoring batch processes. For example, work by Svensson *et. al.* monitored the synthesis and hydrolysis of ethyl acetate [58]. First-order rate constants were determined for the hydrolysis reaction, yielding strong agreement with literature values. Lee et. al. obtained similar results while monitoring imine synthesis with Raman spectroscopy [59]. Physical processes, such as crystallizations, have also been monitored with Raman spectroscopy, as demonstrated by Hu et. al.'s identification of flufenamic acid polymorphic forms [60]. In these and other examples, Raman spectroscopy allows the user to understand what is occurring in a batch system at a near real-time rate.

High performance liquid chromatography (HPLC) and gas chromatography – mass spectroscopy (GC-MS) are popular, widespread tools used for characterization of reactions in almost every modern application [19]. HPLC is the standard for most quantitative determination in both research and industrial environments as many compounds are readily separable by polarity differences and are already in the liquid phase. The oxidation of S-1-phenylethanol to acetophenone is a particularly well-suited chemistry for HPLC analysis, as alcohols and ketones have notably different polarities due to the alcohols' hydrogen bonding abilities. The potential side-products **8** and **9** are also quite different in polarities from reagent and product, allowing for well-defined separation of all anticipated compounds from the reaction.

GC-tandem mass spectroscopy (GC-MS) is occasionally used for determining species present in a post-reactor mixture. GC-MS is an analytical method that separates a mixture via GC and uses MS as a detection method to identify the separated analytes. Mass spectrometry is a detection method that produces spectra of the masses of the molecules comprising a material by ionizing chemical compounds to generate charged molecules. The charged molecules and their fragments are measured via their mass-to-charge ratio, creating spectra that are used to determine the chemical structure of molecules. GC-MS has been widely heralded as a "gold standard" [19] for identification of substances in a mixture. It is particularly useful in situations where a large matrix of compounds is present in unknown quantities, and standards are not easily obtained.

In order to intelligently design a reaction for continuous flow (see Chapter 1), the batch reaction must be well-understood and characterized. In addition, the viability of the reaction in continuous flow with real-time Raman analysis developed in Chapter 2 requires confirmation of Raman activity over the course of a reaction. In this chapter, the Moffat-Swern oxidation, also referred to as the Swern oxidation, is investigated in batch with Raman spectroscopy and chromatographic methods, yielding mechanistic understanding that will inform later CFR design. A reaction vessel is utilized to monitor the oxidation, revealing that product formation in Swern oxidations does not occur at an appreciable rate until temperatures are above -30°C, contradicting previously established mechanisms. This is confirmed via off-line HPLC analysis, and multivariate statistical analysis of the Raman spectra. In addition, the formation of intermediates is discovered to occur at rates counter to literature canon, and a new mechanism for side-product formation is also proposed. All of

this information results in a well-understood chemical system prepared for translation to continuous flow.

Experimental

Batch Apparatus

An apparatus was constructed to deliver chemicals in a controlled, reproducible environment (Figure 3.2). A 50 mL 3-neck round-bottom flask was immersed in a dry-ice acetone bath, maintained at under -70°C for the duration of the experiment. A novel 1/8" O.D. Raman immersion probe (MarqMetrix, Seattle, WA) monitored spectral changes in the flask by collecting spectra every 15 seconds. Thermocouples measured temperature in the reaction vessel and the acetone bath every second. Temperature information was recorded via LabVIEW software (National Instruments Corporation, Austin, TX). The apparatus also consisted of a 20 mL syringe pump, feeding chemicals via a syringe and 1/8" Teflon tubing, through a Corning LF Mixing plate (Corning, France) into the three-neck round-bottom flask. The cooling plate was maintained at a temperature of -20°C via a heat exchange pump (Huber Tango, Huber).

Swern Oxidation Procedure

All reagents were added at 0.5 mL/min for 4 minutes (2mL total volume). 2 mL of dichloromethane (DCM) solvent (Sigma) were initially added to the vessel. After reaching a steady temperature at t=10min, 2 mL of 2.4M dimethyl sulfoxide (DMSO) in DCM

(Sigma) was added to the reaction vessel, and allowed to reach a steady temperature. 10 minutes after the DMSO addition, at t=20min, 2 mL of 2.0M trifluoroacetic anhydride (TFAA) in DCM (Sigma) was added to the reaction vessel. During this exothermic addition, the temperature in the reaction vessel did not exceed -40°C. 10 minutes after the TFAA addition, 2 mL of 2.0M S-1-phenylethanol in DCM (Sigma) was added. After 10 further minutes, at t=40min, 2 mL of 3.6M TEA in DCM (Sigma) was added to quench the reaction. At t=60min, the vessel was removed from the acetone bath. 20 minutes later, at t=80 min, the vessel had reached room temperature.

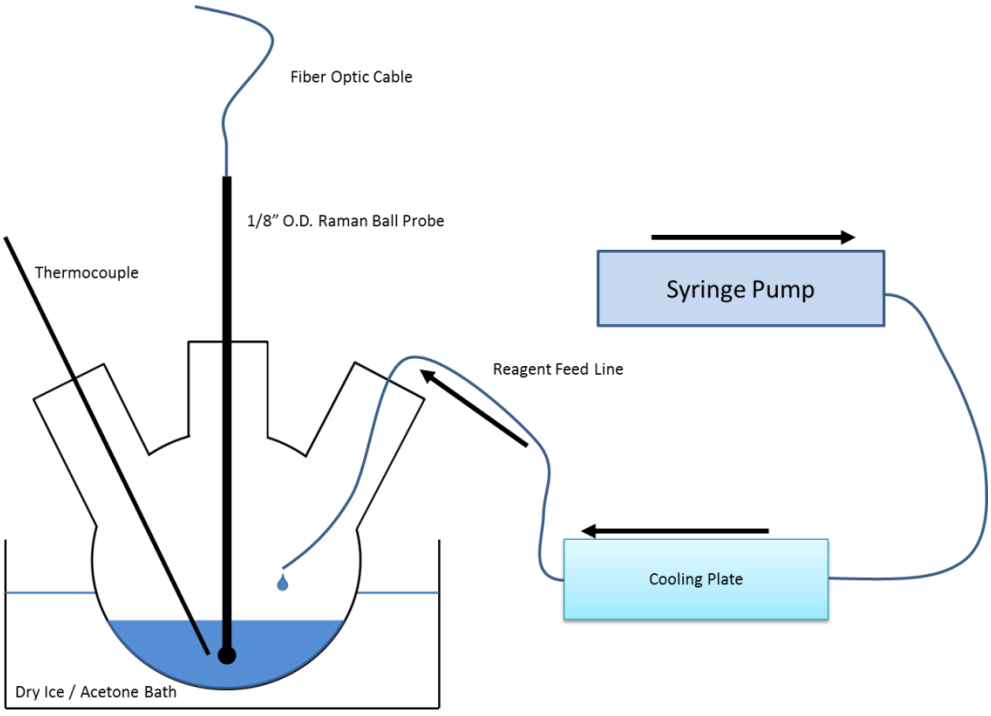

Figure 3.2. A schematic of the reaction vessel designed for this experiment. Key design principles include: reproducible and consistent additions of chemicals via syringe pump; pre-cooled reagent to reduce possibility of intermediate decomposition; temperature monitoring to validate temperatures in reactor; and Raman BallProbe™ designed for monitoring small-volume reactions. Each chemical addition was performed by timed syringe pump additions of 0.5 mL/min for 4 minutes.

Chromatographic Analysis

Through the warming period from t=60min to t=89min, 0.1mL aliquots were taken from the vessel and diluted into DCM for HPLC analysis. All samples were analyzed on an Agilent 1100 Series HPLC (Agilent Technologies, Santa Clara, CA) using a reverse-phase column (Agilent C18 Column). The liquid chromatography was performed using two mobile phases: 0.1% acetic acid in water and acetonitrile. A constant flow of 5% acetonitrile for 2 minutes, then a gradient of 5% acetonitrile to 95% acetonitrile over 5.5 minutes, followed by 2 minutes constant flow resulted in clearly defined peaks for S-1-phenylethanol (**4**), acetophenone (**10**), and side-products **8** and **9**. Acetophenone peak area, compared to reagent and side-products peak areas, was used to determine reaction progress. Aliquots were also investigated via 5973A GC-MS (Agilent Technologies, Santa Clara, CA) to confirm chemical structure and presence. Separations were performed on a model 6890A GC and Agilent DB-5 20m x 0.18mm x 0.4µ column. Oven temperature maintained at 50°C following an injection, then ramped at 10°C/min to 120°C, and finally ramped at 30°C/min to 250°C for a total runtime of 16.33 minutes. The quadrupole MS acquired from mass 50 to 250, at 6 scans per second.

Raman Analysis

Raman spectra were acquired every 15 seconds, with five 1-second acquisitions, on a Kaiser RXN4 (Kaiser Optical Systems, Ann Arbor, MI). Raman data was interpreted in MATLAB 7.5 (Mathworks, Natick, MA). All spectra were preprocessed using a first order baseline removal algorithm to remove variations between spectra. Selective regions were

used for intermediate formation and consumption upon determined correlation with theory and chromatographic analysis. Reaction analysis occurred via peak-monitoring of intermediates, side-products, and products. A PCA model was constructed using PLS Toolbox (Eigenvector Research Inc., Wenatchee, WA), correlating the final 30 minutes of Raman information with 30 HPLC samples taken during the warming period.

Results & Discussion

Chemical reactions are typically translated to continuous flow via a direct conversion of optimized batch reaction steps. This is discussed in Chapter 1, and further discussed in Chapter 5. A central argument in this thesis is the importance of thorough understanding of a reaction before translation to continuous flow. Beginning in this chapter with a Raman investigation of the Swern oxidation, the information gained will inform a reactor design (discussed in chapters 4 and 5) deviating from typical continuous flow reaction design, resulting in a significantly improved continuous flow reactor system.

Swern Oxidation

A reaction system (Figure 3.2) was designed to ensure steady and reproducible additions of reagents to a three neck round-bottom flask. It also allowed for temperature and Raman measurements to be obtained inside the reaction vessel continuously without significantly affecting the reaction. Due to the highly unstable nature of intermediates **3** and **5**, as well as the exothermic reaction between DMSO and TFAA to form intermediate **3**, great care was taken to ensure temperature stability in the reactor. Literature sources [17,18], along with

unreported experiments, indicated that temperatures above -30°C result in poor product conversion (below 10%) due to decomposition of these intermediates. All reagent additions were pre-cooled to -20°C via a mixing plate, and added to the reactor at 0.5 mL/min. The recorded temperature data (Figure 3.3) confirms that the temperature inside the reactor vessel did not exceed -40°C upon addition. In total, the precautions taken ensured that the information recorded was representative of a reaction without the same instrumentation in the vessel.

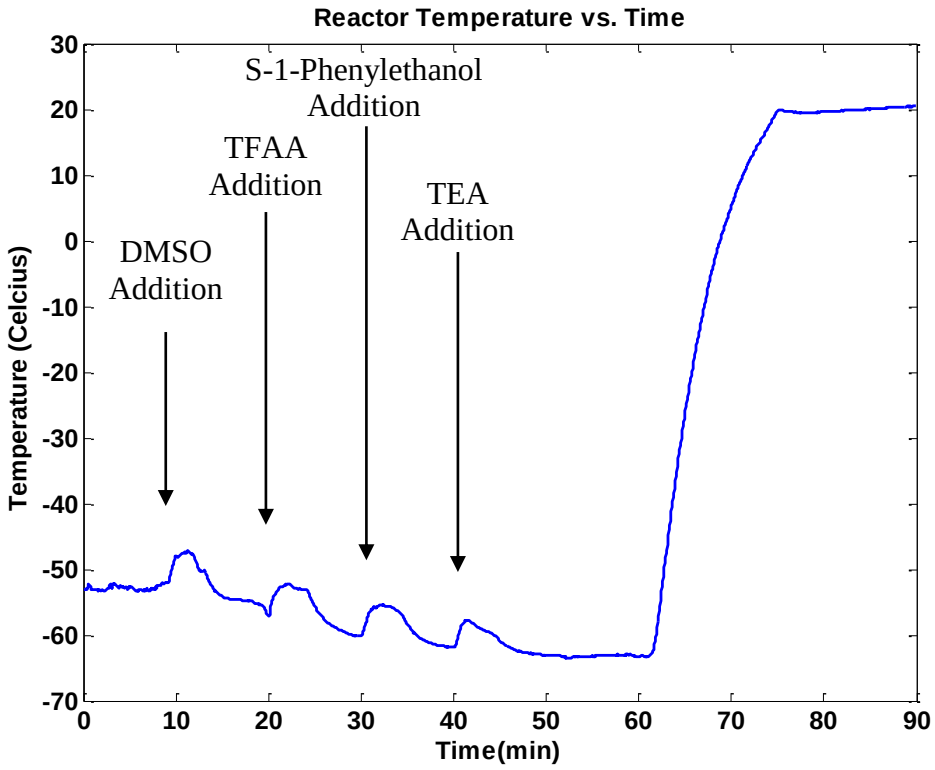

Figure 3.3. Reactor temperature versus time of reaction. Additions of chemicals occurred at 10, 20, 30, and 40 minutes. The batch reactor was removed from the dry ice / acetone bath at 60 minutes.

The chemical system was analyzed via three separate analysis methods to ensure for accurate understanding of the reaction. Raman spectra were acquired every 15 seconds throughout the entire experiment, from initial additions to after the warm-up period (60-90 mins). Aliquots were taken every minute during the warm-up period for analysis via both HPLC and GC-MS. These analysis techniques allowed unprecedented insight into the exact mechanisms occurring in the batch reactor, but occasionally yielded contradictory information. Taken as a whole, however, they offered near-complete picture of what is occurring throughout the Swern oxidation of S-1-phenylethanol, and yielded valuable information that informed the continuous flow reactor design in Chapter 5.

HPLC Analysis

Swern oxidation yield is typically validated with HPLC post-reaction [17,18]. Using peak areas from HPLC analysis, Figure 3.4 tracks the formation of product and side-product over the 30 minutes of warm-up, in addition to side-product formation and unreacted reagent. HPLC aliquots taken during the post-reaction warm-up phase (60 to 90 minutes) demonstrate that while the reaction is still cold, after the TEA quench has been added, minimal product has formed. The amount of product found in solution stays constant for over four minutes until the vessel begins warming up more. Importantly, product formation accelerates after temperatures exceed -40°C, and continues until the vessel reaches room temperature. Final product formation, as determined by HPLC, peaks at 70% conversion. The amount of product detected in the final solution slowly decays afterwards. This is believed to occur due to solvolysis via methanol solvent in the prepared HPLC samples[18]. The yield obtained is also lower than has been obtained elsewhere [18].

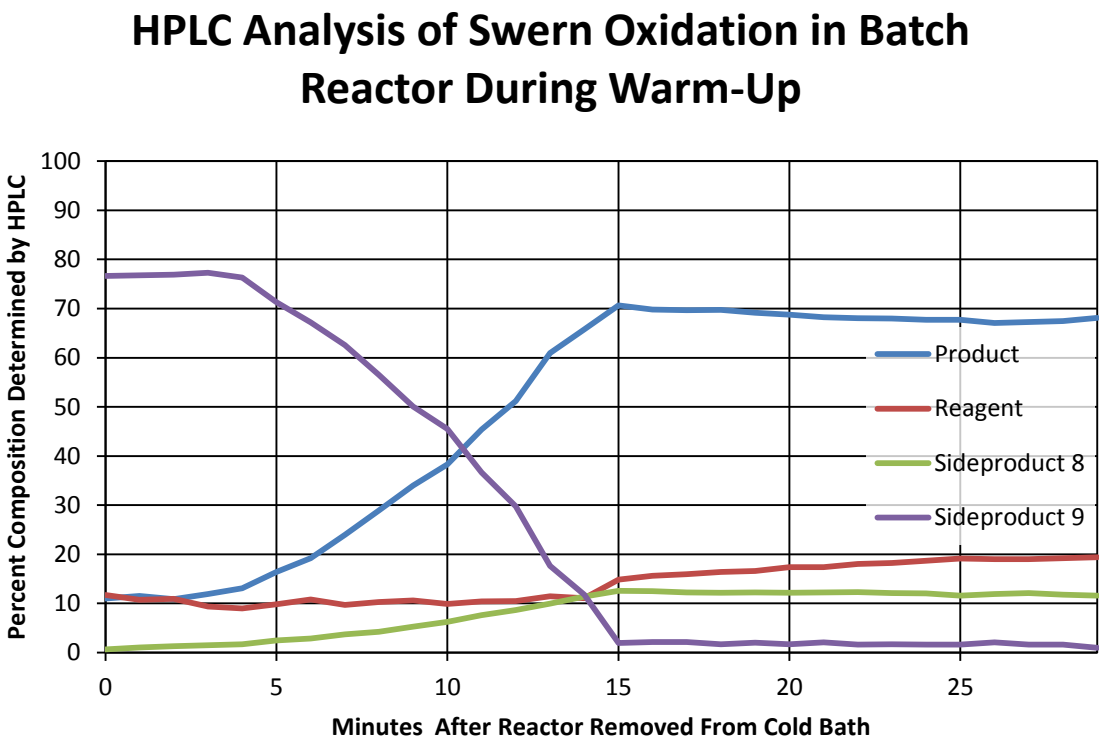

Figure 3.4. HPLC analysis of reaction mixture during 30 minute warm-up period. Acetophenone product formation accelerated approximately 4 minutes after the reactor was removed from the dry ice and acetone bath. Side-product (**9**) decreasing represents the consumption of intermediate 2 (**5**).

This may be attributed to the presence of the Raman immersion probe and thermocouple in the reaction bath. These metal probes conduct heat and possibly resulted in localized elevated temperature. Regardless, maximizing yield of the reaction was not a primary objective for this investigation.

Side-product **9**'s decreasing concentration in HPLC analysis could be interpreted either as the amount of side-product present in the reaction vessel, or as an amount of side-product formed during the preparation of HPLC samples for analysis. In a future section, Raman analysis will reveal which of these cases is taking place in the reactor.

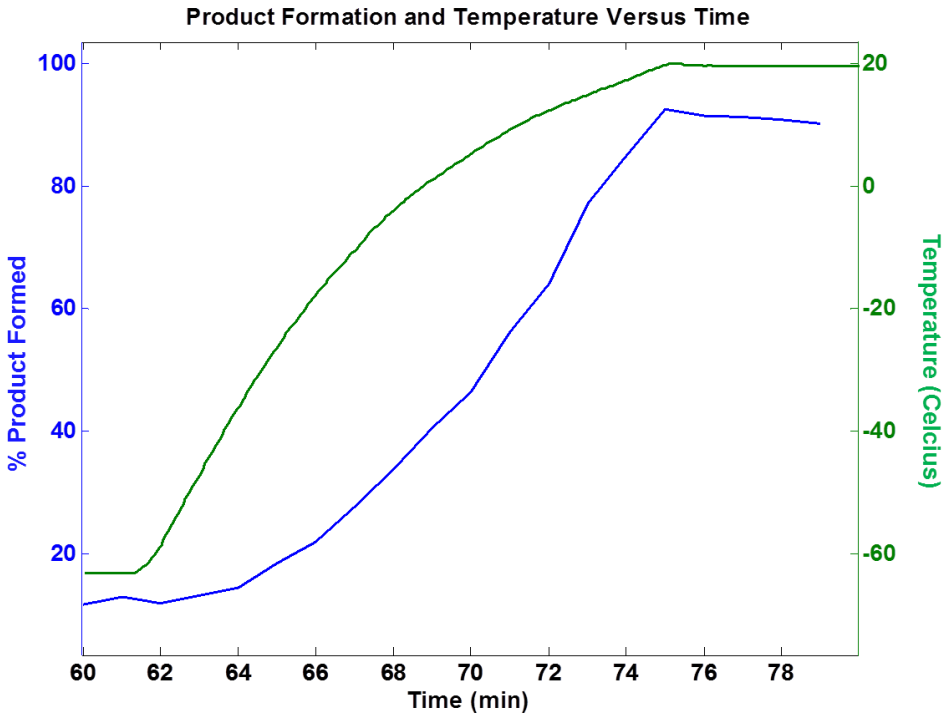

Figure 3.5. Temperature of reactor (green line) versus product formation as determined by HPLC (blue line). TEA quench (**7**) was added at time = 40 minutes, resulting in minimal product formation. Only upon the warming of the reactor does product formation occur.

Figure 3.5 shows the relationship between only product formation and reactor temperature. Beginning at time = 60, the reactor is removed from the dry ice / acetone bath. Only after the temperature reaches above -40°C does product formation occur at an appreciable rate. Product formation ceases after ~ 15 minutes outside of the cryogenic bath.

GC-MS Analysis

GC-MS analysis was also performed on the same aliquots obtained during post-reaction warm-up. This served two purposes: a) to determine mixture composition and correlate HPLC peaks, particularly for compounds which do not contain readily available references; b) independent confirmation of mixture composition. Figure 3.6 shows the chromatogram

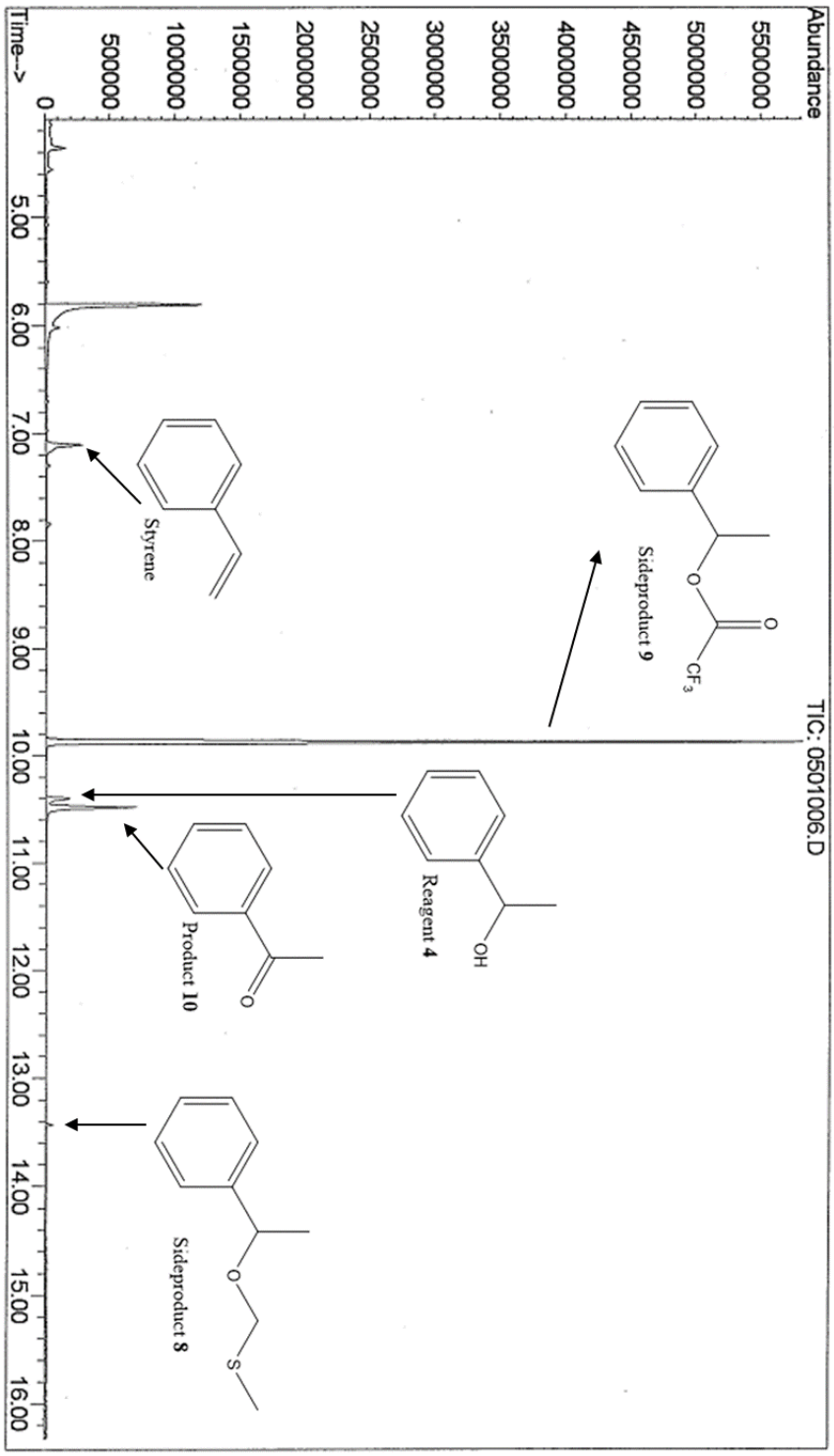

Figure 3.6. Representative chromatogram from GC-MS analysis. Aliquot taken from reactor 5 minutes after removal from dry ice / acetone bath.

from GC analysis, with multiple peaks labeled via MS analysis. Figure 3.7 shows the mass spectrum for the peak at 7.1 minutes in the chromatogram, an unexpected side-product not found in literature. Analysis of the spectrum via assigning fragments, as well as literature comparison, [61] identifies the extra side-product as styrene. A proposed mechanism for the formation of styrene is discussed later in this chapter. Figure 3.8 shows GC-MS composition, calculated by % area of chromatogram. Styrene appears to follow the same trajectory as side-product 9, and is not present at completion of reaction.

Intermediate 2 (**5**) is not observed in GC-MS or HPLC. However, side-product **9** and styrene are found (at a ratio of 19:1) in quantities that intermediate 2 (**5**) is expected. Literature indicates that intermediate 2 can be converted to (**9**) by solvolytic attack by trifluoroacetic acid at warm up, and can only happen in acidic conditions [54,56]. However, this pathway happens after base (TEA) has been added. A possible explanation for this is that as the aliquots are collected for chromatography analysis they are immediately diluted by a factor of 10 into room temperature solvent. This may have a severe impact on the rate-limiting first step of the formation of product; namely the deprotonation by of one of themethyl-hydrogens of intermediate 2 (**5**) by TEA. This deprotonation occurs at a second order kinetic rate, conveyed by the following equation:

$$rate = k1 * [base] * [IM2]. \quad \text{Eq. 2}$$

A 10x dilution of the solution (TEA and intermediate 2) results in a 100-fold rate decrease. competing spontaneous dissociation of intermediate 2 (**5**) into a stable benzylic carbocation

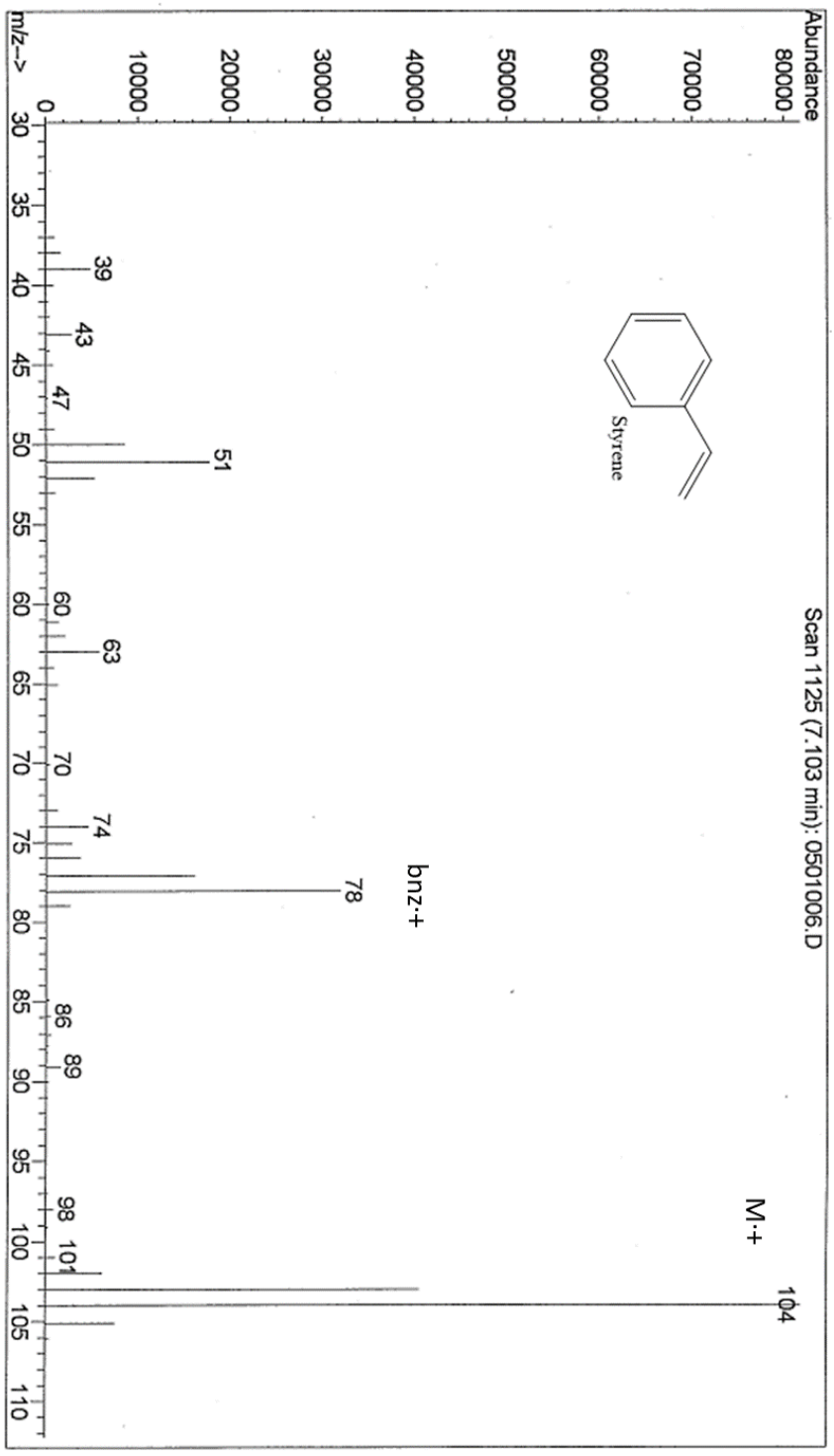

Figure 3.7. Mass spectrum of styrene eluted at 7.1 minutes, with parent ion and the major fragmentation labeled.

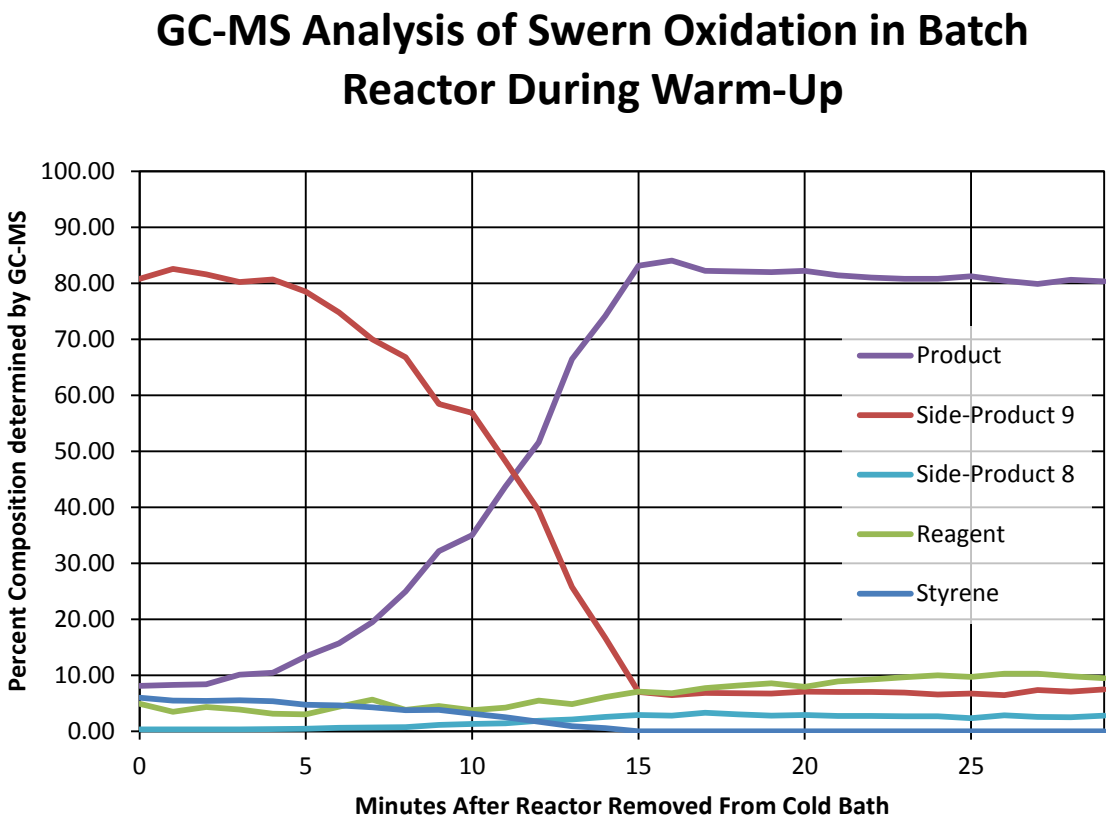

Figure 3.8. HPLC analysis of reaction mixture during 30 minute warm-up period. Product formation accelerating approximately 4 minutes after the reactor was removed from the dry ice and acetone bath. Side-product (**9**) decreasing represents the consumption of intermediate 2 (**5**).

and DMSO happens at a first order kinetic rate and is therefore kinetically favorable when compared to the former SN2 reaction. The benzylic carbocation can now either react by an SN1 reaction path together with trifluoroacetate and form (**9**), or by an E1 path to form styrene as shown in Figure 3.9. Regardless, this path appears to not occur naturally in the reactor, only appearing in samples that are removed from the reactor, thermally shocked to room temperature and diluted by a factor of 10.

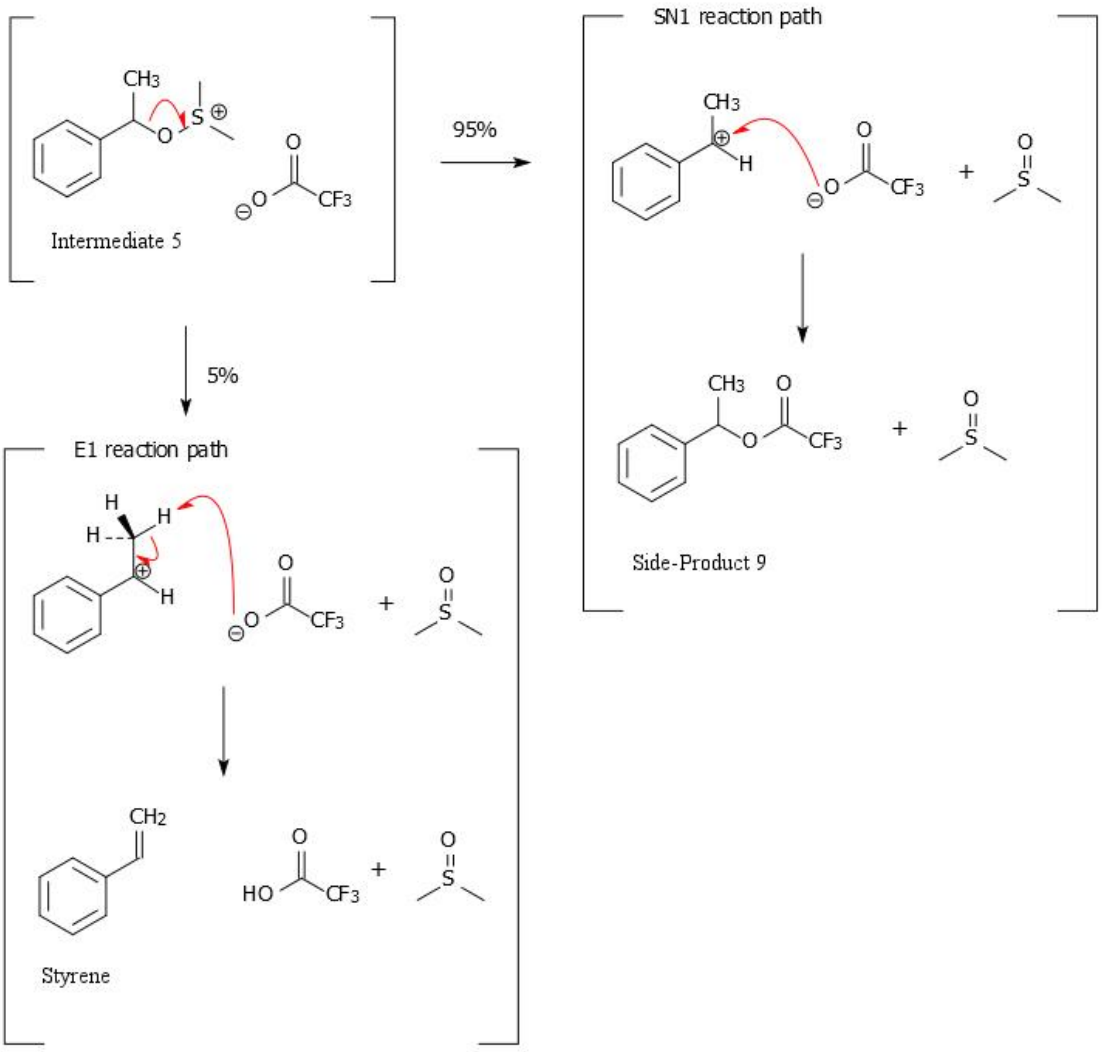

Figure 3.9. Proposed styrene formation mechanism via E1 reaction pathway. Collaboration with Olav Bleie.

Comparison of HPLC and GC-MS Results

There are both similarities and differences between the GC-MS and HPLC results. The HPLC and GC-MS analysis show similar curves for product formation (Figure 3.10), side-

product amounts, and also remaining reagent. Product peak area in GC-MS is inflated compared to HPLC, showing a yield of more than 80% versus under 70% in HPLC (Figure 3.10). Side-product **9** is present in GC-MS analysis at the end of the reaction, while HPLC results indicate that side-product **9** is not present. Additionally, styrene was detected via GC-MS, while not observed in HPLC. Figure 3.11 shows the difference between GC-MS and HPLC composition. These differences can be attributed to not having investigated detector response variations amongst the analytes; standards were not obtainable for the products formed.

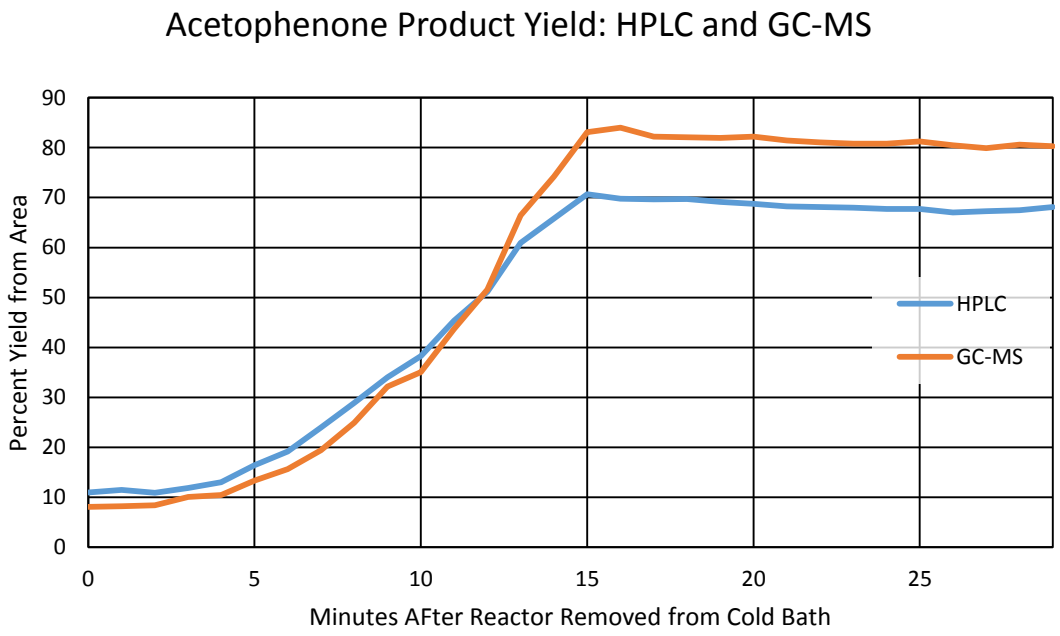

Figure 3.10. HPLC and GC-MS traces of Product formation during reactor warm-up.

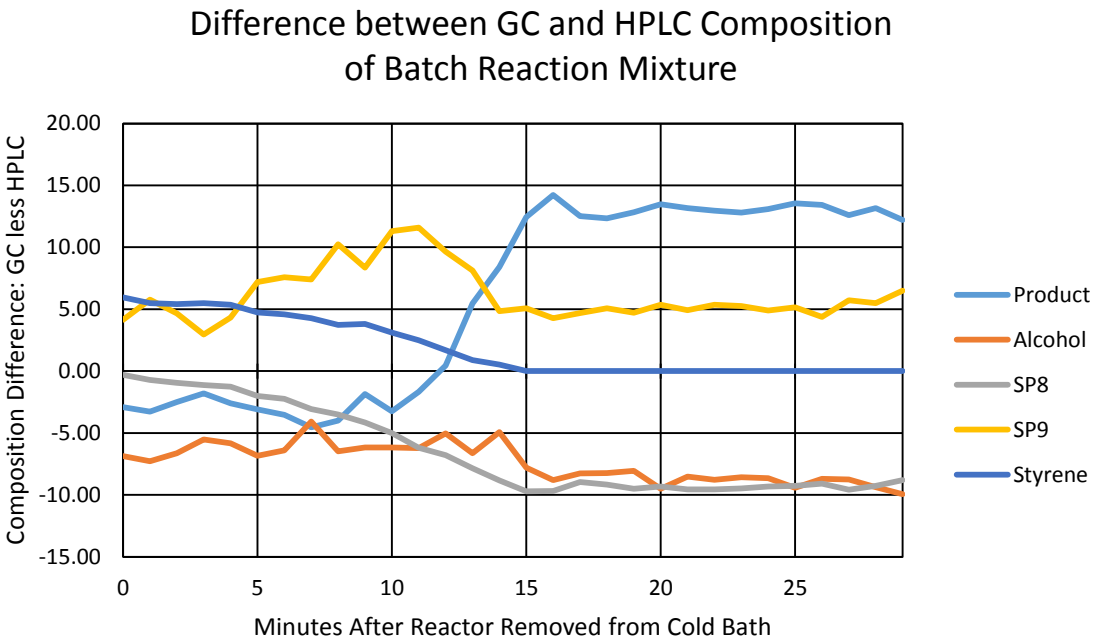

Figure 3.11. GC-MS and HPLC analysis showed disparities between mixture proportions and composition. The final product yield differed by 13%. Styrene was not detected in the HPLC.

Together, HPLC and GC-MS reveal new details about the Swern oxidation of S-1-phenylethanol that was previously unreported or not well understood:

- Product formation occurs not before "quench" addition, but afterwards.
- Product formation occurs primarily during the warm-up of the reactor post-addition of reagents.
- Styrene formation is a possible viable competing pathway if the reaction is significantly diluted.

These insights inform the continuous flow reactor design in Chapter 5, and generally contribute to a greater understanding of the reaction. However, chromatography analysis on its own is not sufficient to fully understand the reaction in the reactor, and do not fully

explain what is occurring in the reactor during warm-up due to decomposition of intermediates and artificial formation of side-products. *In situ* analysis of the reactor is required for complete understanding of the reaction.

Raman Analysis

Raman analysis of the reactor in batch served two purposes. First, confirmation of Raman activity of the reaction, allowing for monitoring in continuous flow. Second, to further understand the oxidation of S-1-phenylethanol, allowing for continuous flow reactor design that takes advantages of the paradigm. Raman allows for quantitative monitoring of a reaction with large temperature shifts with minimal effects. This proved particularly important for the Swern oxidation as product formation occurred during the transition from -70°C to room temperature.

Figure 3.12 shows the concentrations of the major constituents in the reaction, as well as the temperature inside the reaction vessel, as a function of time. From time 0 to 10 minutes the reaction vessel contains only solvent (DCM). The concentration of DCM as the reaction progresses is not shown in Figure 3.12. At time 9 to 13 minutes, 2 ml of DMSO solution is added at 0.5 ml per minute, shown in the green line. During this time, the temperature increases as the addition of DMSO progresses, due to the temperature differential between the reaction vessel and chilled DMSO. The slow addition of the reagent ensures that the temperature of the reaction vessel remained below -40°C. From 13 to 20 min the system is in steady state. This is shown in Figure 3.12 as a plateauing of the DMSO concentration

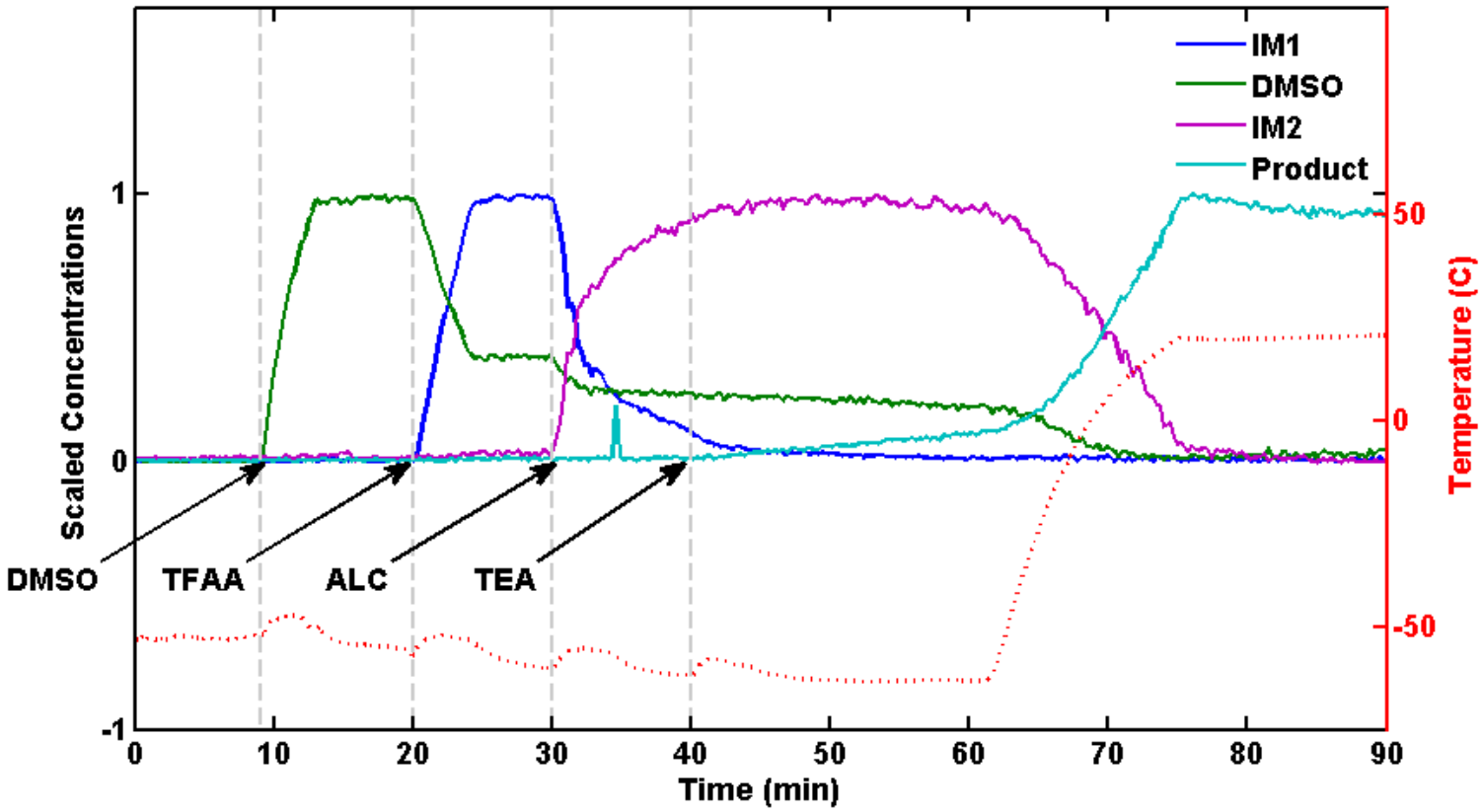

Figure 3.12. Raman Progression of Reaction versus time. Selective Raman regions used for tracking of components. DMSO, Intermediate 1, Intermediate 2, and Product are observed along with Temperature information (red dotted line below). Additions occurred at 10, 20, 30, and 40 minutes, and the reactor was removed from the dry ice / acetone bath.

curve. One also notes that the temperature resumes equilibrium with the ice bath during this time. Between 20 and 24 min, 2 ml of TFAA is injected at 0.5 ml per min. The shape of the curve showing intermediate 1 (**3**) formation, shown in blue in Figure 3.12, demonstrates that TFAA reacts very rapidly with DMSO, requiring no time to reach equilibrium. A rapid ascent and sharp plateau characterizes the speed of formation, mirroring the shape of the curve for the DMSO addition. This conflicts with earlier studies [56]. No spectral features of TFAA are seen in the Raman spectra as well, further indicating instantaneous consumption of TFAA. A steady state is again achieved between time 24 to 30 min, as can be seen from the plateaued concentration curves of DMSO (in excess) and intermediate 1 (**3**).

The S-1-phenylethanol (**4**) is injected from 30 to 34 minutes at 0.5 mL/min. Unlike the previous addition, which caused the instantaneous formation of intermediate 1 (**3**), the formation of intermediate 2 (**5**), shown in the purple line in Figure 3.12, is significantly slower, requiring more than 10 minutes to equilibrate at a maximum. Intermediate 2 is still rising in concentration when TEA (**6**) is introduced in the system from 40 to 44 min, indicating that the reaction between S-1-phenylethanol and intermediate has not reached completion at this point. This is corroborated by the slow consumption of intermediate 1 in blue, which mirrors the shape of the formation of intermediate 2. This contradicts previous understanding of the Swern oxidation, which indicates that this intermediate formation is very rapid. For example, Swern stated "The reaction of alcohols with "activated" DMSO [intermediate 1] is extremely fast irrespective of reaction temperature, at least down to -70°C." [62]. Unfortunately, the alcohol (**4**) has no selective regions in the Raman spectrum to further confirm this observation.

Acetophenone, seen as the light blue "Product" curve in Figure 3.12, starts forming immediately after TEA addition, but at a slow rate. The rate is highly dependent on the temperature, as is demonstrated by a clear acceleration of product formation at 62 min, after the reaction vessel has been removed from its dry ice / acetone bath. Notably, the temperature ramp does not slowly plateau, but instead quickly reaches the maximum temperature then sharply flattens out. This is indicative of an exothermic reaction adding heat to the system, ceasing only when product formation has concluded. Unreacted DMSO is likely broken down to dimethyl sulfide at a steady rate until the temperature ramp-up where this decomposition also accelerates.

The understanding gained from Raman spectroscopy illustrates some important points, most of which will have repercussions for continuous flow reactor design:

- The formation of intermediate 1 (**3**) is, contrary to consensus, very rapid.
- Intermediate 2 (**5**), also contrary to consensus, forms slowly.
- Intermediate 2 is present in the reactor after quench addition.

Combined with temperature information from the thermocouple, GC-MS and HPLC, more information is available:

- Intermediate 2, present after quench, decomposes primarily into side-product 9, and a small amount of styrene. The styrene formation appears to not be possible in normal conditions, but only occurs when removing aliquots followed by dilution. Very little of this new side-product forms product in these circumstances. This is supported by the Raman spectral information showing intermediate 2 present in

solution early in the warm-up period, while HPLC showed side-product 9 and GC-MS showed side-product **9** as well as styrene at these time points.

- In the absence of such a dilution, intermediate 2 forms product slowly during the warming of the reactor. This is supported by Raman information showing the conversion of intermediate 2 to product, while both chromatographies showed side-product 9 decreasing in concentration.

In addition, the speed of formation of intermediates 1 and 2 indicate that the accepted procedure of waiting 10 minutes prior to the addition of the alcohol is not related to the formation of intermediate 1, but rather to the potential of thermal runaway if both intermediates are formed in rapid succession. The temporal delay prior to S-1-phenylethanol allows time for the reactor's temperature to stabilize again (Figure 3.12). This observation is the most important for continuous flow reactor construction, as exothermicity is easily contained in continuous flow, allowing for chemical addition orders to be reconfigured to great effect (this is further explored in Chapter 5).

Conclusions

Through the investigation of the Swern oxidation of S-1-phenylethanol with myriad analytical techniques, a complete understanding of the reaction has emerged. HPLC and GC-MS together allowed for quantitative determination of the solution's components through the entire warm-up period, after the reaction vessel had been removed from the dry ice / acetone bath. These methods reveal that product formation has not occurred before the warm-up, and that the warm-up is in fact what drives product formation. The GC-MS

investigation also revealed a new potential side-product to the reaction, in the event of both rapid thermal shock and dilution. Raman analysis revealed that intermediate formation rates are not as was previously believed; intermediate 1 (**3**) forms rapidly, and intermediate 2 (**5**) forms slowly. The misunderstanding may have occurred through reduced product formation if reactor temperature does not have time to stabilize after the highly exothermic formation of intermediate 1. Online Raman spectroscopy allowed for real-time observation of kinetic and thermodynamic processes occurring in the reactor, resulting in increased understanding of the reaction. These observations bring new understanding to the Moffat Swern oxidation, and significantly affected the continuous flow reactor design discussed in the following chapters.

The work from this chapter is in preparation for publication.

Chapter 4

The Swern Oxidation in Continuous Flow: Steady State Determination and Configuration 1

Introduction

There are many examples of pharmaceutical companies implementing CFR production. Schwalbe *et. al.* from Synthacon demonstrated the synthesis of the antibiotic Ciprofloxacin™, with yields as high as 99% at 96% purity [63]. Fukase and coworkers produced the immunoactivitating natural product Pristine at a capacity of 5 kg $week^{-1}$ [64]. Hopkin *et. al.* demonstrated the synthesis of the active pharmaceutical ingredient (API) Imatinib™, the API of Gleevec [65]. These demonstrations of API production all focus on the increased reliability of CFRs – once producing a target chemical, a reactor will yield the same quality product over time. This assumes that a reactor system is in steady state. A steady state continuous flow system is one that is physically stable with regards to the variables of pressure, flow rate, mixing, and temperature. This results in controlled chemical production with reproducible results, analogous to a hypothetical multi-batch setup performed all at once, with identical physical conditions and chemical additions across all batch reactors. Continuous flow systems offer significant advantages over batch reactors that can fluctuate between different production runs.

Currently, CFRs are determined to be at steady state by either a univariate method, detecting physical stability in the reactor, or a multivariate method determining the stability of chemical output [10,12,15,16,37]. Example univariate detectors include thermocouples and pressure transducers, characterized by a continuous stream of data for a single measurable property. Multivariate detectors include chromatographic and spectrographic information, which produce variable amounts of data per acquisition, depending on the method. Chemical steady state is frequently determined by off-line HPLC analysis [2]; a

typical example is demonstrated by Watts *et. al.* application note demonstrating the esterification of benzoic acid in a continuous flow reactor [12]. In this study, the output from the CFR is sampled at each design point and analyzed via HPLC, requiring 15 minutes of analysis per design point. Adding to analysis time is an uncertainty in reactor steady state that requires multiple measurements. This can be especially problematic when attempting to determine optimal reactor conditions that require the exploration of a large design space. Physical measurements, while rapid, cannot effectively detect problems associated with product quality. Additionally, CFRs are not currently constructed with interfaces to accommodate process analytical technology (PAT). Instead, current physical stability detection methods largely rely on feedback from the temperature or flow controllers without dedicated sensors.

Monitoring of any process requires a reproducible sampling interface for reliable results. New Sampling/Sensor Initiative (NeSSI) sampling systems have previously been shown to be effective tools for enabling process monitoring in fluid and gas systems [30,31], and as interfaces for continuous flow reactor analytics [31]. NeSSI is a modular platform allowing for simple expansion or rearrangement of a sampling platform. This enables rapid prototyping and development of continuous flow reactor systems. The coupling of NeSSI with appropriate PAT creates a dependable interface for the consistent sampling of a flow channel [30,32].

The combination of NeSSI with PAT and multivariate chemical monitoring offers significant advantages for optimizing chemical design space when compared with systems that employ physical or chemical techniques alone. A continuous flow system was

designed that expands traditional physical monitoring while implementing real-time chemical monitoring to accurately and rapidly determine steady state. Additionally, methods developed show potential for quality control and upset detection in production-scale facilities. Critical to the success of this project was the construction and design of a smart reactor system for monitoring and control of a defined chemistry with PAT. To demonstrate the smart reactor system, the Moffatt-Swern oxidation of 1-phenylethanol (Figure 4.1) was investigated. The formation of unstable intermediates **3** and **5** is highly exothermic and unstable, requiring accurate temperature control [12,13].

The reactor design described in this chapter follows the batch addition order investigated in Chapter 3, allowing for direct comparison to batch. Yield results demonstrate a significant advantage over batch production, allowing for high yield production at temperatures above -30°C, where the reaction fails in batch. The overall results demonstrate that the application of PAT to accurately detect physical and reaction stability in CFRs improved the time required to determine steady state by more than an order of magnitude. This reduced the time required to process the DoE and determine optimal reactor conditions. The final goal of this work was to develop a procedure for optimizing CFRs independent of the chemistry performed.

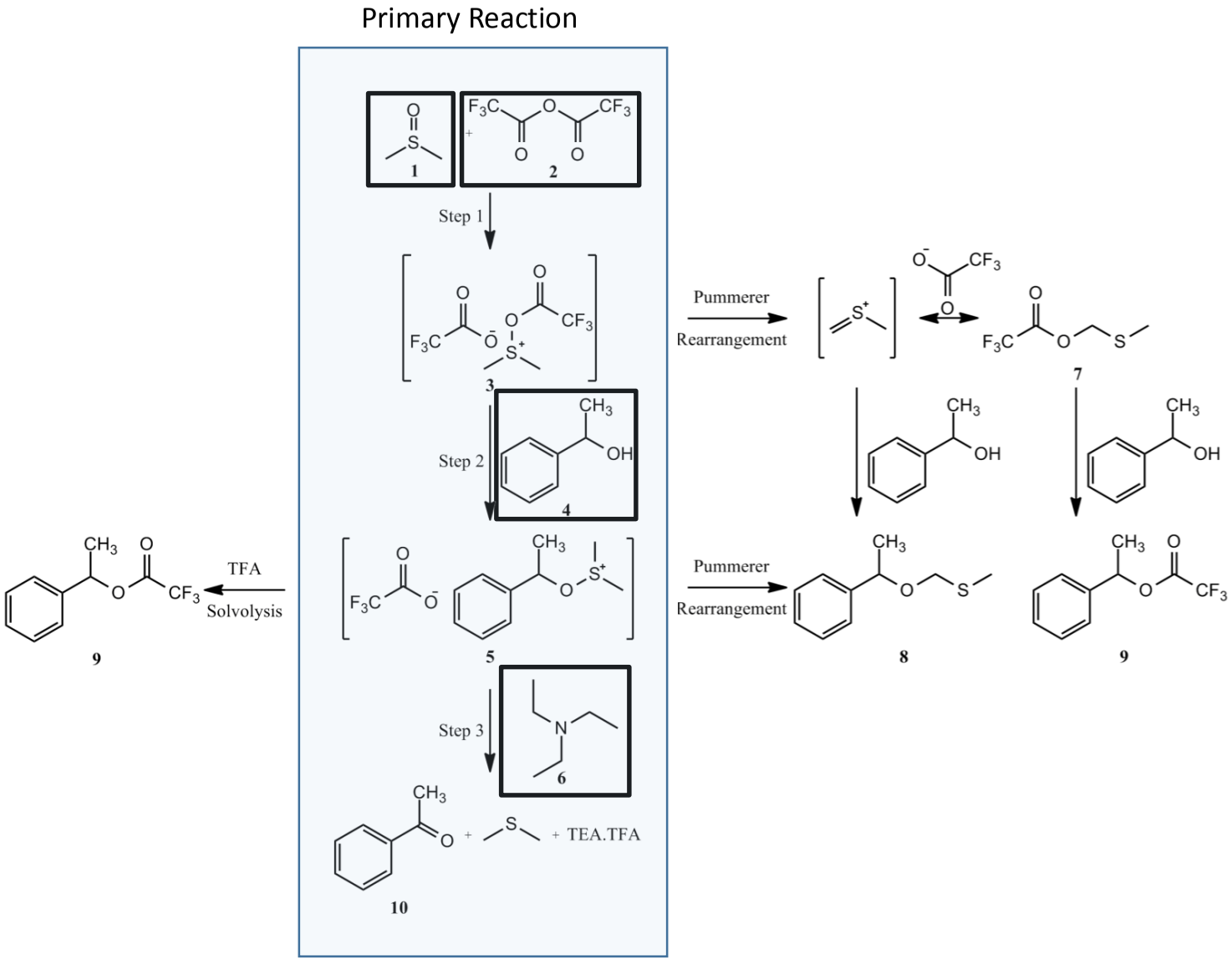

Figure 4.1. The Swern Oxidation. In the primary reaction pathway, DMSO (**1**) reacts with TFAA (**2**) to form intermediate 1 (**3**) quickly. S-1-phenylethanol (**4**) then reacts with intermediate 1 to form intermediate 2 (**5**). TEA (**6**) quenches the reaction, resulting in product acetophenone (**10**). Possible side-products include **8** and **9** through Pummerer rearrangements or solvolysis.

Experimental

The CFR was comprised of 4 main components: The Intraflow NeSSI sampling system, the analytics and controllers, the reactor mixing plates, and the control software. The Intraflow sampling system, provided by Parker Hannifin (Cleveland, OH, USA), consisted of four identical reagent lines and a product line. Four reagents: 2.4 M trifluoroacetate anhydride (Sigma-Aldrich, St. Louis, MO, USA), 4.0 M DMSO (Sigma-Aldrich, St. Louis, MO, USA), 2.0 M *S*-1-phenylethanol (Sigma-Aldrich, St. Louis, MO, USA), and 5.8 M triethylamine (Sigma-Aldrich, St. Louis, MO, USA) all in dichloromethane (Sigma-Aldrich, St. Louis, MO, USA) are pumped into the system by HPLC Pumps (two FLOM FS10A HPLC pumps, FLOM USA, San Diego, CA, USA, and two SSI Series I HPLC pumps, SSI, State College, PA, USA). These pumps actively controlled the residence time and stoichiometry of the reactor system. Pressure relief valves were installed on each line to ensure safe reactor operating conditions. Temperature was controlled by a Huber Tango heat-exchanger (Huber USA, Northport, NY, USA) and was pumped across three sequential Corning LF Reactor plates (Corning Glass, Avon, France), each with a reactor volume of 1 mL, that included heart-shaped mixers to ensure turbulent mixing throughout.

Univariate sensors deployed on the reactor were: a pressure transducer on each reagent line (HEISE, Stratford, CT, USA), a flow meter on each reagent line, (FCI Incorporated, San Marcos, CA, USA), and a thermocouple (Omega Engineering, Stamford, CT, USA) on the product line and two thermocouples before and after the reactor plates to determine the temperature loss across the reactor. The sensors and controllers were all monitored and controlled via an in-house designed LabVIEW 7.5 (National Instruments Corporation,

Austin, TX) GUI environment. All of the analytics were interfaced to the reaction flow via NeSSI sampling system. The sensors and digital controllers were queried once per second; the GUI reported temperature, pressure, and flow information in real-time. Raman probes provided multivariate information and were interfaced to all reagent lines and the product line via a 0.5" O.D. Raman BallProbe™ (MarqMetrix, Seattle, WA, USA) A four-channel 785 nm Raman system, supplied by Kaiser Optical Systems (Ann Arbor, MI, USA) was used to collect Raman spectra from four BallProbes™ mounted on the reactor sequentially.

Raman investigation of the reaction chemistry was performed prior to exploring the full temperature and flow rate design space. Spectra were collected by performing chemistry at a constant flow rate of 4 mL/min from −20 °C to 20 °C at 10 °C intervals. Five Raman spectra were recorded; each consisting of five one-second exposures, for a total of 25 calibration spectra. All calibration samples were validated on an Agilent 1100 Series HPLC (Agilent Technologies, Santa Clara, CA, USA) using a reverse-phase column (Agilent C18 Column, Santa Clara, CA, USA). The liquid chromatography was performed using two mobile phases: 0.1% acetic acid in water and acetonitrile. A constant flow of 5% acetonitrile for 2 min, then a gradient of 5% acetonitrile to 95% acetonitrile over 5.5 min, followed by 2 min constant flow resulted in clearly defined peaks for *S*-1-phenylethanol (**4**), acetophenone (**10**), and side-products **8** and **9**. Acetophenone peak area was used to determine reaction progress.

Raman spectra were imported into MATLAB 7.5 (Mathworks, Natick, MA, USA) for analysis and modeling. All spectra were preprocessed using a 1st order baseline removal to remove unwanted baseline variation between spectra. PCA was performed with PLS

Toolbox 5.0 (Eigenvector Research, Inc., Wenatchee, WA, USA) using mean-centered, background corrected spectra to monitor reactor steady state via changes in the multivariate scores. These scores were plotted in real-time in the control software for monitoring of steady state.

Software Development

The backbone of the control software was a controller loop, able to monitor inputs from the user and execute them in the order received. Figure 4.2 shows a portion of the front panel, with status lights, flow and temperature inputs, and the temperature line plot. Once a second, the software queried all univariate sensors. Upon interaction with specific elements on the front panel, such as the "Flow Pumps" button (Figure 4.2), the software transmits the flow commands to the pumps, and then resumes status queries. The digital instruments gave feedback upon receiving commands properly, and the software required a second confirmation of status before updating the control panel.

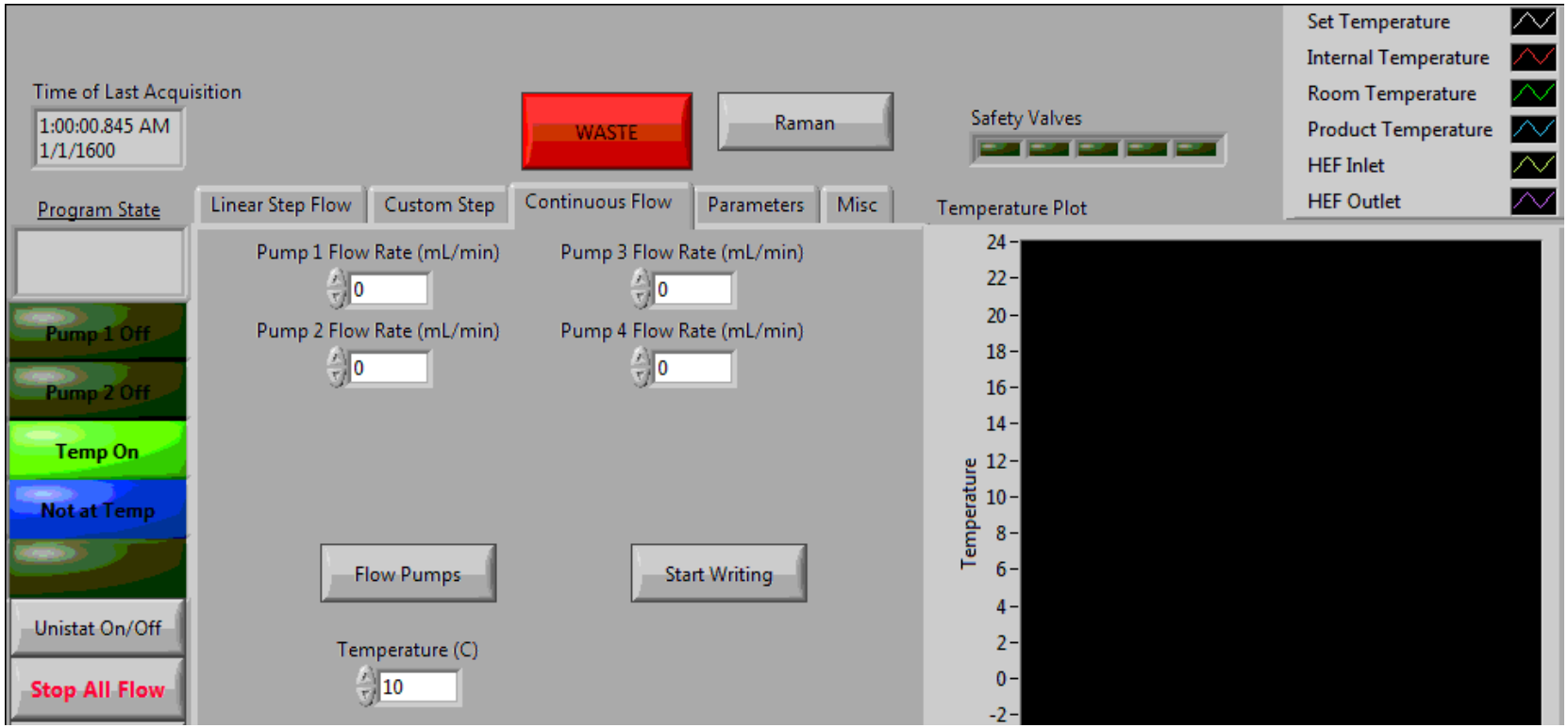

Figure 4.2. A section of the front panel of the control software. Notable elements include status indicators for pumps, temperature control, and safety valves. The "Continuous Flow" tab is shown, able to control flow rates and temperature manually.

Results and Discussion

A system was developed using a CFR, NeSSI sampling system, and PAT to monitor chemical and physical variation in real-time (Figure 4.3). The PAT served two purposes: To determine reaction steady state, and to detect process upsets in the reactor. The variables temperature, pressure, and flow were recorded at one second intervals at specific locations in the reactor (Figure 4.3, "A" and "B"). When the lowest deviation of each physical measurement had been obtained the reactor was considered physically stable. Upon reaching physical stability the reactor requires a lead time in order for the physical changes to be reflected in the chemical output downstream. Lead time is dependent upon the flow rate and the total volume of the reactor system by the equation:

$$Residence\ Time = \frac{Reactor\ Volume}{Flow\ Rate} \qquad \text{Eq. 4.1}$$

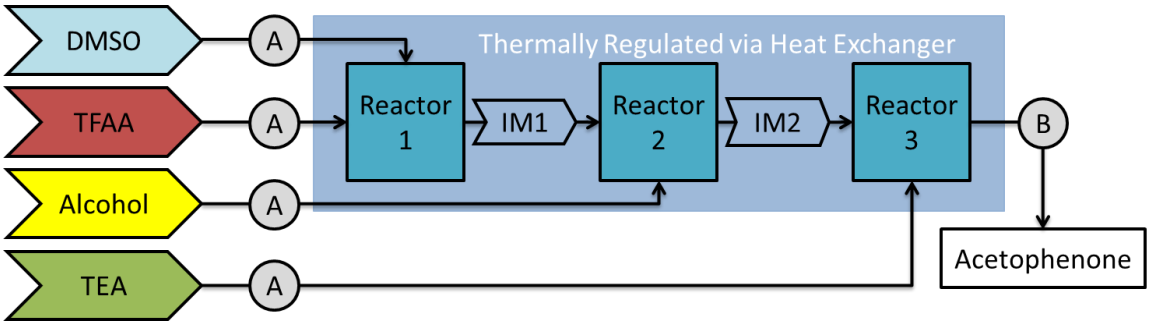

Figure 4.3. Schematic of continuous flow reactor configuration 1. Each reagent line is equipped with identical suite of analytics (labeled as A) – flow meter, pressure sensor, and Raman probe – and safety valves for operator safety. The product line (B) contains a Raman probe, a pressure regulator, and a pneumatic valve to route the completed reaction material to product or to waste, depending on product quality.

A Raman BallProbe™ on the product line (Figure 4.3, "B") performed spectral acquisitions every 15 s. Raman spectroscopy is particularly suitable for monitoring the Swern oxidation due to the strength of the C=O band of the product at 1691 cm^{-1} (Figure 4.4). Upon exiting the final reactor plate, all chemicals rapidly reached room temperature in the tubing before the NeSSI sampling system prior to Raman analysis. This was confirmed by a thermocouple upstream of the Raman BallProbe™ on the product line. Chemical steady state was determined via monitoring of the first PC score from the Raman spectra in real-time. Four sequential scores within an acceptable statistical confidence were used to define chemical steady state (approximately 1 min of sample time). Upon attaining chemical steady state, a single HPLC sample was extracted and analyzed to quantitatively determine the yield of product.

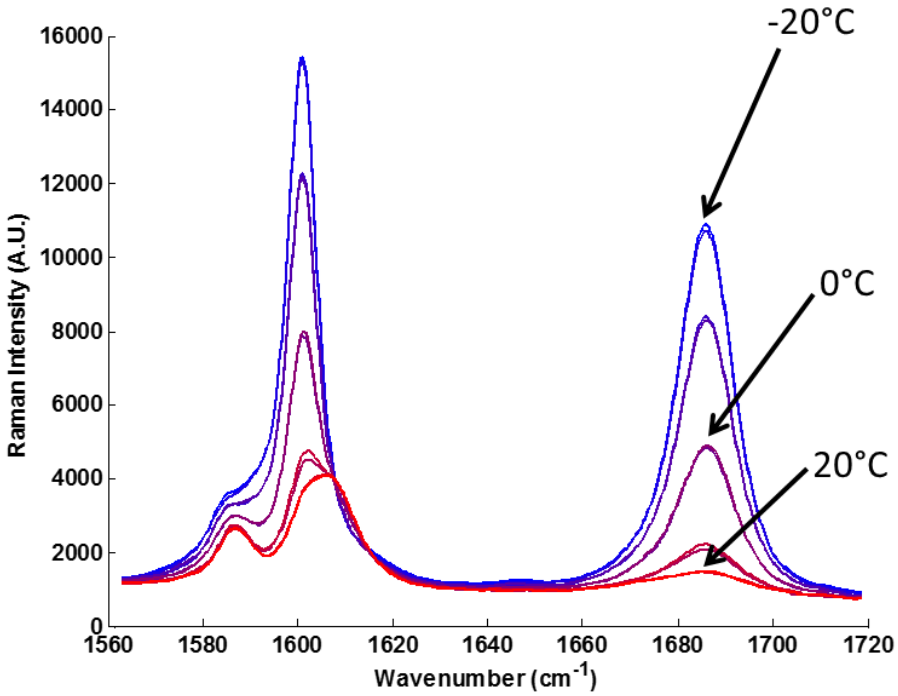

Figure 4.4. Wavelength subset of Raman spectra at five different temperatures. While the entire spectrum was used for PCA modeling, this region in particular shows the temperature dependence of the production of acetophenone, with peaks at 1691 cm^{-1} and 1602 cm^{-1}.

An example of how physical stability and chemical steady state relate to each other is shown in Figure 4.5. The dark dotted line shows the measured pressure in one of the four reagent lines. At 3 min, the flow rates of the four reagents were doubled from 2 to 4 mL/min. Physical stability is established in 1.5 minutes. The first change in the PCA scores is observed at 4 min, shown in the lighter dotted line. Chemical steady state is reached by 13 min, 10 min after the change in physical conditions. Determining chemical steady state using HPLC would have significantly increased the time to complete reactor optimization. Four consecutive HPLC measurements require an analysis cycle of more than one hour.

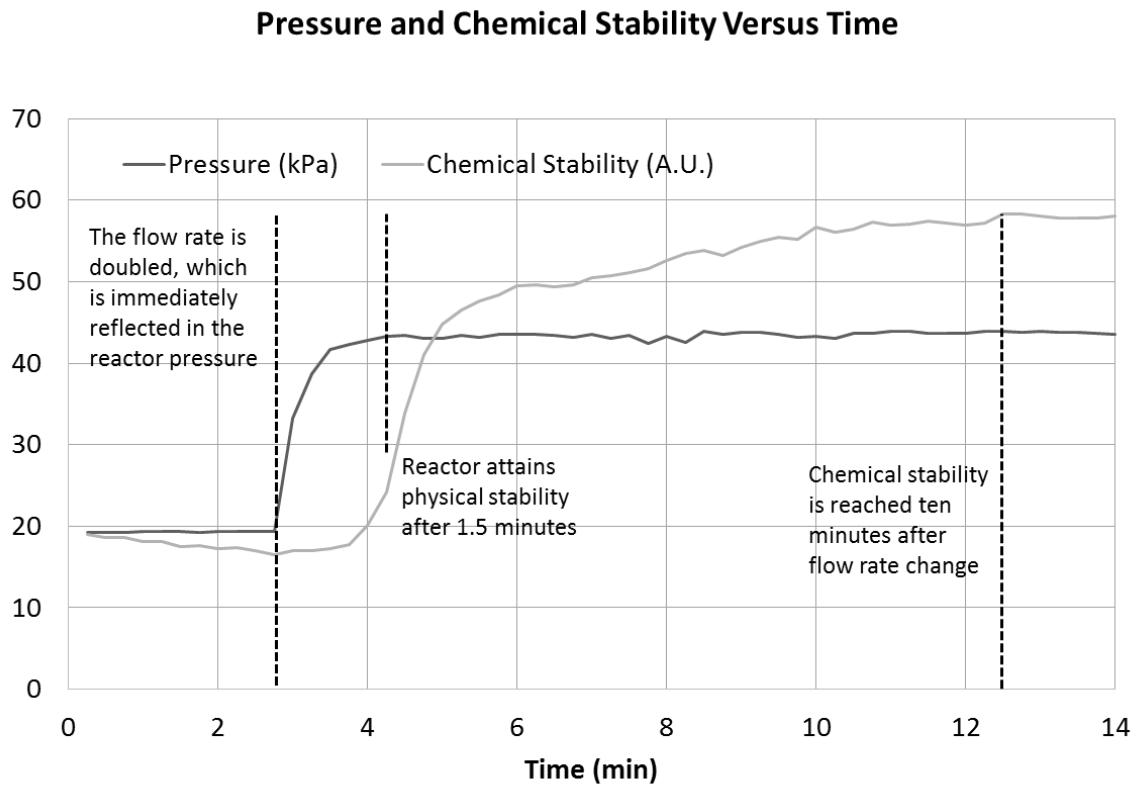

Figure 4.5. Pressure response in a reagent line (**dark line**) and chemical steady state information (**light line**) that demonstrate physical and chemical steady states and changes in the system.

This is 60 times longer than Raman monitoring to determine steady state. The real-time Raman information enabled a more effective use of HPLC for validation.

The chemical yield results obtained by using offline HPLC are shown in Table 4.1. In batch, at temperatures above −30 °C, no significant product yield is detected (<2%) [13]. In continuous flow, the Moffat Swern oxidation had yields of 81% at −20 °C , 37% at 0°C, and 5% at room temperature. As expected due to the exothermicity of the reaction, yield decreases with increasing temperature. The unstable nature of intermediates 3 and 5 also resulted in lower chemical yield at slower flow rates (Table 4.1). This effect has been previously reported by Yoshida et al. [12] and Kemperman et al. [13].

		Temperature				
Configuration 1		**-20°C**	**-10°C**	**0°C**	**10°C**	**20°C**
Flow Rate (mL/min)	**2**	34	17	15	4.5	1
	4	73	58	31.5	7.5	2.28
	6	80	68.5	32.5	8.5	3
	8	81	73	37	14	5
	10	81	74	37	14.5	5

Table 4.1. % Yield of Swern oxidation of S-1-phenylethanol in CFR Yield is proportional to flow rate and inversely proportional to temperature. Highest yield of 81% is higher than was attained in batch (Chapter 3)

The information from the PAT allowed for rapid exploration of a design of experiments in the CFR. Using HPLC to validate chemical steady state would have required at least 30 hours of experiment time, compared to under 4 hours in the described experiment. These results demonstrate that the real-time monitoring of physical and chemical steady state in a CFR offers significant advantages for optimizing a reactor system when compared with systems that employ either physical or chemical techniques. This was accomplished through coupling a reactor to PAT using a NeSSI sampling system. The fast optimization

technique is chemistry and hardware agnostic, making this approach a viable means of optimizing any CFR for any suitable chemical reaction.

Conclusions

The Swern oxidation (previously discussed in Chapter 3) was used as a model chemistry and investigated in continuous flow. Physical sensors, providing information on physical stability combined with Raman spectroscopy and multivariate modeling, allowed for real-time detection of steady state in a CFR. The investigation of a design space to optimize reactor conditions was improved through the rapid detection of steady state. The design of experiments was explored in under four hours, with improved confidence in the reproducibility of quality product. In addition, the optimization was achieved via a chemistry agnostic platform that allows for determination of optimum parameters for future production based on quality, volume, and energy needs, regardless of chemistry. In the following chapter, the reactor system is redesigned using information and results from this chapter combined with the knowledge from batch monitoring (Chapter 3)

Portions of this chapter were published in *Processes* in 2013 [66].

Chapter 5

The Swern Oxidation in Continuous Flow: Configuration 2 and Real-Time Yield Prediction

Introduction

The advantages of CFRs are usually demonstrated through translating a batch process directly to continuous flow, resulting in improved production capabilities of a target product. Suga et al. [67] evaluated a Friedel-Crafts alkylation of thiophene. Performed in batch, the authors reported a 14% yield of the mono-alkylated product, with 27% unwanted di-alkylated product. In a micromixer, the yield improved to 81% mono-alkylated product, with only trace amounts of di-alkylated product. Wahab [68] reported a study of the bromination of indoles in continuous flow. Reporting batch conversions of under 75%, the continuous synthesis of bromoindole derivatives proved to have a 99.9% conversion yield. Other studies report significantly reduced times to product formation. Wiles and Watts report that the continuous flow esterification of benzoic acid generated product in under 3 minutes, compared to more than an hour in batch, by surpassing boiling point limitations [12]. Kobayashi *et. al.* [69] demonstrated the alkylation of 2-oxocyclopentane carboxylate in continuous flow. In their study, product yield of 96% was obtained in 10 minutes, while batch reactors achieved 60% conversion in the same timeframe.

In all of these examples, which constitute only a small fraction of similar studies, the continuous flow production scheme is directly translated from the batch production scheme, taking advantage of the efficient temperature gradients and thermal capabilities of continuous flow. However, continuous flow allows not only for a translation of batch production paradigms, but for an informed production scheme by designing for continuous flow from scratch. This is possible following a thorough investigation of a reaction in batch. Through the understanding of intermediate formation rates, side-product production

pathways, target chemical production mechanisms, and understanding of batch reaction method limitations, a chemistry reaction can be fundamentally improved for production of a target compound.

The Swern Oxidation of S-1-phenylethanol

In Chapter 3, the Swern Oxidation (Figure 5.1) was investigated in batch. Raman spectroscopy and HPLC monitoring of the reaction revealed several mechanisms of the reaction that were previously unknown, or poorly understood. These included intermediate

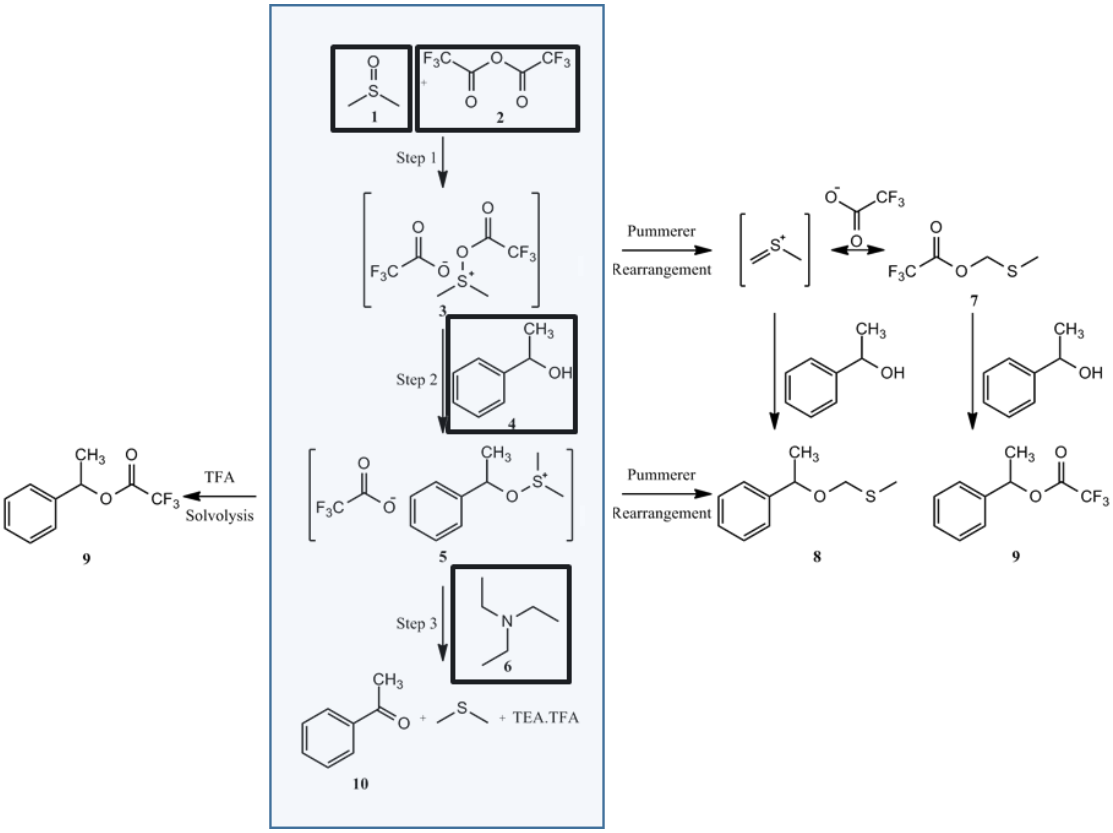

Figure 5.1. The Swern Oxidation. In the primary reaction pathway, DMSO (**1**) reacts with TFAA (**2**) to form intermediate 1 (**3**) quickly. S-1-phenylethanol (**4**) then reacts with intermediate 1 to form intermediate 2 (**5**). TEA (**6**) quenches the reaction, resulting in product acetophenone (**10**). Possible side-products include **8** and **9** through Pummerer rearrangements or solvolysis.

formation rates, product formation rates and the role of temperature in product formation. These studies also informed why the reagents have always been added in a specific order [54]. For example, the reaction vessel temperature rose notably following each intermediate formation in batch (**4** and **6**), requiring an addition order that separated the formations to reduce the possibility of thermal runaway. The instability of the intermediates (intermediate 1 (**4**) in particular) required a cryogenic bath of -70°C, introducing a significant cost burden on the manufacturing process. However, these limitations do not apply to continuous flow through efficient temperature control and mixing schemes. In this chapter, the Swern oxidation is investigated with two different reaction orders. Configuration 1, preliminarily explored in Chapter 4, is a direct translation of the Swern oxidation from batch to continuous. Configuration 2 is a revised reaction schematic that is only possible in continuous flow, taking advantage of the temperature control attainable in a CFR.

Spectroscopic Validation

As previously discussed in Chapter 2, a significant limitation for CFRs is the lack of effective in-line and real-time monitoring techniques. Current monitoring methods for CFRs largely rely on offline chromatographic methods. These techniques introduce significant delays and inefficiencies into CFR monitoring [39]. HPLC and GC-MS techniques are largely incompatible with flow systems, and frequently require an operator to collect and prepare samples [70]. In addition, chromatographic methods frequently require long analysis times and require consumable materials. This has inhibited long-term industrial implementation of CFRs due to continuous consumption of materials for both

generation and validation of product. To address these inefficiencies, Raman spectroscopy was used for CFR monitoring, as discussed in Chapter 4.

Spectroscopic methods contain chemical and physical information that can be used for effective online monitoring of a continuous flow reaction. However, deconvolution of spectral data is challenging in complex chemical systems that contain many species. Chemometric tools, such as principal component analysis (PCA) and partial least squares (PLS), are often used to process and analyze spectral data quickly and effectively [20-23]. PCA monitoring was discussed in Chapter 4 as a qualitative method for monitoring a reactor. Partial least squares (PLS), as introduced in Chapter 2, is a method of forming quantitative predictions from multivariate measurements based on correlation to a standard reference measurement [71]. Using PLS regression models built from Raman spectra, Cooper *et. al.* demonstrated accurate predictions of chemical and physical properties including octane numbers and vapor pressures of petrochemical solutions [72]. This was further demonstrated by Dearing *et. al.* who predicted more physical properties of crude distillates when combining IR, Raman, and nuclear magnetic resonance (NMR) information into data-fused models [25]. Regardless of specific application, real-time PLS modeling of multivariate data has allowed for fast and accurate quantitative information to be acquired from both batch and continuous flow systems.

The work in this chapter demonstrates that while Configuration 1 results in an improvement over batch, a configuration built upon batch understanding from Chapter 3 offers greater improvements through taking full advantage of the continuous flow paradigm. Thus, a thorough investigation of batch followed by designing a reaction

pathway from the information gathered represents a new path for process development that should be applicable to a wide range of chemical reactions, enabling better use for the continuous flow paradigm for target production.

Experimental

The reactor system, as discussed in Chapter 4, was comprised of 5 main components: an Intraflow New Sampling and Sensor Initiative (NeSSI) sampling system, PAT, controllers, chemical reactor plates, and control software. The NeSSI Intraflow sampling system, provided by Parker Hannifin (Cleveland, OH), consisted of reagent lines and a product line (Figure 5.2). The pumps actively controlled the residence time and stoichiometry of the reactor system under software control. Pressure relief valves were installed on each line to ensure that the reactor system did not exceed pressure limits. Temperature was controlled by a Huber Tango heat-exchanger (Huber USA, Northport, NY) and was connected to a commercial CFR reactor, composed of a Corning LF Reactor plate (Corning Glass, Avon, France) followed by four Corning LF residence time plates, each with a reactor volume of 1 mL for a total reactor volume of 5 mL. The sensors, PAT, controllers, and chemicals are all as previously described in Chapter 4.

Reactor Configurations for Swern Oxidation of S-1-phenylethanol

In configuration 1 (Figure 5.2), DMSO (**1**) and TFAA (**2**) are added first forming intermediate 1 (**3**). Intermediate 1 reacts with the S-1-phenylethanol (**4**) in the next reactor to form intermediate 2 (**5**). Finally, TEA quench (**6**) is added for acetophenone product

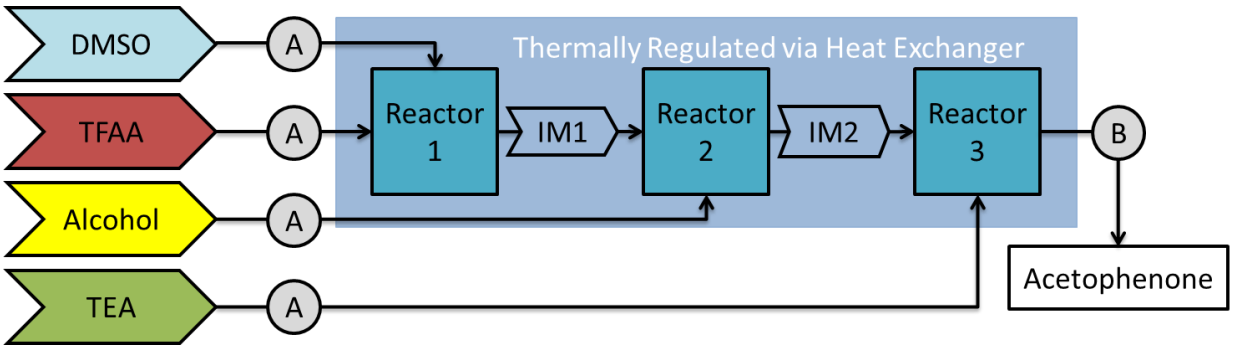

Figure 5.2. Schematic of continuous flow reactor **Configuration 1**. Each reagent line is equipped with identical suite of analytics (labeled as A) – flow meter, pressure sensor, and Raman probe – and safety valves for operator safety. The product line (B) contains a Raman probe, a pressure regulator, and a pneumatic valve to route the completed reaction material to product or to waste, depending on product quality. In configuration 1, DMSO and TFAA react in the first reactor, forming intermediate 1, which subsequently reacts with the S-1-phenylethanol to form intermediate 2. TEA, acting as quench, is added in the third reactor.

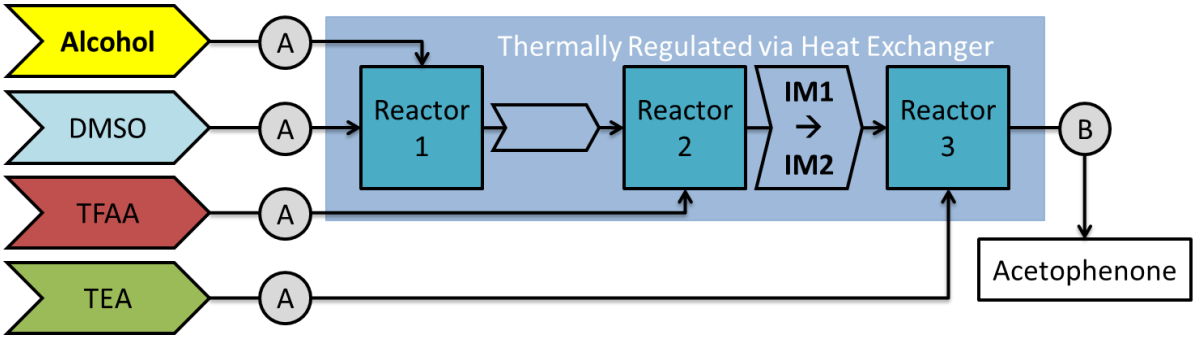

Figure 5.3. Schematic of continuous flow reactor **Configuration 2**. See Figure 5.2 for description of analytics. In configuration 2, S-1-phenylethanol and DMSO mix in the first reactor, causing no reaction. This mixture is subsequently added to reactor 2, where TFAA and DMSO react to form intermediate 1. reacts with the S-1-phenylethanol to form intermediate 2. TEA, acting as quench, is added in the third reactor.

formation (**10**) in the reactor. In configuration 2 (Figure 5.3), DMSO (**1**) and S-1-phenylethanol (**4**) are mixed in reactor 1, causing no reaction. TFAA (**2**) is added to this mixture in reactor 2, causing the rapid formation and immediate consumption of intermediate 1 (**3**), forming intermediate 2 (**5**). TEA quench (**6**) is added in the last reactor plate as in configuration 1. A full factoral design of experiment (DoE) using temperatures from -20°C to 20°C and flow rates from 2mL/min to 10mL/min at 5 levels per variable was investigated in both reactor configurations. For configuration 1, % conversion was determined for all design points via HPLC as discussed in Chapter 4. For configuration 2, % conversion was determined with Raman spectroscopy via PLS analysis, with random points in the design validated via offline HPLC for PLS model. Chemical identities from HPLC were validated with GC-MS (see Chapter 3 for further discussion).

Data Analysis

Raman spectra were imported into MATLAB 7.5 (Mathworks, Natick, MA) for data analysis and modeling. All spectra were preprocessed using a first order baseline removal algorithm to remove unwanted baseline variations between spectra. For configuration 2, a PLS model was constructed with PLS Toolbox (Eigenvector Research Inc., Wenatchee, WA) using the spectra collected as part of the DoE. Five HPLC aliquots were collected at each temperature and analyzed offline to construct a 50-point PLS model. For all real-time modeling, upon the control software receiving a new spectral file, a prediction of yield was made using the PLS calibration model. The predicted yield was then sent to the LabVIEW control software for display. Chromatographic methods are described in chapter 3.

Results and Discussion

The process of optimizing batch chemistry for continuous flow is based upon understanding. If a chemical reaction is well-understood, it is not limited to a direct translation to continuous flow where all stoichiometries, reagent additions, and temperatures are applied from batch. It can instead be redesigned for optimal use of the continuous flow paradigm, making use of the mixing schemes, temperature gradients, and modular design. However, this is rarely the case. As discussed in Chapter 1, continuous flow offers notable yield improvements compared to batch, but this is frequently the result of direct translation of a chemistry rather than wholesale redesign of the reaction for continuous flow. In this chapter, the initial configuration discussed in Chapter 4 is further investigated with Raman spectroscopy, and a quantitative PLS model is constructed for this system. The reactor is then redesigned to Configuration 2, using he knowledge gained from previous chapters to make informed design choices for a continuous flow reactor.

Configuration 1

In Chapter 4, the Swern oxidation was quantified using off-line HPLC, demonstrating that a straight translation of the chemistry performed in a continuous flow reactor offers significant advantages over batch. High yields were obtained at fast flow rates and low temperatures, with temperatures significantly higher than batch (Table 5.1). Raman monitoring was also present on the product line, showing distinctly different levels of product formation depending on flow rates and pressure. Figure 5.4 shows a subset of the

entire Raman spectrum over time, showing a clear regression of a product peak with increasing temperature.

Configuration 1		Temperature				
		-20°C	**-10°C**	**0°C**	**10°C**	**20°C**
Flow Rate (mL/min)	**2**	34	17	15	4.5	1
	4	73	58	31.5	7.5	2.28
	6	80	68.5	32.5	8.5	3
	8	81	73	37	14	5
	10	81	74	37	14.5	5

Table 5.1. % Yield of Swern oxidation of S-1-phenylethanol in CFR configuration 1 (as discussed in Chapter 4). Yield is proportional to flow rate and inversely proportional to temperature. Highest yield of 81% is higher than was attained in batch (Chapter 3)

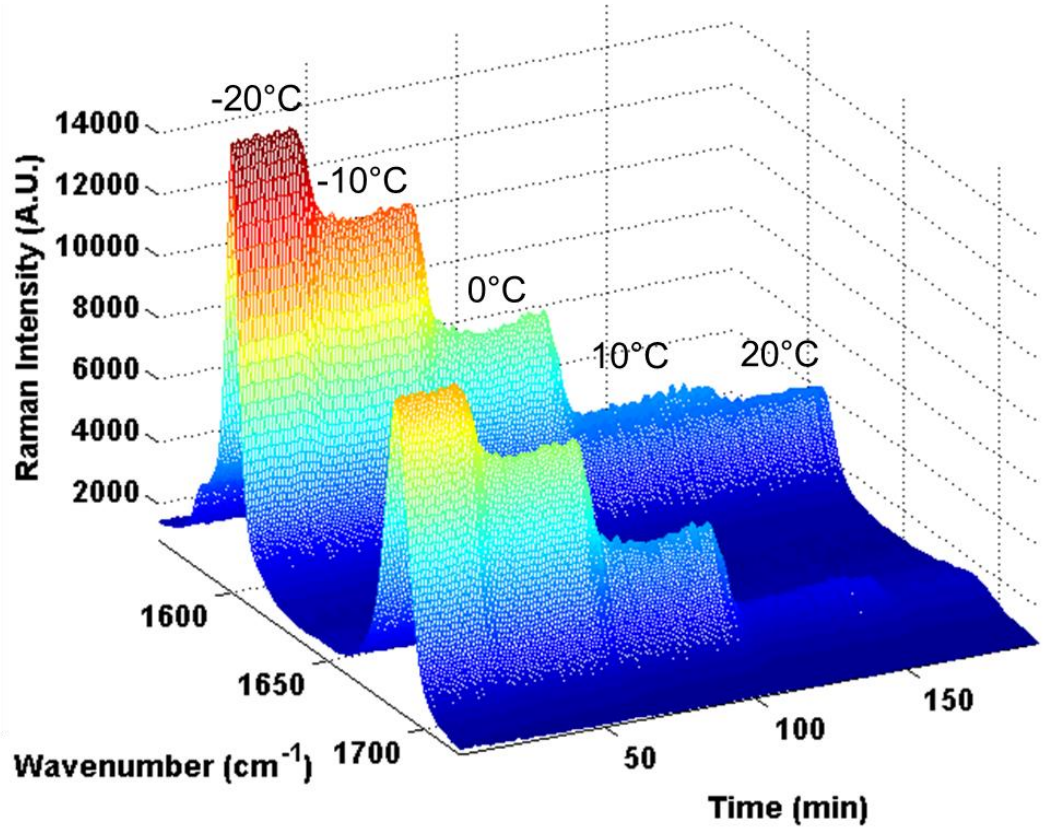

Figure 5.4. Waterfall plot of select region of Raman spectrum from configuration 1. Peak formation at ~1600 represents the carbonyl stretch of acetophenone. Product formation decreases with increasing temperature.

Following this demonstration of Raman capability for monitoring acetophenone production in a CFR, multivariate statistical modeling was investigated using Raman spectra and HPLC information. 25 HPLC aliquots were collected from five temperature points (-20°C to 20°C) at 8 mL/min, and analyzed off-line. Control software was used to step through each temperature; aliquots were taken when the reactor was determined to be at physical and chemical equilibrium (see Chapter 4). Each temperature design point paired one Raman spectra per HPLC sample, and a 25-point PLS model was constructed (Figure 5.5, black circles). Only one latent variable was necessary for accurate modeling; two latent

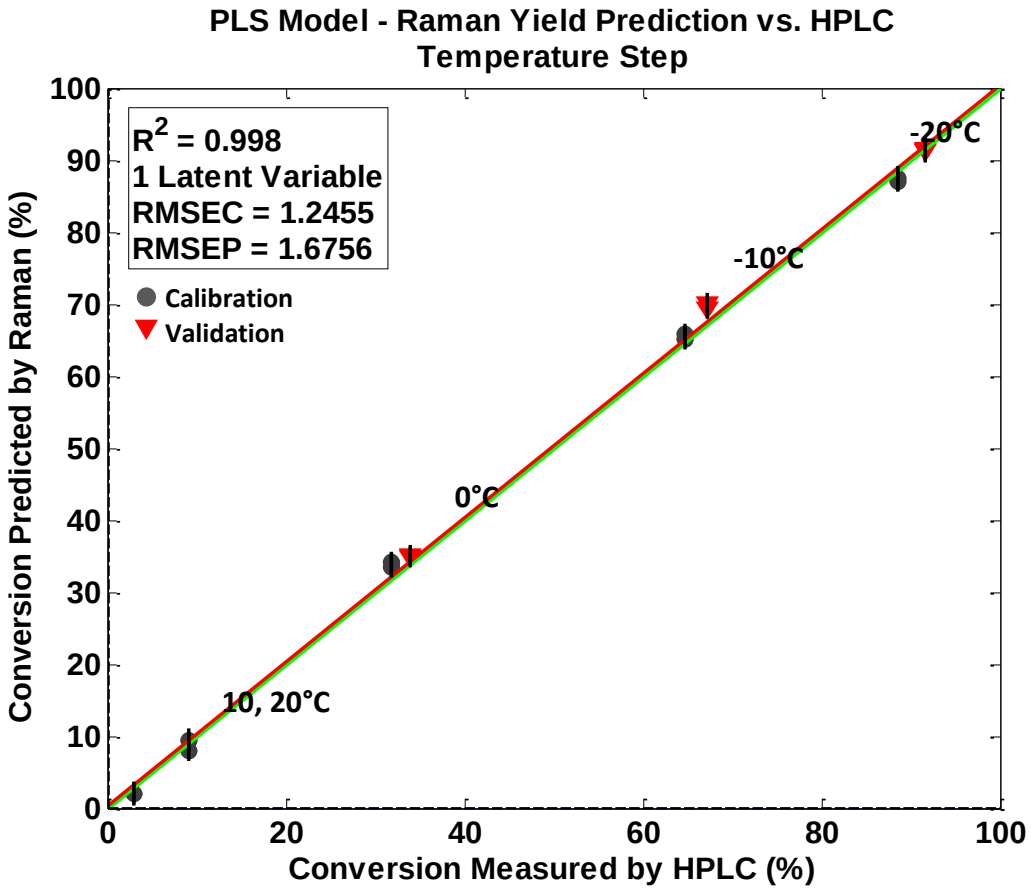

Figure 5.5. PLS model for the esterification of S-1-phenylethanol in configuration 1. Calibration points obtained at 10°C intervals from -20°C to 20°C. Validation points taken at 0°C, -10°C, and -20°C.

variables was found to overfit the data. The RMSEC across the full range was 1.2% error. Three validation samples were taken at -20°C, -10°C, and 0°C in a separate temperature step experiment (Figure 5.5, red triangles). The prediction error was 1.7% (root mean square error of prediction, "RMSEP"). This demonstrated the viability of Raman spectroscopy for quantitative validation of the Swern oxidation of S-1-phenylethanol, allowing for the adaptation of the real-time modeling capabilities demonstrated in Chapter 2 to the Swern oxidation.

Configuration 2

In Chapter 3, the Swern oxidation of S-1-phenylethanl was investigated with Raman, HPLC, and GC-MS monitoring. In-situ monitoring throughout the reaction with Raman spectroscopy combined with chromatographic analysis of the final 30 minutes granted significant insights into the kinetics and mechanisms of the reaction. Of critical importance was that the formation of intermediate 1 was very fast, and the formation of intermediate 2 was slow. In batch, the additions of DMSO (1) and TFAA (2) are performed very slowly, and require ~10 minutes to reattain thermal equilibrium. If S-1-phenylethanol is added before this, thermal runaway may occur, degrading intermediates into undesired side-products. This may have caused the misunderstanding that the rate of formation of intermediate 1 is slow. In translating the chemistry to continuous flow, this information would prove critical for optimizing the continuous flow reactor design. Intermediate 1's instability, whether due to temperature effects or short longevity, could be completely avoided if the reagents were added in a different order. This possibility is difficult to investigate in batch due to the exothermicity of batch of these reactions. If uncontrolled, the

reaction could exothermically run away. In continuous flow, however, the efficient heating gradients and high surface-to-volume ratio of the thermal control results in a significantly reduced possibility of thermal runaway. As a result, the rapid formation of intermediate 1 can be immediately followed by the formation of intermediate 2 without an increased chance of side-product formation in this new configuration.

A new addition order that takes advantage of the continuous flow paradigm was investigated. Configuration 2 combines DMSO and S-1-phenylethanol in the first reactor, which do not react with each other. Upon the addition of TFAA in the second reactor, intermediate 1 and intermediate 2 are formed in rapid succession (Figure 5.3). This configuration ensures that intermediate 1 is immediately consumed upon formation.

Following the redesign of the reactor, a new PLS model was constructed allowing for real-time Raman investigation of yield for configuration 2 rather than requiring off-line HPLC analysis. Five duplicate aliquots at 10 temperature and flow combinations resulted in a 50-point PLS calibration model, with a calibration error of 0.76 % yield (Figure 5.6, black circles). Note that the % yields covered by this model are a significantly narrower range, as yields below 60% were not attained in Configuration 2. One latent variable was used, as more resulted in an overfit model.

This new model was implemented with the same in-house real-time modeling software used in Chapter 2's investigation of the esterification of benzoic acid. All of the yields determined for Configuration 2 were determined in real-time from the control software. The same 25-point design space of temperatures and flow rates that was studied in

Configuration 1 was investigated in Configuration 2. This configuration has been previously investigated by Yoshida *et. al.* [17]. To validate the new chemistry model, aliquots were taken from random points in the design. HPLC aliquots were procured only for model validation purposes, and were not used for yield determination comparisons. These validation samples (Figure 5.6, red triangles) show strong correlation with the calibration model, with a prediction error of 1.4% yield. The results of this configuration, determined in real-time using Raman spectroscopy, are shown in Table 5.2.

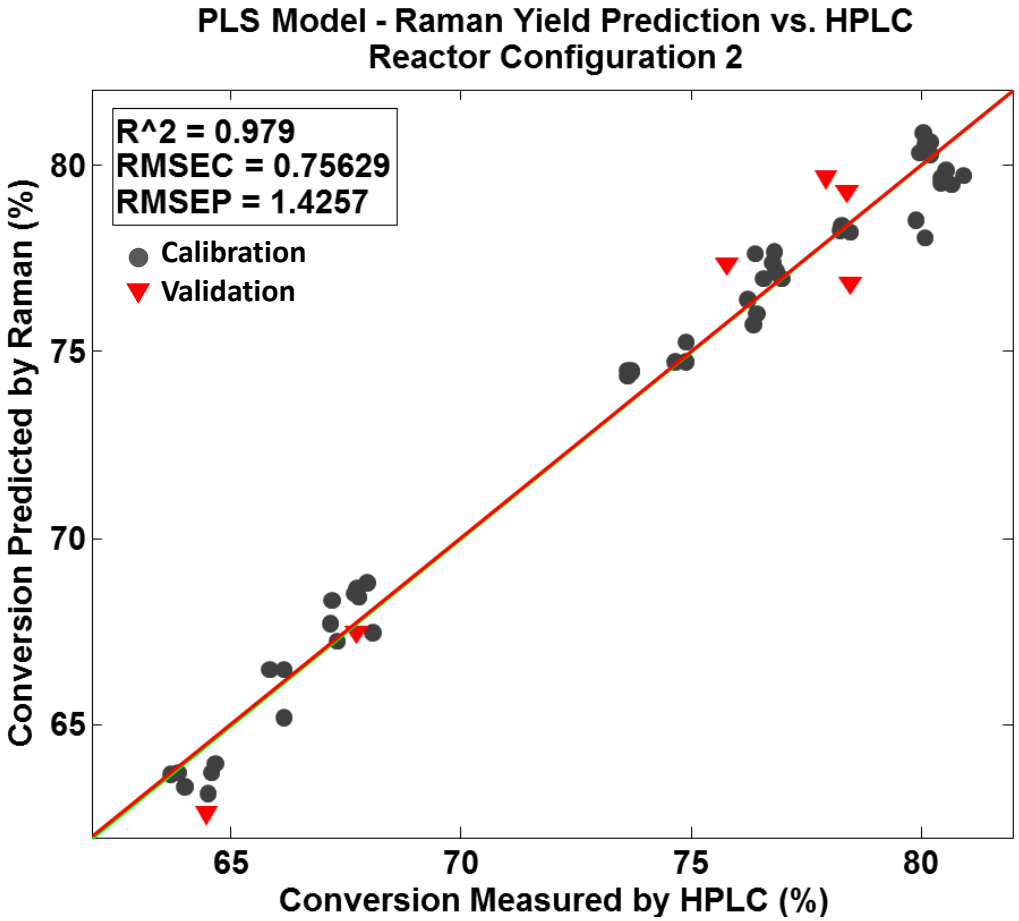

Figure 5.6. PLS model for the esterification of S-1-phenylethanol in configuration 2. A 55-point calibration model (black circles), with validation (red triangles). The calibration error was 0.76% yield of acetophenone. The prediction error was 1.43% yield of acetophenone. The configuration 2 results cover a narrow range due to the high efficiency of this reactor configuration disallowing low yield.

The results show that yield is significantly higher at warmer temperatures in this Configuration than in Configuration 1 – as high as 67% yield at room temperature. Compared to batch, which shows <2% yield at -30°C [18], this new reaction scheme significantly improves the viability of an industrial process that requires cryogenic temperatures (i.e. a Swern oxidation). The DoE required 4 hours of total experiment time, without the need for offline HPLC. This is a fivefold improvement in experimental time over a design that requires HPLC validation of every design point [66].

		Temperature				
Configuration 2		**-20°C**	**-10°C**	**0°C**	**10°C**	**20°C**
Flow Rate (mL/min)	**2**	79	79	76.75	63	61.5
	4	79.75	79.5	78.5	72	65.5
	6	79.75	79.5	78	71	63.5
	8	79.5	79.5	77	71	67
	10	79.5	79.5	77	71	67

Table 5.2. % yield results from Configuration 2 of the CFR. Configuration 2 results show higher yield at all temperature and flow rate combinations compared to configuration 1. Flow rate dependence is minimal, with no change in % yield in all flow rates at -10°C. Temperature dependence is significantly reduced as well. All results for Configuration 2 were obtained in real-time via Raman spectroscopy monitoring of the product line.

Comparison of Configurations

Configuration 2 results in a significant difference in yield at high temperatures, as high as 67% in Configuration 2 compared to 5% in Configuration 1. The formation and consumption of intermediate 1 (**3**) occurring in the same reactor in Configuration 2 is likely the cause of this improved yield, while Configuration 1 allows for the thermal degradation of **3**. This is further validated by the strong dependence on flow rates in Configuration 1

which further prolongs the presence of intermediate 1 (**3**), while Configuration 2 yields remain more consistent at a given temperature.

Figure 5.7 compares the results from batch and these two configurations. Even the straight conversion of reagent addition order (Configuration 1) demonstrates the power of continuous flow, showing marked improvement over batch synthesis. When continuous flow is combined with design decisions that are made to take advantage of this new paradigm – as in Configuration 2 – the improvement is even greater. At most temperatures and flow rates, Configuration 2 outperforms Configuration 1 by minimizing the presence of intermediate 1. The cases of Configuration 1 outperforming Configuration 2 are limited to <2% yield difference between the configurations, and are not statistically significant.

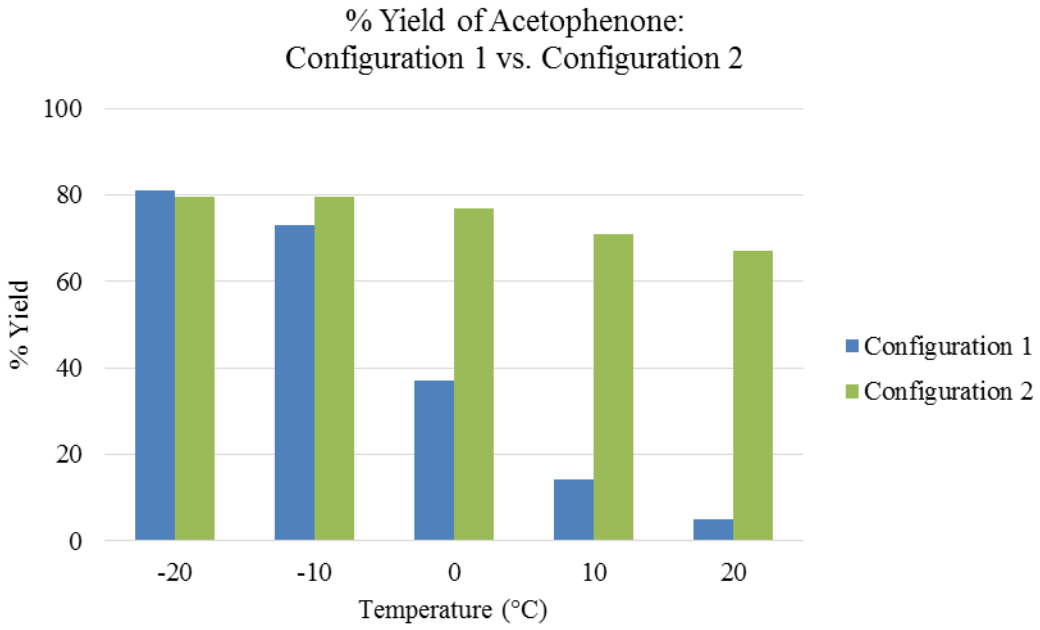

Figure 5.7. Batch and continuous flow configurations' percent yield. High yield in batch is only feasible at cryogenic temperatures of -70°C or below. Yield is negligible at temperatures of -30°C or higher. Configuration 1 shows high yield at -20°C, slowly decreasing as temperature increases until yield of 5% is obtained at room temperature. Configuration 2 shows high yield at -20°C which is largely maintained as temperature increases, reaching a minimum of 67% yield at room temperature.

The information from real-time quantitative monitoring of the chemistry allowed for rapid exploration of a design of experiments in the CFR in less than four hours. Using HPLC to validate chemical steady state would have doubled the experiment time. If not for random aliquots for validation, the entire experiment could have been performed via remote control. These results demonstrate that the real-time monitoring of product yield offers significant advantages for optimizing a reactor system when compared with systems that employ chromatographic methods. Most advantageous is the ability to alter a DoE based upon real-time information occurring in the reactor. The chemistry investigated (compare Chapter 2) and configuration of the reactor had no effect on the ability to predict chemical yield with Raman spectroscopy, demonstrating that this system is chemistry and hardware independent.

Additionally, continuous flow optimization thorough investigation of batch synthesis offered significant advantages over current optimization methods. Currently, optimization is almost exclusively focused on temperature and flow design space after a straightforward conversion to continuous flow. This method has proven effective – converting a reaction to continuous flow almost always results in improved yield compared to batch (see results from Configuration 1). But as a new synthesis paradigm, continuous flow allows for a rethinking of not just temperature and flow limitations but kinetics, runaway, and other physical limits as well. In continuous flow, a reflux reaction isn't limited by boiling point, but by pressure [2]. And, in this case, a cryogenic reaction isn't limited by exothermicity but by stability of intermediates. This is understood through a thorough investigation of batch using Raman spectroscopy, yielding a more efficient continuous flow configuration.

Conclusions

Investigation of the Swern oxidation via batch monitoring yielded significant information about the mechanisms and kinetics of the reaction. Instead of converting a batch chemistry directly to continuous flow, the information gained from batch informed continuous flow reactor design to take advantage of the continuous flow paradigm. As a result, yields from Configuration 2 showed marked improvements compared to a straight conversion of a batch chemistry for continuous flow. In addition, the overall analytical results demonstrate that the combined techniques of Raman spectroscopy and PLS allow for real-time quantitative monitoring of chemical yield with low errors. The real-time modeling was performed via a chemistry agnostic platform that allows for rapid determination of product formation, side product formation and product yield. Subsequent expansions of this platform could apply chemometric methods to Raman spectra collected from reagent lines as well, enabling not only feedback control but also feed-forward prediction of quality and subsequent validation of yield.

The work from this chapter is in preparation for publication.

Chapter 6: Conclusions

In this body of work, a project has been presented from conception and initial study to the cohesive and thorough case study of how to design a reaction for continuous flow. In Chapter 2, the esterification of benzoic acid was investigated in continuous flow with PAT. A PLS model that accurately predicted product formation using Raman spectroscopy was constructed using off-line. This model was integrated with the control software, and was able to predict product yield in real-time using Raman spectroscopy. This work, published in 2010, is the first implementation of spectroscopic real-time monitoring of a production-scale CFR using PLS modeling. This simple equilibrium reaction proved to be a valuable proof of concept for multiple techniques investigated later: CFR reactor construction, NeSSI implementation of reaction analytics, software development for CFR control, Raman integration with the CFR and the control software, chemometric modeling of yield from a CFR, and eventually the real-time predictions of product conversion in a CFR. Subsequent work relied heavily on these understandings, proving invaluable.

In Chapter 3, the cryogenic Swern oxidation of S-1-phenylethanol was thoroughly investigated in batch via Raman spectroscopy, HPLC, and GC-MS. An apparatus was constructed to ensure consistent delivery of pre-cooled reagents while obtaining analytical measurements throughout the experiment. Raman spectroscopy monitored the reaction from start to finish, yielding multiple insights into the kinetics of the reaction and correcting misunderstandings. Notably, the intermediate formation observed with Raman spectroscopy revealed that the formation of the second intermediate was the rate-determining step, rather than the formation of the first intermediate. Raman also revealed that product formation in the Swern oxidation occurs post-quench reaction, contradicting beliefs and step-by-step instructions found elsewhere. The chromatographic methods

confirmed these observations through rapid sampling of chromatography samples. This began the work for translating a reaction from batch to continuous flow. The reaction itself is far from the most important part of this work; I believe that a similar process of trying to understand many multistep reactions via analytical methods would yield similarly fascinating insights.

In Chapter 4, the CFR is thoroughly detailed and preliminary results of performing the Swern oxidation in continuous flow are discussed. The work in this chapter further explains the software and hardware developments, including some discussion of points that were not fully described earlier. The addition order in Chapter 4 is solely informed by a direct translation of the Swern oxidation from batch to continuous flow. The Swern oxidation obtains great results in continuous flow at temperatures as high as -20°C, while highly dependent upon both temperature and residence time.

In Chapter 5, the reactor from Chapter 4 is redesigned into Configuration 2, taking into consideration the findings from Chapter 3 and implementing the real-time modeling developed in Chapter 2. While the reactor described in Chapter 4 obtained great yields, Configuration 2 takes advantage of many facets of the continuous flow paradigm, resulting in significantly higher yield across the board. Figure 6.2 shows the overall improved results obtained throughout, culminating in 67% conversion at room temperature for a reaction that requires cryogenic temperatures in batch. The data obtained in batch directly informed the reactor design and construction, leading to astounding results in continuous flow. Coupled with real-time modeling of a reaction, which significantly reduced the time

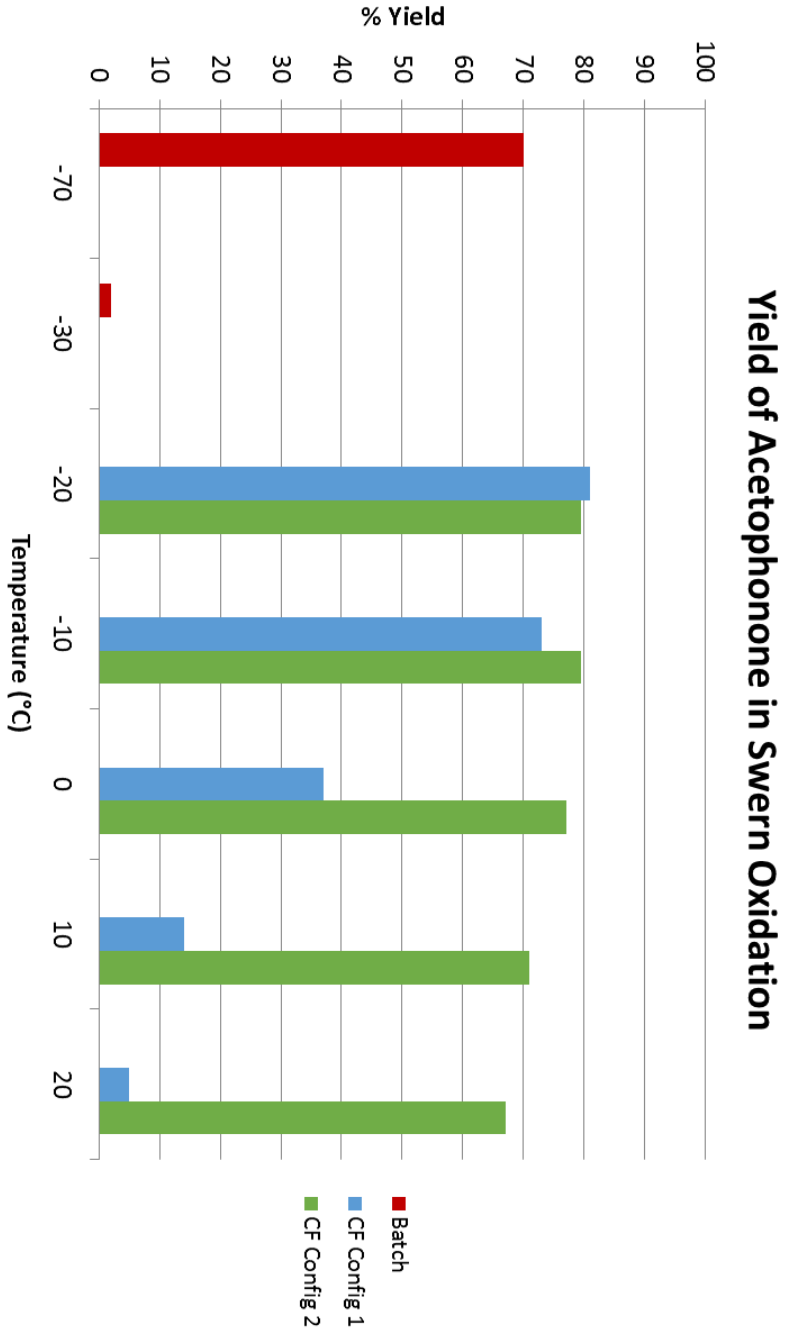

Figure 6.2. Batch and continuous flow configurations' percent yield. High yield in batch is only feasible at cryogenic temperatures of -70°C or below. Yield is negligible at temperatures of -30°C or higher. Configuration 1 shows high yield at -20°C, slowly decreasing as temperature increases until yield of 5% is obtained at room temperature. Configuration 2 shows high yield at -20°C which is largely maintained as temperature increases, reaching a minimum of 67% yield at room temperature.

required to optimize the reactor, a strong case is made for advanced analytics use in continuous flow.

Presented as a whole, this work describes a thorough investigation of batch, coupled with optimization of a reaction in continuous flow through understanding of a chemistry via PAT and chemometrics. While continuous flow offers numerous advantages for production, this improved CFR development pathway offers significant advantages over the current paradigm, and is applicable to most CFRs. A cohesive vision for designing a CFR pathway from the information gathered by a thorough investigation of batch represents a new path for CFR process development that should be applicable to a wide range of chemical reactions, enabling better use of the continuous flow paradigm for industrial production of target chemicals.

References

1. Wong-Hawkes, S.Y.F.; Matteo, J.C.; Warrington, B.H.; White, J.D. In *Microreactors as new tools for drug discovery and development*, Ernst Schering Foundation Symposium on New Avenues to Efficient Chemical Synthesis, Berlin, GERMANY, August 31 -September 01, 2007; Berlin, GERMANY, pp 39-55.
2. Wiles, C.; Watts, P. *Micro reaction technology in organic synthesis*. CRC Press: 2011.
3. HIBARA, A.; TOKESHI, M.; UCHIYAMA, K.; HISAMOTO, H.; KITAMORI, T. Integrated multilayer flow system on a microchip. *Analytical sciences* **2001**, *17*, 89-93.
4. Beato, P.; Kraehnert, R.; Engelschalt, S.; Frank, T.; Schlögl, R. A micro-structured quartz reactor for kinetic and< i> in situ</i> spectroscopic studies in heterogeneous catalysis. *Chemical Engineering Journal* **2008**, *135*, S247-S253.
5. Adamschik, M.; Hinz, M.; Maier, C.; Schmid, P.; Seliger, H.; Hofer, E.; Kohn, E. Diamond micro system for bio-chemistry. *Diamond and Related materials* **2001**, *10*, 722-730.
6. De la Iglesia, O.; Sebastian, V.; Mallada, R.; Nikolaidis, G.; Coronas, J.; Kolb, G.; Zapf, R.; Hessel, V.; Santamaria, J. Preparation of pt/zsm-5 films on stainless steel microreactors. *Catalysis today* **2007**, *125*, 2-10.
7. McCreedy, T. Rapid prototyping of glass and pdms microstructures for micro total analytical systems and micro chemical reactors by microfabrication in the general laboratory. *Analytica chimica acta* **2001**, *427*, 39-43.
8. Yoon, T.-H.; Park, S.-H.; Min, K.-I.; Zhang, X.; Haswell, S.J.; Kim, D.-P. Novel inorganic polymer derived microreactors for organic microchemistry applications. *Lab on a Chip* **2008**, *8*, 1454-1459.
9. Becker, H.; Gaertner, C. Polymer based micro-reactors. *Reviews in Molecular Biotechnology* **2001**, *82*, 89-99.
10. Watts, P.; Wiles, C. Recent advances in synthetic micro reaction technology. *Chemical Communications* **2007**, 443-467.
11. Cotí, K.K.; Wang, Y.; Lin, W.-Y.; Chen, C.-C.; Liu, K.; Shen, C.K.-F.; Selke, M.; Yeh, A.; Lu, W.; Tseng, H.-R. A dynamic micromixer for arbitrary control of disguised chemical selectivity. *Chem. Commun.* **2008**, 3426-3428.
12. *Wiles, C.*; *Ngamsom, B.* **Continuous flow esterifications**. Application Note: chemtrix.com, 2010.
13. Baek, J.; Allen, P.M.; Bawendi, M.G.; Jensen, K.F. Investigation of indium phosphide nanocrystal synthesis using a high-temperature and high-pressure continuous flow microreactor. *Angewandte Chemie-International Edition* **2011**, *50*, 627-630.
14. McMullen, J.P.; Stone, M.T.; Buchwald, S.L.; Jensen, K.E. An integrated microreactor system for self-optimization of a heck reaction: From micro- to mesoscale flow systems. *Angewandte Chemie-International Edition* **2010**, *49*, 7076-7080.
15. Wiles, C.; Watts, P.; Haswell, S.J.; Pombo-Villar, E. The aldol reaction of silyl enol ethers within a micro reactor. *Lab on a Chip* **2001**, *1*, 100-101.

16. Wiles, C.; Watts, P.; Haswell, S.J.; Pombo-Villar, E. 1,4-addition of enolates to alpha,beta-unsaturated ketones within a micro reactor. *Lab on a Chip* **2002**, *2*, 62-64.
17. Kawaguchi, T.; Miyata, H.; Ataka, K.; Mae, K.; Yoshida, J.i. Room-temperature swern oxidations by using a microscale flow system. *Angewandte Chemie International Edition* **2005**, *44*, 2413-2416.
18. van der Linden, J.J.M.; Hilberink, P.W.; Kronenburg, C.M.P.; Kemperman, G.J. Investigation of the moffatt-swern oxidation in a continuous flow microreactor system. *Organic Process Research & Development* **2008**, *12*, 911-920.
19. Skoog, D.A.; Holler, F.J.; Crouch, S.R. *Principles of instrumental analysis*. 6 ed.; Thomson Brooks/Cole: 2007.
20. Barthus, R.C.; Poppi, R.J. Determination of the total unsaturation in vegetable oils by fourier transform raman spectroscopy and multivariate calibration. *Vibrational Spectroscopy* **2001**, *26*, 99-105.
21. Pelletier, M.J.; Fabiilli, M.L.; Moon, B. On-line analysis of a continuous-flow ozonolysis reaction using raman spectroscopy. *Applied Spectroscopy* **2007**, *61*, 1107-1115.
22. Misra, M.; Yue, H.H.; Qin, S.J.; Ling, C. Multivariate process monitoring and fault diagnosis by multi-scale pca. *Computers & Chemical Engineering* **2002**, *26*, 1281-1293.
23. Chen, J.; Liu, K.-C. On-line batch process monitoring using dynamic pca and dynamic pls models. *Chemical Engineering Science* **2002**, *57*, 63-75.
24. Geladi, P. Chemometrics in spectroscopy. Part 1. Classical chemometrics. *Spectrochimica Acta Part B: Atomic Spectroscopy* **2003**, *58*, 767-782.
25. Dearing, T.I.; Thompson, W.J.; Rechsteiner, C.E., Jr.; Marquardt, B.J. Characterization of crude oil products using data fusion of process raman, infrared, and nuclear magnetic resonance (nmr) spectra. *Applied Spectroscopy* **2011**, *65*, 181-186.
26. Szostak, R.; Mazurek, S. Quantitative determination of acetylsalicylic acid and acetaminophen in tablets by ft-raman spectroscopy. *Analyst* **2002**, *127*, 144-148.
27. Shah, R.B.; Tawakkul, M.A.; Khan, M.A. Process analytical technology: Chemometric analysis of raman and near infra-red spectroscopic data for predicting physical properties of extended release matrix tablets. *Journal of Pharmaceutical Sciences* **2007**, *96*, 1356-1365.
28. Sulub, Y.; Wabuyele, B.; Gargiulo, P.; Pazdan, J.; Cheney, J.; Berry, J.; Gupta, A.; Shah, R.; Wu, H.; Khan, M. Real-time on-line blend uniformity monitoring using near-infrared reflectance spectrometry: A noninvasive off-line calibration approach. *Journal of pharmaceutical and biomedical analysis* **2009**, *49*, 48-54.
29. Peinado, A.; Hammond, J.; Scott, A. Development, validation and transfer of a near infrared method to determine in-line the end point of a fluidised drying process for commercial production batches of an approved oral solid dose pharmaceutical product. *Journal of pharmaceutical and biomedical analysis* **2011**, *54*, 13-20.
30. Pawliszyn, J. *Comprehensive sampling and sample preparation: Analytical techniques for scientists*. Elsevier: Amsterdam, 2012; Vol. 1.34.

31. Roberto, M.F.; Dearing, T.I.; Martin, S.; Marquardt, B.J. Integration of continuous flow reactors and online raman spectroscopy for process optimization. *Journal of Pharmaceutical Innovation* **2012**, *7*, 69-75.
32. Undey, K.; Low, D.; Menezes, J.; Koch, M. *Pat applied in biopharmaceutical process development and manufacturing: An enabling tool for quality-by-design*. CRC Press: Boca Raton, FL, 2012.
33. Roberge, D.M.; Ducry, L.; Bieler, N.; Cretton, P.; Zimmermann, B. Microreactor technology: A revolution for the fine chemical and pharmaceutical industries? *Chemical Engineering & Technology* **2005**, *28*, 318-323.
34. Roberge, D.M.; Zimmermann, B.; Rainone, F.; Gottsponer, M.; Eyholzer, M.; Kockmann, N. Microreactor technology and continuous processes in the fine chemical and pharmaceutical industry: Is the revolution underway? *Organic Process Research & Development* **2008**, *12*, 905-910.
35. Roberge, D.M.; Bieler, N.; Mathier, M.; Eyholzer, M.; Zimmermann, B.; Barthe, P.; Guermeur, C.; Lobet, O.; Moreno, M.; Woehl, P. Development of an industrial multi-injection microreactor for fast and exothermic reactions - part ii. *Chemical Engineering & Technology* **2008**, *31*, 1155-1161.
36. Styring, P.; Parracho, A.I.R. From discovery to production: Scale-out of continuous flow meso reactors. *Beilstein Journal of Organic Chemistry* **2009**, *5*.
37. Leung, S.A.; Winkle, R.F.; Wootton, R.C.R.; deMello, A.J. A method for rapid reaction optimisation in continuous-flow microfluidic reactors using online raman spectroscopic detection. *Analyst* **2005**, *130*, 46-51.
38. de Boer, A.R.; Letzel, T.; van Elswijk, D.A.; Lingeman, H.; Niessen, W.M.A.; Irth, H. On-line coupling of high-performance liquid chromatography to a continuous-flow enzyme assay based on electrospray ionization mass spectrometry. *Analytical Chemistry* **2004**, *76*, 3155-3161.
39. Basheer, C.; Shahitha, F.; Hussain, J.; Lee, H.K.; Valiyaveettil, S. Design of a capillary-microreactor for efficient suzuki coupling reactions. *Tetrahedron Letters* **2004**, *45*, 7297-7300.
40. Kim, J.; Han, J.; Noh, J.; Chung, H. Feasibility of a wide area illumination scheme for reliable raman measurement of petroleum products. *Applied Spectroscopy* **2007**, *61*, 686-693.
41. Workman, J.J. Interpretive spectroscopy for near infrared. *Applied Spectroscopy Reviews* **1996**, *31*, 251-320.
42. Workman Jr., J. A review of process near infrared spectroscopy: 1980-1994. J. Near Infrared Spectrosc., 1993; Vol. 1, pp 221-245.
43. Cooper, J.B.; Wise, K.L.; Welch, W.T.; Sumner, M.B.; Wilt, B.K.; Bledsoe, R.R. Comparison of near-ir, raman, and mid-ir spectroscopies for the determination of btex in petroleum fuels. *Applied Spectroscopy* **1997**, *51*, 1613-1620.
44. Santos, V.O.; Oliveira, F.C.C.; Lima, D.G.; Petry, A.C.; Garcia, E.; Suarez, P.A.Z.; Rubim, J.C. A comparative study of diesel analysis by ftir, ftnir and ft-raman spectroscopy using pls and artificial neural network analysis. *Analytica Chimica Acta* **2005**, *547*, 188-196.
45. De Beer, T.R.M.; Vergote, G.J.; Baeyens, W.R.G.; Remon, J.P.; Vervaet, C.; Verpoort, F. Development and validation of a direct, non-destructive quantitative method for medroxyprogesterone acetate in a pharmaceutical suspension using ft-

raman spectroscopy. *European Journal of Pharmaceutical Sciences* **2004**, *23*, 355-362.
46. Vergote, G.J.; De Beer, T.R.M.; Vervaet, C.; Remon, J.P.; Baeyens, W.R.G.; Diericx, N.; Verpoort, F. In-line monitoring of a pharmaceutical blending process using ft-raman spectroscopy. *European Journal of Pharmaceutical Sciences* **2004**, *21*, 479-485.
47. Reich, G. Near-infrared spectroscopy and imaging: Basic principles and pharmaceutical applications. *Advanced Drug Delivery Reviews* **2005**, *57*, 1109-1143.
48. Hao, H.; Su, W.; Barrett, M.; Caron, V.; Healy, A.-M.; Glennon, B. Org. Proc. Res. Dev., 2010; Vol. 14, p 1209.
49. Yates, F. The design and analysis of factorial experiments. Imperial Bureau of Soil Science: Harpenden, Eng., 1937.
50. Annadurai, G.; Juang, R.S.; Lee, D.J. Factorial design analysis for adsorption of dye on activated carbon beads incorporated with calcium alginate. *Advances in Environmental Research* **2002**, *6*, 191-198.
51. Negro, M.J.; Manzanares, P.; Oliva, J.M.; Ballesteros, I.; Ballesteros, M. Changes in various physical/chemical parameters of pinus pinaster wood after steam explosion pretreatment. *Biomass & Bioenergy* **2003**, *25*, 301-308.
52. Afseth, N.K.; Segtnan, V.H.; Wold, J.P. Raman spectra of biological samples: A study of preprocessing methods. *Applied Spectroscopy* **2006**, *60*, 1358-1367.
53. Lieber, C.A.; Mahadevan-Jansen, A. Automated method for subtraction of fluorescence from biological raman spectra. *Applied Spectroscopy* **2003**, *57*, 1363-1367.
54. Omura, K.; Swern, D. Oxidation of alcohols by "activated" dimethyl sulfoxide. A preparative, steric and mechanistic study. *Tetrahedron* **1978**, *34*, 1651-1660.
55. Albright, J.D.; Goldman, L. Dimethyl sulfoxide-acid anhydride mixtures. New reagents for oxidation of alcohols1. *Journal of the American Chemical Society* **1965**, *87*, 4214-4216.
56. Omura, K.; Sharma, A.K.; Swern, D. Dimethyl sulfoxide-trifluoroacetic anhydride. New reagent for oxidation of alcohols to carbonyls. *The Journal of Organic Chemistry* **1976**, *41*, 957-962.
57. Tidwell, T.T. Oxidation of alcohols by activated dimethyl sulfoxide and related reactions: An update. *Synthesis* **1990**, *1990*, 857-870.
58. Svensson, O.; Josefson, M.; Langkilde, F.W. Reaction monitoring using raman spectroscopy and chemometrics. *Chemometrics and intelligent laboratory systems* **1999**, *49*, 49-66.
59. Lee, M.; Kim, H.; Rhee, H.; Choo, J. Reaction monitoring of imine synthesis using raman spectroscopy. *BULLETIN-KOREAN CHEMICAL SOCIETY* **2003**, *24*, 205-208.
60. Hu, Y.; Liang, J.K.; Myerson, A.S.; Taylor, L.S. Crystallization monitoring by raman spectroscopy: Simultaneous measurement of desupersaturation profile and polymorphic form in flufenamic acid systems. *Industrial & engineering chemistry research* **2005**, *44*, 1233-1240.
61. *(SDBS), S.D.f.O.C.* Mass spectrum.

62. Mancuso, A.J.; Huang, S.-L.; Swern, D. Oxidation of long-chain and related alcohols to carbonyls by dimethyl sulfoxide" Activated" By oxalyl chloride. *The Journal of Organic Chemistry* **1978**, *43*, 2480-2482.
63. Schwalbe, T.; Kadzimirsz, D.; Jas, G. Synthesis of a library of ciprofloxacin analogues by means of sequential organic synthesis in microreactors. *QSAR & Combinatorial Science* **2005**, *24*, 758-768.
64. Tanaka, K.; Motomatsu, S.; Koyama, K.; Tanaka, S.-i.; Fukase, K. Large-scale synthesis of immunoactivating natural product, pristane, by continuous microfluidic dehydration as the key step. *Organic Letters* **2007**, *9*, 299-302.
65. Hopkin, M.D.; Baxendale, I.R.; Ley, S.V. A flow-based synthesis of imatinib: The api of gleevec. *Chemical Communications* **2010**, *46*, 2450-2452.
66. Roberto, M.F.; Dearing, T.I.; Branham, C.W.; Bleie, O.; Marquardt, B.J. Rapid determination of optimal conditions in a continuous flow reactor using process analytical technology *Processes* **2014**, *2*, 24-33.
67. Suga, S.; Nagaki, A.; Yoshida, J.-i. Highly selective friedel–crafts monoalkylation using micromixing. *Chemical Communications* **2003**, 354-355.
68. Wahab, B. Advances in organic synthesis: Expedient radiosynthesis of substituted indoles for pharmaceutical lead development within microreactors. University of Hull, 2010.
69. Ueno, M.; Hisamoto, H.; Kitamori, T.; Kobayashi, S. Phase-transfer alkylation reactions using microreactors. *Chemical Communications* **2003**, 936-937.
70. Knothe, G. Rapid monitoring of transesterification and assessing biodiesel fuel quality by near-infrared spectroscopy using a fiber-optic probe. *Journal of the American Oil Chemists' Society* **1999**, *76*, 795-800.
71. Thomas, E.V. A primer on multivariate calibration. *Analytical Chemistry* **1994**, *66*, 795A-804A.
72. Cooper, J.B.; Wise, K.L.; Groves, J.; Welch, W.T. Determination of octane numbers and reid vapor pressure of commercial petroleum fuels using ft-raman spectroscopy and partial least-squares regression analysis. *Analytical Chemistry* **1995**, *67*, 4096-4100.